1-1-2017

Navigating Human Cytomegalovirus (hcmv) Envelopment And Egress

William Longeway Close
Wayne State University,

NAVIGATING HUMAN CYTOMEGALOVIRUS (HCMV) ENVELOPMENT AND EGRESS

by

WILLIAM LONGEWAY CLOSE

DISSERTATION

Submitted to the Graduate School

of Wayne State University,

Detroit, Michigan

in partial fulfillment of the requirements

for the degree of

DOCTOR OF PHILOSOPHY

2017

MAJOR: IMMUNOLOGY & MICROBIOLOGY

Approved By:

_____

Advisor Date

_____

_____

_____

DEDICATION

With love, I dedicate this dissertation to the memory

of my father, Duane Edgar Close.

ACKNOWLEDGEMENTS

The work presented herein is the result of countless hours spent trying to answer a seemingly straightforward question. While my name is the one on the cover, this work was anything but an individual endeavor. In the years leading up to and including my time at Wayne State University, I have been extremely fortunate to find individuals who believed in me and supported me at every step along the way.

First and foremost, I would like to thank my mentor, Phil, for letting me independently grow in my scientific career. I knew I would always find help when I needed it. I would also like to thank the members of the Pellett Lab, past and present. Steve, Danny, and Subhendu put up with me when I was still new to the lab and helped me get to where I am today. Amit, Marwa, and Imran all helped immensely with my work and provided more than a couple laughs. Lastly, thank you to Ashley, James, Christina, and Ashlei for helping with the day-to-day grind and making lab enjoyable.

To Wayne State as a whole, thank you for believing I had what it takes and helping me realize my goals. Thank you to my committee members: Phil, Jeff, Tom, and Bhanu for guiding me along throughout my degree and keeping me focused. Thank you to the everyone in the former Department of Immunology and Microbiology and current Department of Microbiology, Immunology, and Biochemistry. With the support of the office staff, Mary, Lynette, and April, I knew I only had to worry about my research and the rest would be taken care of (even if I did forget an occasional receipt). To the other faculty, thank you for helping me develop a broad foundation of knowledge which I know will continue to benefit me going forward. Most importantly though, I would like to thank my fellow graduate students in the department. From eating lunch together and talking

about our experiments to going out and grabbing drinks, the camaraderie, the inside jokes, and the friendship made my time at Wayne State far more enjoyable than I could have ever anticipated.

To my family and my friends, thank you for being there for me when I needed it. To my brother, Ben, and sister, Steph, thank you for believing in me and keeping me grounded. To my mother, Cindy, thank you for always supporting me no matter what. Ever since I was a child, you helped me embrace my love of science and if I ever needed anything, I knew I could count on you. To my father, Duane, I miss your presence most at times like these. I knew I always had your unwavering support and you were always so interested in what I was doing. Even though you aren't here to see what I've accomplished, I hope I've made you proud. To my mother- and father-in-law, Afaf and Tony, plus the rest of the family, I can't thank you enough for always making sure I have a warm meal and pleasant company when I needed it.

Finally, I would like to thank my wife, Lisa. When I came to Wayne State, I never anticipated I would meet someone as talented, ambitious, or caring as her, especially not in the same department. Your support as both a fellow graduate student and as my partner has meant far more than I could possibly put into words. I can't thank you enough for all that you've done for me and for us.

TABLE OF CONTENTS

LIST OF TABLES

LIST OF FIGURES

CHAPTER 1: INTRODUCTION

I. Herpesviruses

The name herpes comes from the Greek verb "ἕρπειν" meaning "to creep" and was originally used to describe various recurring skin infections (4). Since the time of Hippocrates, the use of the term "herpes" has been continually refined based on observed characteristics of infection. Eventually, herpes came to describe infections resulting in formation of small transient pustules that were resistant to other treatments. In the initial 17th through 19th century classifications of the genus *Herpes*, *H. zoster* and *H. simplex* were first identified.

Through advances in technology and the characterization of viruses in modern times, the genus *Herpesvirus* was officially recognized by the International Committee of Taxonomy of Viruses (ICTV) starting in 1971 (5). Since then, the genus has been elevated to the order *Herpesvirales* and now contains over 130 species divided into three families based on host speciation: *Herpesviridae* (mammal, bird, and reptile), *Alloherpesviridae* (fish and frog), and *Malacoherpesviridae* (mollusks). The human herpesviruses (HHVs) are contained within *Herpesviridae* and help comprise three subfamilies: *Alphaherpesvirinae* includes herpes simplex virus 1 (HSV-1, HHV-1), herpes simplex virus 2 (HSV-2, HHV-2), and varicella zoster virus (VZV, HHV-3); *Betaherpesvirinae* includes human cytomegalovirus (HCMV, HHV-5), HHV-6A, HHV-6B, and HHV-7; finally, *Gammaherpesvirinae* includes Epstein-Barr virus (EBV, HHV-4) and Kaposi's sarcoma-associated herpesvirus (KSHV, HHV-8). Based on evolutionary phylogeny, divergence of the *Herpesviridae* subfamilies happened ~180-220 million years

ago whereas *Homo sapiens* are estimated to have evolved only ~1.3-1.8 million years ago (6).

HHVs vary broadly in their tissue tropism and, as a result, are associated with a wide range of etiologies with contrasting degrees of severity in healthy individuals. HSV-1 and HSV-2 cause oral and genital lesions, respectively, and are classified as cofactors for sexually transmitted infections. VZV is the causative agent of chicken pox and shingles. HHV-6A, HHV-6B, and HHV-7 are all associated with roseola in infants. Infectious mononucleosis is caused by EBV and to a lesser degree, HCMV. Lastly, HSV-1, EBV, and KSHV infections have also been correlated with the development of cancer.

Despite differences in virion tropism and disease progression, HHV virions maintain a conserved structure similar to all herpesviruses (7). Mature virions range from 100-200 nm in size and contain a large linear double-stranded DNA genome packaged within an icosahedral nucleocapsid (Fig. 1.1). Within HHVs, genomes range from 145-240 kbp in size and vary in terms of coding potential and sequence organization (Fig. 1.2) (8). The capsid is then wrapped in a proteinaceous tegument which serves as a bridge between the capsid and the envelope in addition to several key effector functions upon infection. Ultimately, mature virions are wrapped in a host-derived lipid bilayer containing membrane bound glycoproteins and accessory factors required for receptor binding and membrane fusion during initiation of infection.

Similar to structure, the general replication cycle for HHVs is also conserved between subfamilies (Fig. 1.3) (8). During lytic infection, virions attach the receptors on host cell membranes. Following adherence, the virion envelope fuses with the plasma membrane or endocytic vesicle thus releasing the tegument and nucleocapsid into the

cytoplasmic space. The tegument downmodulates host immune responses while also aiding in transport of the capsid to the nuclear membrane. Upon arrival at the nucleus, the capsid portal is opened and the high internal pressure of the capsid ejects the viral genome. Through a combination of tegument trans-activating proteins and host factors, transcription of viral genes is initiated. This leads to the sequentially regulated expression of viral proteins. Generally, immediate early (IE, α) genes promote replication by altering the host environment, early (E, β) genes lead to DNA replication, and late (L, γ) genes produce structural components used in assembly of nascent virions. When the infection has sufficiently progressed, genome concatemers are packaged into the capsid which is then exported out of the nucleus and into the cytoplasm. An amorphous tegument layer is added and virions are enveloped. Finally, HHV progeny are exported out of host cells into the extracellular space.

A hallmark of HHV infection is the ability to establish latency within host tissues. In these instances, a low level of IE gene expression is maintained while the majority of downstream genes are repressed through various mechanisms. Following cellular stress or another appropriate stimulus, viral gene expression is induced and lytic replication proceeds normally.

A. Global health burden of HCMV infection

Of all the HHVs, HCMV is one of the most pervasive and opportunistic pathogens worldwide. Seroprevalence has been shown to increase as a function of age with approximately 60% of individuals being positive at 50 years of age (9). Rates of seroprevalence also tend to be disproportionately higher in both non-white and low socioeconomic groups suggesting lifestyle-associated risk factors. In healthy individuals,

primary symptoms are typically mild and may go unnoticed. Conversely, in individuals with naïve or compromised immune systems, infection can have severe and lasting effects.

HCMV is the leading infectious cause of congenital birth defects in the United States (10). If a seronegative woman becomes infected prior to becoming pregnant, the likelihood of fetal infection is low (11). If the same woman were to instead become infected while pregnant, there is a 50% probability that the fetus will also be infected. Even in healthy individuals, the normal immune response to HCMV is weakly protective. Thus, if a mother contracts a previously unencountered strain of HCMV during pregnancy, the risk for fetal infection increases. Of infected children, only 10% will show symptoms although the other 90% may develop symptoms later. The primary outcomes of congenital infection are microcephaly, hearing loss, and growth retardation, among others (12). During infection, the virus is able to access the fetus through infection of placental cytotrophoblasts unless sufficiently controlled by the maternal immune response. Infection of cytotrophoblasts also alters cellular gene expression and may impact the support structures required for fetal development, particularly if infection occurs within the first trimester.

In addition to congenital cases, HCMV is particularly problematic for immunocompromised individuals, including HIV/AIDS patients and organ transplantation patients. Because HCMV is so prevalent and establishes latency in hosts, individuals with diminished immune systems are at high-risk for experiencing frequent viral reactivations.

Individuals infected with HIV were 2.5-times more likely to develop AIDS if they were also HCMV-seropositive (13). For those who already developed AIDS, infection with HCMV most often results in virally induced retinitis (14). The inability to mount a sufficient neutralizing response to HCMV infection is correlated with decreased $CD4^+$ leukocyte populations. The development of highly active antiretroviral therapy (HAART) has led to dramatic improvements in the prognosis of AIDS patients but treatment can also lead to temporary uveitis from reconstituted immune populations attacking remaining viral antigens in the eye (15).

For solid organ transplant patients, CMV can be particularly problematic because the virus exhibits an extraordinarily broad tissue tropism and is able to infect most major organ systems. If a transplanted organ is directly infected or carries latently infected monocytes, the new host may mount a strong $CD8^+$ response against the new tissue resulting in graft versus host disease and ultimate rejection of the organ.

For all at risk populations, the combination of improved screening techniques and development of HCMV antiviral treatments has greatly reduced the incidence of complications (16). Currently, there are four treatments available for HCMV: ganciclovir, valganciclovir, cidofovir, and foscarnet. Thus far, vaccination strategies against HCMV have been unsuccessful due to its unique immune evasion tactics meaning the antivirals are the only option for treating patients. Unfortunately, all available drugs target either viral DNA polymerase (UL54) or the phosphokinase, pUL97, so antiviral resistance has increased. Hindering the development on novel therapies is a lack in understanding of HCMV replicative processes. In relation to several other clinically relevant viruses,

comparatively little is known regarding HCMV virion assembly and egress. If these processes were better understood, drug targets could be pursued.

B. HCMV replication and formation of the assembly compartment

During infection, HCMV follows a replication cycle similar to other herpesviruses (Fig. 1.3). Where HCMV replication deviates most notably from the other herpesviruses, is the formation of the assembly compartment. Approximately three days post-infection, the host organelle structure is significantly altered through a process dependent on viral gene expression (17-19). The internal reorganization of host membranes leads to the generation of the cytoplasmic virion assembly compartment (cVAC; Fig. 1.4). The cVAC is a structure unique to HCMV infection and consists of one or more enlarged nuclei bent around a perinuclear ring-like Golgi structure with various endosome populations at the center (18-20). In tissue sections of clinical specimens, these structures are referred to as “owl’s eye inclusions.” The prevailing idea is that the cVAC functions as a viral assembly line where the maturing capsids pass through the subsequent layers, gathering the requisite structural proteins, until envelopment and egress.

Several studies have looked for proteins integral to cVAC biogenesis leading to identification of both viral and cellular factors. An siRNA screen of viral genes identified UL48, UL94, and UL103 as being important for induction of cVAC structures (21). After establishing a direct role for UL103, a follow-up proteomics study characterized several cellular proteins that interact with UL103 (22). By this study and others, the Golgi-resident motor protein, MYO18A, was found to facilitate cVAC structure formation (22, 23).

The induction of cVAC formation is not required for virion growth but does augment it. Several studies seeking to understand envelopment and egress of HCMV virions have

found arrest of virion maturation is typically accompanied by improper localization of virion structural proteins typically found in the cVAC. These observations lead to the question: does cVAC development drive envelopment and egress or do envelopment and egress drive cVAC development as a byproduct of virion production? To look at this interplay further, we need to take a closer look at events required for envelopment and egress.

II. Envelopment and Egress

Several components are required for virion biogenesis including: i) the viral genome, ii) capsid proteins, iii) viral microRNAs (miRNAs), iv) tegument proteins, v) lipid membranes, and iv) membrane-bound glycoproteins. During infection with HCMV and other herpesviruses, the host environment is heavily modified to generate the various components and organize them along a novel biosynthetic pathway. If any one of the components is absent or mislocalized, the stability of maturing particles is compromised because the scaffold-like assembly of virions requires accurate construction at the preceding stages. As an example, the ability for nascent virions to acquire the lipid envelope is dependent on proper tegumentation.

Secondary envelopment of maturing virions takes place in the cytoplasmic space and only proceeds following successful tegumentation. Similar to replication of HSV-1 and other herpesviruses, the lipid envelope is essential because it carries the necessary glycoproteins and other signaling molecules to initiate infection upon release from the host cell (24, 25). Envelopment is mediated by layers of tegument proteins interacting with cellular lipid membranes in the assembly compartment, either directly through lipid modifications or indirectly via membrane bound proteins (26). Through these interactions, HCMV particles are engulfed by the target membranes and virion maturation is completed

upon membrane scission (27). For the replication cycle to complete, the last remaining stage is virion egress.

In addition to factors required for initiation of infection, membranes used during envelopment define the route of virion egress (28, 29). The lipid composition of co-opted membranes determines which cellular mediators of vesicle trafficking are able to interact and by extension, the direction of transport (23). HCMV influences the route of exocytosis through manipulation of fatty acid (FA) synthesis and resultant shifts in the balance of various lipid moieties in the assembly compartment during infection (30, 31). Likewise, several viral gene products also influence the stability and localization of proteins required for vesicle transport, further driving the process (21, 32, 33). Through this multi-faceted approach, HCMV virions are carried along a pathway that appears to connect Golgi-derived membranes to the plasma membrane (20, 29). Following fusion of the transport vesicle at the plasma membrane, viral particles are released and infection can start anew.

Because secondary envelopment and exocytosis are the last stages required to produce infectious virions, upstream disruptions of replicative processes can manifest as defects in envelopment or export. To increase replication efficiency, HCMV expresses several miRNAs and viral proteins with overlapping functions. Some alter the host cell metabolic profile and internal morphology while others participate in virion construction and recruitment of essential components. This observed functional redundancy is one of the primary cofounding factors to studying HCMV replication.

In this section, we explore the impact of virally induced mechanisms leading to secondary envelopment and egress. Through understanding the cooperative nature of viral and host-derived factors, we seek to outline a progressively more detailed map of

these complex and often interwoven processes critical for virion maturation. Generation of a map of HCMV replication enables identification of critical control points which can then be exploited for the development of novel antiviral treatments.

A. Host-derived compartments as the site of secondary envelopment

Due to the dramatic restructuring of infected cells and the resultant shifts in organelle identity (19), the source of membranes used for the process of envelopment is unclear but correlations can be made using known cellular markers (23). Though it is not strictly necessary, formation of the cytoplasmic virion assembly complex (cVAC) appears to facilitate envelopment of nascent particles (21, 34). Following the cVAC model, nascent particles are enveloped during translocation through a Golgi-derived ring-like structure and upon entrance into the predominantly endosomal-staining central compartment (18, 19, 34). Three-dimensional reconstruction of immune electron micrographs (EMs) from infected human foreskin fibroblasts (HFFs) suggests that envelopment likely occurs in a region coinciding with markers for both the *trans*-Golgi Network (TGN) and various endosome populations as seen in other herpesviruses (19, 35-37).

Through immunofluorescence imaging and immunogold staining of EMs, it was found that membranes targeted for envelopment based on glycoprotein accumulation colocalize with typical Golgi-derived markers (TGN46, mannosidase II, Rab3, syntaxin 5) and endosomal markers (CD63, EEA1, Rab11) but not lysosomal markers in HFFs (17-20, 38-41). Supporting the role of endosomes in herpesvirus replication, HSV-1 or HCMV infected cells labeled with horse radish peroxidase (HRP), a fluid phase marker of uptake and release through the endocytic recycling compartment (ERC), had an accumulation of

HRP in the interstitial space between the lipid bilayers of successfully enveloped particles (42, 43). HRP accumulation is indicative of a change in the net flux of endocytic and exocytic pathways throughout the ERC during infection. Transferrin receptor (TfR) also appears to be sequestered in a perinuclear secretory trap coinciding with markers of the cVAC (20).

Formation of the secretory trap is partly induced by HCMV miRNA-mediated downregulation of recycling activity by targeting host genes involved in ERC trafficking (44), a pattern also seen in Epstein-Barr virus (EBV) and Kaposi's sarcoma-associated herpesvirus (KSHV) (45, 46). Characterization of the HCMV transcriptome late in infection shows a much broader effect with 112 host vesicular trafficking genes being differentially modulated by infection, far more than are targeted by miRNAs alone (44, 47, 48). This activity is multi-faceted because it both blocks innate immune signaling through cytokines such as IL-6 or TNF-α and leads to the perinuclear pooling of virion components, thus contributing to cVAC formation (44, 47, 49).

The immediate-early viral protein pUL37x1 also contributes to altered host morphology and cVAC development by potentiating actin remodeling. pUL37x1 is a multi-function protein responsible for releasing Ca^{2+} stores from the endoplasmic reticulum (ER) before traveling to mitochondria where it inhibits apoptosis (50-52). The Ca^{2+} efflux activates PKCα which remodels actin along with RhoB (53), leading to altered morphology. In addition, the efflux causes the accumulation of large cytoplasmic vesicles approximately 0.5-5 μm in diameter through a process requiring FA synthesis and elongation (50, 51, 54). When pUL37x1 is not expressed, the cVAC is disrupted and there is an buildup of nonenveloped particles in the perinuclear region (51).

It is not enough that the virion structural components are made in sufficient quantities, they must also be spatially organized in the appropriate order. Only through extensive rearrangement of host morphology, are virions efficiently produced. The complex orchestration of viral products and host factors underscores the complexity of understanding virion envelopment.

B. Regulation of envelopment as a function of tegumentation

For envelopment to take place, one of several prerequisite steps that must be completed is tegumentation. The tegument layer of herpesvirus virions provides a scaffold-like interface for membrane-associated viral proteins to adhere to during envelopment. Because of this, alterations in tegument composition can ultimately cause defective envelopment.

As an example, products of the *UL35* ORF have been implicated as having a role in tegument recruitment (55). At early time points, both ppUL35^{A} and ppUL35 localize to the nucleus where they interact with ppUL82 and activate the major IE promoter. At late timepoints, however, the longer form, ppUL35, helps shuttle ppUL82 and pp65 (ppUL83) out of the nucleus as it translocates to the cytoplasm for incorporation into the tegument (55-58). If the UL35 ORF is deleted, nonenveloped capsids accumulate in the cytoplasmic space and infectious output is reduced 10-fold likely due to improper tegument structure and inability to bind lipid recruiting molecules (55).

During infection, the tegument proteins pUL103 and pUL71 also contribute to the process of envelopment (21, 59). pUL103 is required for cVAC biogenesis and efficient release of nascent virions (21, 60, 61). Using the UL103-Stop-F/S deletion mutant or UL103-FKBP destabilization mutant, decreased pUL103 expression correlated with

altered trafficking of pp28 (viral UL99), golgin-97, GM130, and CD63 and decreased plaque size (21, 60). Further imaging shows virions stalled during envelopment or with abnormal structure accumulating in the perinuclear region (21). Because pUL103 has several interacting partners during infection (22), it isn't clear which process leads to the observed phenotypes but it appears to be linked to the two C-terminal ALIX-binding motifs. ALIX-binding motifs are also important in the maturation of other enveloped viruses including during the primary envelopment of EBV (62-64). Alternatively, the defective phenotypes may be linked to pUL103 interacting with pUL71 under normal conditions (22, 65).

pUL71 is a component of mature virions and HCMV infected patients mount a B cell response against it suggesting it may be exposed on virions or it is otherwise released from host cells (58, 66). pUL71 deficient virus causes the aberrant localization of viral proteins in the cVAC and the formation of large Lamp1/CD63 positive multi-vesicular bodies (MVBs) near the cVAC in infected cells (59, 67). Structural analysis of the pUL71 null mutants, TBstop71 and BAD*in*UL71STOP, showed the accumulation of HCMV particles unable to complete envelopment on the cytoplasmic side of MVBs (59, 67). During TBstop71 infection, 26.90% of particles were enveloped and 70.14% were budding compared to 86.64% and 12.95%, respectively, during wild-type infection (68). This behavior can be recapitulated when pUL71 is expressed with a mutated basic leucine zipper (bZIP)-like domain suggesting oligomerization is necessary for pUL71 to function properly (68, 69). Positional homologs of pUL71 are involved in envelopment and are conserved amongst other herpesviruses including pUL51 in HSV-1 (70), UL51 in pseudo-rabies virus (PRV) (71), and GP71 in guinea pig CMV (GPCMV) (72). The

observed phenotypes of pUL71 suggest that it is involved in membrane scission events during envelopment.

Despite being low abundance compared to other virion-associated proteins (58), the outer tegument protein, pp28, is important for envelopment as well (73). After the amino terminus of pp28 is myristoylated, it attaches to target membranes before localizing to the cVAC and forming multimers late in infection (17, 39, 74, 75). When the first 50 residues at the amino terminus of pp28 are mutated, infectious yield is hindered due to aberrant trafficking of pp28 and a corresponding accumulation of nonenveloped particles in the cytoplasm (26, 76). The irregular trafficking of mutated pp28 does not affect the level of other tegument proteins in mature virions suggesting it forms part of the outermost layer of tegument proteins (26). Expression of only the amino-terminus of pp28 was necessary and sufficient for reconstituting infectious output, accumulation of pp28 in mature virions, and proper envelopment (76). Further characterization found the most important sites of the pp28 amino terminus to be the second residue, glycine, which serves as the site of myristoylation (39), amino acids (aa) 26-43 which are responsible for multimerization in the cVAC (75), and aa 37-39 which allow interaction with the cysteine residue at position 250 of the viral protein UL94 (77, 78). The ability of pp28 to be incorporated in maturing virions is also dependent on its interaction with UL94 which serves as a scaffold on the outside of the tegument (77, 78). Without UL94, secondary envelopment and cVAC formation is hindered (79). In HSV-1, KSHV, mouse cytomegalovirus (MCMV), and murine herpesvirus 68 (MHV-68), homologs of pp28 and UL94 play an analogous role but in contrast to HCMV infection, they are not considered essential for virus replication (80-84).

Genes within the HCMV U_L*/b'* region influence maturation through cell-specific mechanisms. Within this region, the *UL133-UL138* (*UL133/8*) locus is nonessential for growth in fibroblasts but required for other cell types (85). Proteins produced by HCMV *UL135* and *UL136* are transcribed as part of *UL133/8* polycistronic mRNAs (86), localize to Golgi membrane structures (87, 88), and are required for latency and virion maturation (86, 88-93). *UL135* and *UL136* ORFs were responsible for the dispersion of cVAC markers and abnormal particle formation when human lung microvascular endothelial cells (HMVECs), but not fibroblasts, were infected with a TB40/E-*UL133-UL138*$_{NULL}$ virus (88-91). Using a TB40/E-*UL135*$_{STOP}$ mutant defective in *UL135* expression to infect HMVECs, only 27% of virions exhibited normal morphology with the remainder being non-infectious enveloped particles (NIEPs) or aberrantly enveloped particles (90). *UL135* mutation also resulted in smaller dense bodies, caused by a 2- to 3-fold decrease in pp65 and pp150 expression, and, furthermore, dense bodies were excluded from MVBs where they normally aggregate with progeny virus in endothelial cells (89, 90). In fibroblasts, the only phenotype of infection with TB40/E-*UL135*$_{STOP}$ was a slight increase in NIEPs relative to wild type (91). Using similar methodology as the *UL135* studies, a TB40/E-*UL136*$_{GalK}$ mutant with a disrupted *UL136* ORF produced aberrantly enveloped virions 65% of the time and dense bodies that were 2.5 times larger on average despite having comparable levels of tegument proteins compared to wild type (90). Of the several different sized proteins encoded by *UL136* splice variants, the 26 kDa and 33 kDa products were shown to be the most important in facilitating normal cVAC biogenesis and particle formation (92, 93). Although specific mechanisms have yet to be determined, HCMV pUL135 appears to direct maturation and envelopment through interactions with

other tegument proteins while *UL136* ORF isoforms are needed for interacting with target membranes. The endothelial-dependent phenotypes exhibited by *UL133/8* locus mutations are a prime example of the manipulative nature of HCMV in distinct host environments.

The herpesvirus tegument serves essential functions during replication and initiation of new infections. During HCMV infection, the diverse, yet overlapping, mechanisms of recruiting lipids demonstrate how important this function is to virion replication. Through their interactions between capsids and envelope-associated glycoproteins, tegument proteins are responsible for bringing together the various biosynthetic pathways and initiating secondary envelopment.

C. Outcomes of envelopment as determined by glycoprotein composition

The variability in cellular tropism of nascent virions from different cell types suggests different maturation events occur leading up to egress. As in other herpesviruses, including GPCMV and rhesus CMV (RhCMV), HCMV glycoprotein composition plays a role in establishing sites of envelopment (94-100). HCMV isolates contain approximately 70 ORFs with predicted features of glycoproteins but only a few have been directly studied (95, 101, 102). The most abundant HCMV glycoproteins are gM (UL100), gN (UL73), gB (UL55), gH (UL75), gL (UL115), gO (UL74), and UL128-131 (58) but most have not been detected in virions suggesting non-structural roles. The gM/gN complex is the most abundant glycoprotein complex in mature HCMV virion envelopes and if either is deleted, the virus is unable to replicate (103).

Similar to EBV (104, 105), gM and gN form a complex (gM/gN) when present in the ER before they can be trafficked to cytoplasmic vesicles and colocalize with other

markers of the cVAC (106, 107). Translocation of HCMV gM to the cVAC occurs when the cytoplasmic region of gM interacts with cellular FIP4, FIP4 binds Rab11, and Rab11 recruits further effector proteins until gM is transported in complex with gN (108). gM and gN also contain other C-terminal endocytic trafficking motifs, including an acidic cluster used for binding cellular transport proteins, such as PACS-1, and a YXXΦ tyrosine motif (109-111). The highly-conserved nature of the C-terminal acidic clusters in herpesvirus glycoproteins suggests a common mechanism for direct transport to the site of virion envelopment using membranes believed to be TGN-derived (112-116). YXXΦ motifs are also conserved across all subfamilies of *Herpesviridae* and allow various envelope proteins to be retrieved from the plasma membrane through interactions with the AP-2 complex leading to clathrin-mediated, dynamin-dependent, endocytosis and accumulation in endosomes or the TGN (98, 117-120).

Cell-to-cell spread during HSV-1 infection is dependent on the UL51 (HCMV pUL71 homolog)/gE (US8) interaction (121, 122), an important mediator of syncytia formation (123, 124), before both are transported to the site of envelopment through use of terminal YXXΦ tyrosine motifs (70, 122, 125-128). When the motif is mutated in pUL51, neither pUL51 nor gE is incorporated into nascent virions and spread is hindered in Hep-2 human epithelial cells but not Vero monkey epithelial cells suggesting cell type dependent mechanisms for spread (122).

In HCMV, the more defined assembly compartment results in greater concentration of envelope proteins compared to other herpesviruses. Inclusion of both the acidic cluster and YXXΦ motifs in most envelope proteins ensures proper localization to the assembly compartment. Neither trafficking pattern is essential for virus production

but they both serve to augment infectious output as seen in HCMV gB, gM/gN, and gpUL132 (109, 119, 129-132), varicella-zoster virus (VZV) gE, gH, and gB (99), HSV-1 gB, pUL51, and gE (98, 122, 133), or PRV gB (134), amongst others. During HSV-1 infection, UL20 helps chaperone gK and gE from the ER to Golgi and without it, neither glycoprotein is incorporated resulting in accumulation of nonenveloped particles and inability to form syncytia (135, 136).

The incorporation of gH/gL complexes into the envelope of nascent virions is another example of maturation events defining HCMV tropism (137-140). HCMV and GPCMV virions require the gH/gL/gO complex for entering fibroblasts by fusion at the plasma membrane and the gH/gL/UL128-131 pentameric complex for entry into epithelial and endothelial cells by pH dependent endocytosis (24, 94, 96, 141). Some laboratory strains are fibroblast-restricted because serial passaging has led to loss of functional UL128-UL131 and a compensatory increase in gH/gL/gO concentration (142-144). The ratio between gH/gL/gO and gH/gL/UL128-131 complexes is determined within the ER prior to transport to Golgi or post-Golgi membranes for use in envelopment (96, 140, 145, 146). After gH and gL interact and stabilize each other in the ER (147), a single gH/gL complex can either form a disulfide bond with gO or a noncovalent bond with UL128-131 but not both (96, 148). During formation of the pentameric complex, UL128, UL130, and UL131 are each capable of binding to gH/gL and help recruit the remaining components of the pentameric complex (96). To a lesser degree, the UL116 glycoprotein also appears to compete for gH binding in the ER but its role is still unknown (149). Only after formation of gH/gL/gO or gH/gL/UL128-131 do the complexes migrate to the Golgi where they mature through glycosylation and become incorporated into virions (96, 145, 150).

Glycoprotein complex formation and incorporation in HCMV infected cells is driven by several viral proteins including US17, UL148, and gO (1, 151, 152). In addition to its immune modulatory role, when the transmembrane protein US17 was deleted, gH was mislocalized and there was a 3-fold decrease in the level of gH found in virions (1).

UL148 is a glycoprotein with a RXR motif that retains it in the ER where it appears to bind and sequester gH/gL/UL130 or gH/gL/UL131 thus reducing the formation and trafficking of completed gH/gL/UL128-131 complexes to the cVAC leading to an enrichment of gH/gL/gO in virions (151). Using the TB40/E deletion strain TB_Δ148, high MOI infections were similar to parent in HFFs but yielded 100x more infectious output in ARPE-19 human retinal pigment epithelial cells (151). The deletion also caused substantially less gH/gL/gO complexes to form (151). Insertion of UL148 into the laboratory strain ADr131 which previously lacked it decreased ARPE-19 tropism four-fold (151). A related tropism effect was seen when comparing B cell-derived to epithelial cell-derived EBV suggesting mechanisms for selecting envelope glycoprotein complexes may be a conserved feature of herpesviruses (147). Positional homologs of HCMV gO exhibit approximately 40% aa similarity on average and are maintained in HHV-6A (U47), HHV-6B (KA8L), HHV-7 (U47), and MCMV (M74) (153, 154). Binding properties of HCMV gO vary in efficiency and are strain dependent (146). When aligning the aa sequences of HCMV gO in 40 clinical and 6 laboratory strains, gO isoforms group into 8 different families with increased diversity between sequences at aa 1-100 of the N-terminus and residues in the 270-340 region (146, 155). While gO isoforms from HCMV strains Towne, TR, Merlin, TB40/E, and AD169 were all able to form disulfide bonds with TR gH/gL in HFFs, virions produced in the presence of Merlin gO incorporated significantly more

gH/gL/UL128-131 than gH/gL/gO as opposed to the other strains in which the ratios were reversed (146). Infecting fibroblasts using strains without gO expression caused accumulation of nonenveloped particles in the cytoplasm and mature virions had increased levels of gH/gL/UL128-131 but 50% less gH/gL overall (143, 152). Interestingly, when HUVECs were infected with a UL131 deletion mutant, an identical phenotype was observed but virions accumulated increased levels of gH/gL/gO instead emphasizing the cell specific pathways and competitive nature of glycoprotein complex selection in virion maturation.

By altering glycoprotein expression during infection, HCMV is able to diversify the spread of infection and avoid complete elimination from infected hosts. On a more basic level than determining cellular tropisms, herpesvirus glycoproteins serve a crucial role as bridges between the lipid membrane and tegument layer, without which, production of infectious particles is severely diminished.

D. Fatty acid metabolism as a driver of envelopment

As part of the process that leads to cVAC formation, envelopment, and egress, HCMV induces significant alterations in the metabolic profile of host cells (156). As opposed to HSV-1 infection which upregulates pyrimidine nucleotide synthesis, HCMV induces a metabolic shift that favors long chain FA synthesis (30, 156-158). By altering the metabolic profile during infection, HCMV upregulates saturated FA, which increase membrane curvature at sites of envelopment. As seen with other enveloped viruses, increased curvature promotes envelopment through concentration of membrane-bound viral proteins and decreased energy cost during membrane budding (159-162).

The first committed step of FA acid synthesis is catalyzed by acetyl-CoA carboxylase (ACC) generating malonyl-CoA from byproducts of glycolysis and the tricarboxylic acid (TCA) cycle (163, 164). Malonyl-CoA is then used as a substrate by cellular acyl-CoA synthetases and elongases to create long chain FA (LCFA; 14-21 C chain) and very long chain FA (VLCFA; 21 < C chain) (163, 164).

Following HCMV infection, uptake of cellular glucose required for glycolysis was increased as a downstream result of the antiviral protein viperin becoming activated (165-167). Cellular ACC levels also increased coincident with HCMV infection. By increasing glucose and ACC, host malonyl-CoA production capacity increases and drives downstream FA synthesis. If this process is blocked as during inhibition of ACC by siRNA or the inhibitor TOFA, virion output decreased by 10-100-fold ostensibly due to loss of FA (157, 158).

In addition to viperin, infected cells also upregulate the plasma membrane-bound low-density lipoprotein related receptor 1 (LRP1) as part of the antiviral response (28). Offsetting the adipogenic outcome of viperin upregulation, LRP1 depletes cellular- and virion-associated cholesterol because of amplified FA synthesis during infection. Inhibition of LRP1 by siRNA or antibody binding was sufficient to increase cholesterol concentration and infectivity of nascent virions (28).

An extensive siRNA screen identified 172 cellular enzymes associated with FA metabolism and adipogenesis as having a role in HCMV replication (30). From the screen, several acyl-CoA synthetases, including ACSM2A, 3-5, ACSBG1-2, ACSL1, 3-6, and SLC27A1-6 plus the ELOVL1-7 family of elongases, were found to be important for HCMV biogenesis (30). Pharmacological inhibition of either set of enzymes caused

reduced viral infectivity with elongase inhibitors delaying expression of viral genes and causing a reduction in overall abundance of the tegument protein pp28 (30). In addition to acyl-CoA synthetases and elongases, class III phosphatidylinositol 3-kinase (Vps34) was also identified in the screen as being required for growth; without it, nonenveloped virions accumulate in the cytoplasm (30, 51).

During HCMV infection, Vps34 and ACC cooperatively form large cytoplasmic vesicles, presumed to be the sites of virion envelopment, and act downstream of the viral protein pUL37x1 in the process of envelopment (51). Through carbon labeling and mass spectrometry, the increased acyl-CoA synthetase, elongase, and Vps34 expression were found to cause an upregulation of saturated VLCFA in the viral envelope due to C18 FA elongation, not *de novo* synthesis (30). Accumulation of VLCFA in defined regions is associated with increased membrane curvature (162, 168-171). The lack of *de novo* synthesis suggested HCMV uses preexisting stores of FAs to generate VLCFA for virion envelopes. The source was later found to be lipid droplets within the host cell (30).

The ability to maintain elevated lipogenesis during HCMV infection is dependent on cleavage of the cellular sterol regulatory element binding protein (SREBP) by SREBP activation protein (SCAP) (172). Under normal conditions, the interaction of SREBP1 and SCAP is inhibited by increased sterol formation but HCMV overrides the failsafe through expression of pUL38 (31, 172). pUL38 removes a repressor of mTOR activity which is sufficient for maintaining cleavage and activation of SREBP1 thereby inducing elongase ELOVL7 and VLCFA is synthesized for use in virion envelopment (31, 173, 174).

E. Completion of envelopment by membrane scission

After maturing virions have initiated the budding process, membrane scission events are required to seal the envelope. In cellular pathways, scission is mediated by dynamin- or endosomal sorting complex required for transport (ESCRT)-dependent mechanisms (175, 176). Dynamin is required for pinching off membranes during inbound trafficking and ESCRT stitches membranes closed as they bud into topologically extracellular vacuoles within cells as seen in MVB formation. While both are used for replication of enveloped viruses (177-179), the propensity for HCMV virions to accumulate in structures resembling MVBs suggests a dependence on ESCRT-mediated pathways (67, 90, 175, 176).

ESCRT machinery is comprised of five main cytoplasmic complexes, ESCRT-0, -I, -II, III, and Vps4-Vta1, and assists in both budding and scission of cellular vesicles through recognition of ubiquitin signals (175, 180-182). There is some conflicting evidence but ESCRT-0, -I, and -II appear to act in parallel, not sequentially, to facilitate budding (175, 180-182). ESCRT-III and Vps4-Vta1 act downstream of the other complexes and control the scission and release events, respectively (175, 176).

Following cVAC formation during HCMV infection, components of the ESCRT machinery are intermingled with Golgi and endosomal markers near sites of envelopment (19, 183). During infection of RPE1 retinal pigment epithelial cells with a GFP labelled variant of AD169, siRNA silencing of Tsg101, a component of ESCRT-I, and Alix, which helps recruit ESCRT-III, did not reduce virion output (184). Conversely, siRNA silencing of Vps4A/B resulted in increased infectious output suggesting ESCRT recruitment was nonessential and, in some cases, inhibitory to virion maturation (184). In a separate

study, HFFs were infected with the HCMV strain Towne followed by transfection with dominant negative (DN) forms of Vps4, Tsg101, and CHMP1, a component of ESCRT-III (183). $CHMP1_{DN}$ and $Vps4_{DN}$ reduced infectious output in contrast to the previous study (183).

Results from both studies combined with other observations suggest that HCMV utilizes ESCRT machinery for membrane budding and scission but may have functional redundancies that allow it to bypass requirements for recruitment of upstream ESCRT complexes (67, 90, 183, 184). For example, HCMV UL103 contains ALIX binding domains so through interactions with other tegument proteins, including membrane associated pUL71, and ALIX, UL103 may be able to recruit ESCRT-III to membranes for envelopment without involving ESCRT-0, -I, or -II (21, 22, 59, 65, 67). Another possible explanation for the discordant results is ESCRT complexes are multi-protein formations so only targeting select proteins may not be enough to abrogate budding and scission. As a potential confounding variable, the studies were conducted in different cell types with strains containing divergent coding potential so the results may indicate nuanced differences in virion maturation.

What is known is that other herpesviruses also utilize ESCRT functions for envelopment which suggests this may be a conserved mechanism for viruses within *Herpesviridae*. HSV-1 and HHV-6 particle envelopment is dependent on MVB formation and HSV-1 utilizes a Vps4-dependent mechanism (185-188), however, it is independent of Tsg101 and ALIX similar to HCMV (189). Alternatively, the observed defects following targeting of ESCRT machinery may be related to events required for entry into cells, as seen during KSHV infection (190-192), or membrane remodeling as seen with EBV (64).

F. Virion egress completes HCMV replication

Following successful envelopment, fully matured virions must be exported out of host cells. For herpesviruses, HCMV in particular, the mechanism of viral egress is poorly understood.

In vesicle-mediated transport, divergent pathways maintain unique lipid and protein signatures because the concentration of various FA moieties in a given region defines membrane physiology and restricts the array of interacting proteins (193-196). By analyzing the lipid composition of mature virions, correlations can be made with known trafficking pathways and exocytic events can be better understood.

To identify potential pathways, liquid chromatography-mass spectrometry (LC-MS) was used analyze the lipidome of HCMV infected fibroblasts by measuring the relative abundance of 146 unique glycerophospholipid (GPL) species with chain lengths of 30-42 carbons (29). Except for a four-fold enrichment of phosphatidic acid (PA) during infection, the cellular GPL profile did not deviate greatly from mock-infected cells (29). The GPL composition of virions, however, was markedly different compared to HCMV- or mock-infected cells and was dominated by phosphatidylcholine (PC) and phosphatidylethanolamine (PE) species (29). When compared to known subcellular compartments, the lipid composition of virion envelopes most closely matched profiles seen in neuronal synaptic vesicle membranes suggesting HCMV particles follow a related secretory vesicle (SV) pathway that operates in non-neuronal cells (29).

Secretion via SVs is dependent on a highly-conserved trafficking pipeline used in cells from diverse lineages including mast cells in the immune system and β cells in the pancreas (197-201). Usage of such a widely available pathway would potentially enable

infection of diverse cell types as seen during HCMV infection. Assuming this is the same pathway HCMV uses, it would dramatically reduce the coding potential required to facilitate release in the functionally disparate group of cell types subject to HCMV infection *in vivo*. Starting at the TGN, SV release is mediated by several factors acting in sequence. Various Rab GTPases, cytoskeletal motors, and SNAP/SNARE complexes associate with the target vesicle and relay it towards the plasma membrane where fusion occurs by a Ca^{2+} dependent mechanism (202-207).

Several proteins involved in SV transport have been implicated in exocytosis of HCMV and other herpesviruses. Rab GTPases control specific vesicle-mediated trafficking events within cells (208, 209). For SV exocytosis, Rab3 and Rab27 work cooperatively to transport and dock vesicles at the plasma membrane prior to fusion (201, 210, 211). Maturing HCMV and HSV-1 virions associate with Rab3 containing membranes following immunogold staining and EM imaging (38, 212). Likewise, infectious output was dramatically reduced in Rab27A deficient cells when infected with HCMV and HSV-1 (33, 213).

Once docked at the plasma membrane, SVs require SNAP/SNARE complexes to mediate fusion. Syntaxin 3 (STX3) is one of several SNARE proteins capable of initiating SV-plasma membrane fusion events (214). During HCMV infection, STX3 expression is highly upregulated and localizes to the cVAC. When knocked down using shRNA, production of infectious material was reduced four-fold (32). In neurons, SNAP25 is the major SNAP protein involved in SNAP/SNARE-mediated SV exocytosis (204, 207). In other cell types including fibroblasts, SNAP23, a homolog of SNAP25, is more widely

used for exocytic events. SNAP23 abundance was unaffected by HCMV infection but shRNA knockdown of SNAP23 decreased infectious output 1,000-fold (29).

There are several lines of evidence that predict HCMV uses a SV-like pathway for final egress but it is noteworthy that inhibition of key proteins was not sufficient to completely eliminate HCMV egress. This suggests either there are alternative pathways for virion egress or the SV pathway may only be important for one aspect of virion replication not necessarily specific to egress. For example, despite correlations with a SV pathway, HSV-1 and PRV infectious particles in neurons associate with and are released via a Rab6A/Rab8A/Rab11A-dependent pathway as opposed to Rab3A/Rab27A-staining vesicles (212, 215-217). The difference in HSV-1 and PRV function may a result of increased cellular dependence for Rab3A/Rab27A pathways during maintenance of homeostasis compared to other cell types.

III. This Work

Complications from HCMV infection place a high burden on society due to their frequency and severity. An effective vaccine has yet to be developed and current treatments are limited in target diversity due to a lack of understanding of HCMV replicative processes. By exploring the cellular-associated aspects of HCMV envelopment and egress, we aim to build a map of maturing HCMV virions as they traverse the cytoplasmic assembly compartment.

To accomplish this, I will first describe the structure and function of a novel HCMV transduction vector, TB40/E/Cre, for use in studying various genes of interest in the context of infection. Through demonstration of its growth properties, we were able to make preliminary observations relating HCMV genome length to replicative efficiency in

fibroblasts. Using various protein tags, we also show the utility of expressing genes from TB40/E/Cre. The flexibility of TB40/E/Cre allows it to be adapted to a wide range of experiments such as studying cellular trafficking pathways.

Next, I transition into our current model of pathways involved in HCMV assembly and egress. By analyzing previously generated microarray data (1), we were able to identify clusters of cellular transcripts significantly altered over the course of infection that have defined roles in host vesicle mediated transport. By mapping the transcriptional data onto known pathways, we establish a model for which transport events are favored during HCMV virion maturation.

Lastly, I will summarize the contributions made to herpesvirus biology as part of this work. Inherent to that is the current state of knowledge and the potential for future directions. Through our work, we have developed various tools and models that will continue to benefit researchers going forward. By applying these concepts to HCMV replication, we have generated a road map of HCMV maturation as virions navigate through host compartments.

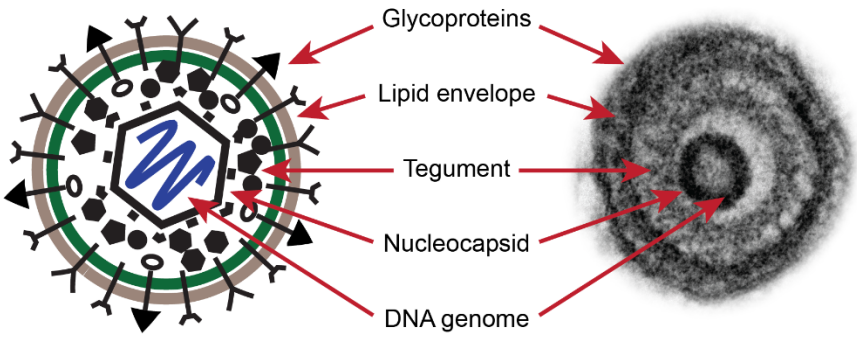

Fig. 1.1. Structure of an HCMV virion. An artist representation and an electron micrograph image of an HCMV virion are shown with the corresponding layers.

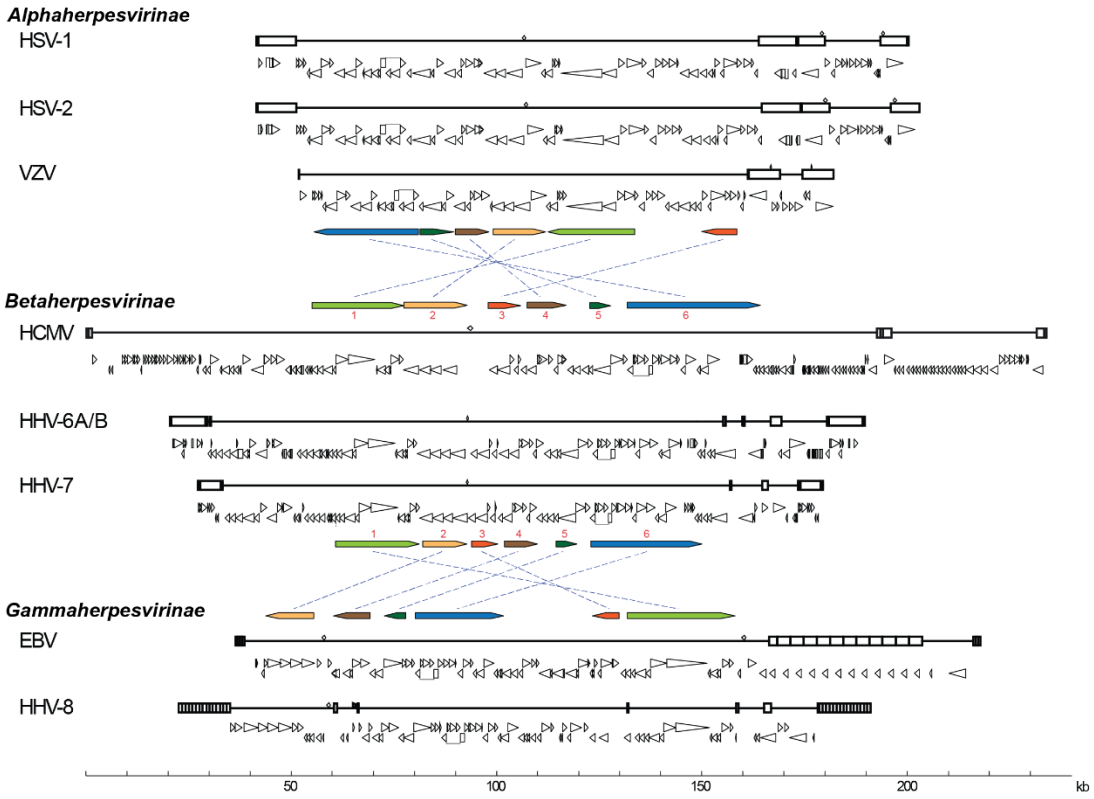

Fig. 1.2. Comparative alignment of herpesvirus genomes demonstrates conserved regions and strain-specific differences. Small triangles depict virally encoded open reading frames (ORFs), boxes represent repeat regions, and colored boxes denote conserved gene blocks. Abbreviations: herpes simplex virus 1 (HSV-1), herpes simplex virus 2 (HSV-2), varicella zoster virus (VZV), human cytomegalovirus (HCMV), human herpesvirus 7 (HHV-7), Epstein-Barr virus (EBV), human herpesvirus 8 (HHV-8)

Figure adapted, with permission, from P.E. Pellett and B. Roizman, Fields Virology, 6th ed., 2013, p 1802-1822

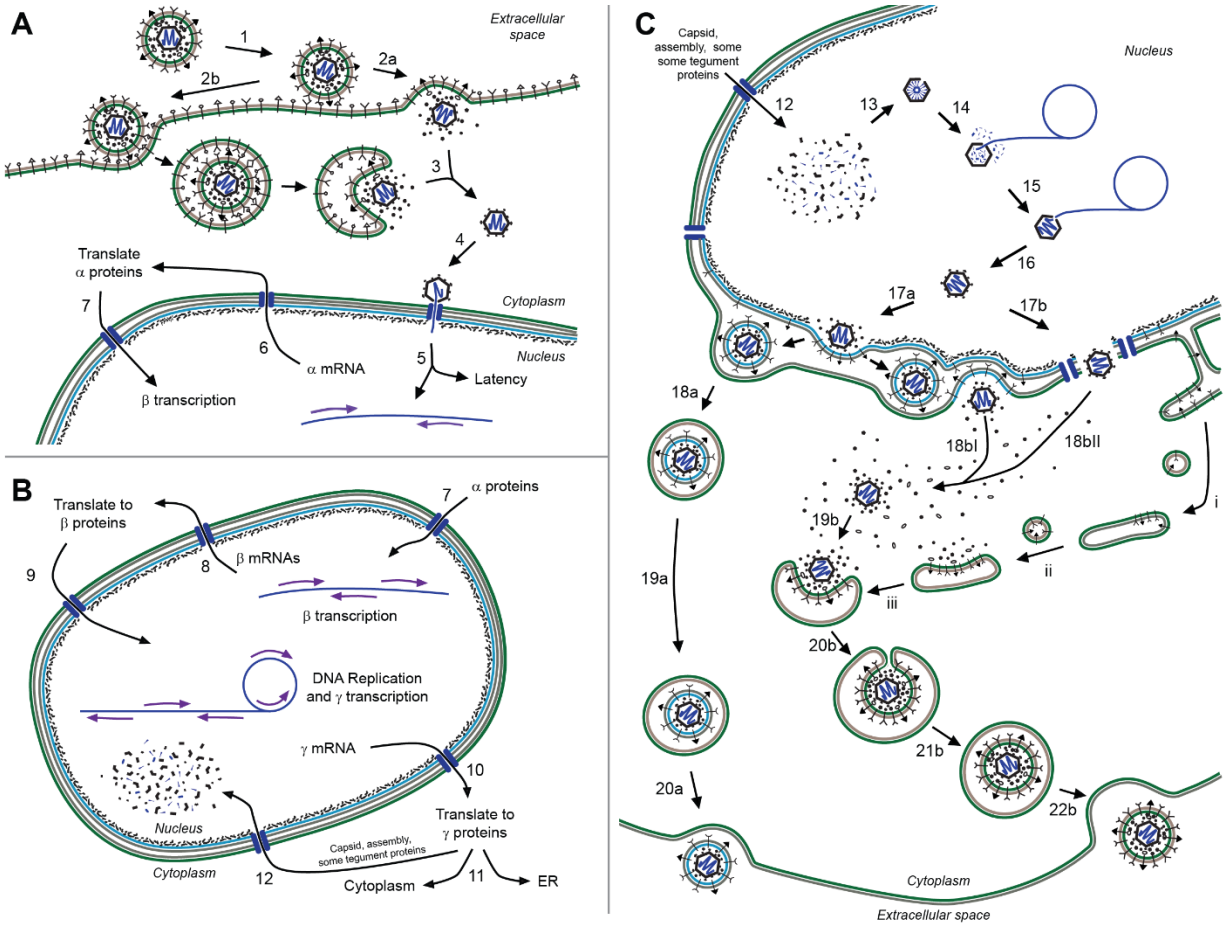

Fig. 1.3. General replication cycle of herpesviruses. (A) Adherence, entry, and initiation of infection. Extracellular virions adhere to target host cells; the capsid and tegument are released following fusion at the plasma membrane or within endocytic vesicles; the viral genome is delivered to the nucleus and immediate early (IE, α) transcripts are expressed or latency is induced. (B) Early (E, β) protein expression leads to DNA replication of the viral genome and late (L, γ) gene expression. (C) Herpesvirus assembly. Structural L proteins assemble into the capsid prior to genome packaging and nuclear export. Viruses follow two general pathways: a) capsids associate with nuclear tegument proteins and bud through the nuclear membrane, thereby becoming enveloped, before final exocytosis or b) capsids are exported to the cytoplasm where they acquire the tegument and host-derived envelope prior to being exported from host cells.

Figure adapted, with permission, from P.E. Pellett and B. Roizman, Fields Virology, 6th ed., 2013, p 1802-1822

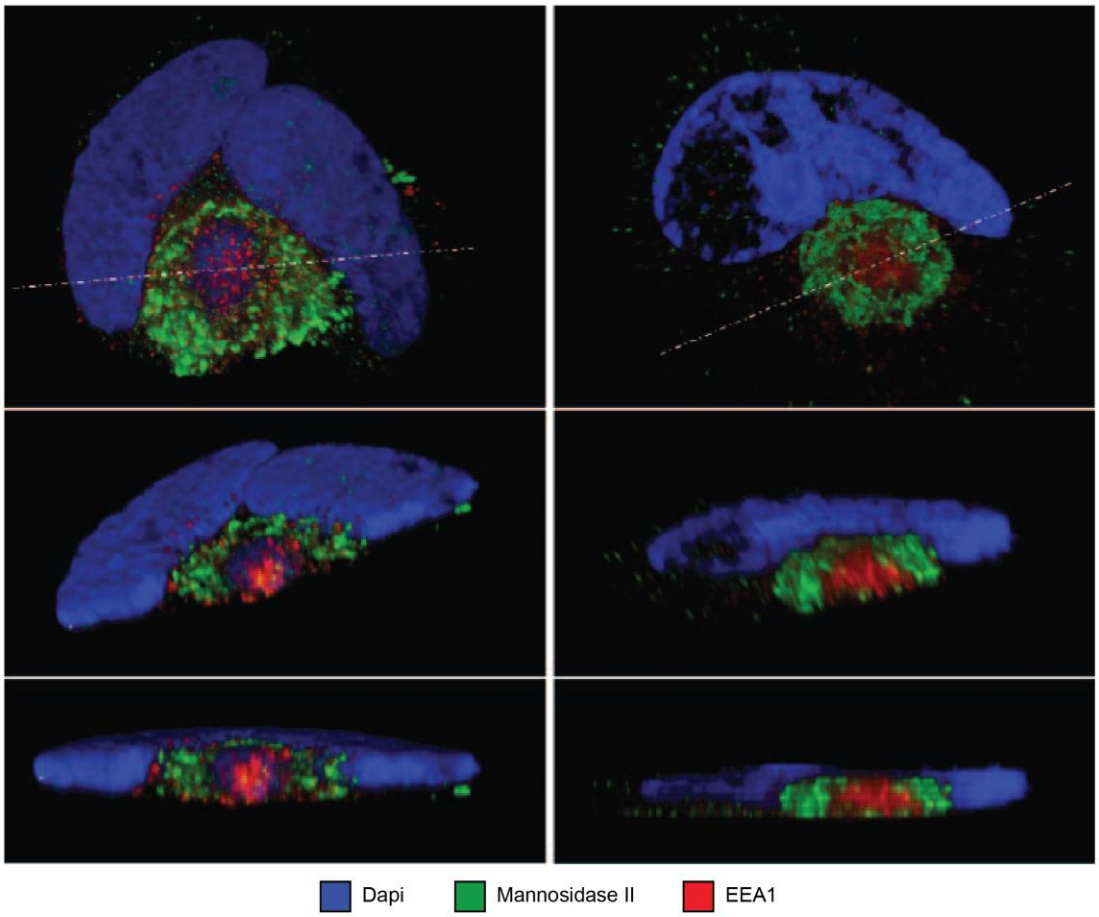

Adapted, with permission, from S Das *et al.*, Journal of Virology, Nov. 2007, p. 11861-11869

Fig. 1.4. Three-dimensional structure of the HCMV cytoplasmic virion assembly complex (cVAC). Immunofluorescence imaging shows the characteristic reniform nuclei (DAPI) surrounding the ring-like Golgi structure (mannosidase II) with endosome populations at the center (EEA1)

CHAPTER 2: GENERATION OF A NOVEL HUMAN CYTOMEGALOVIRUS BACTERIAL ARTIFICIAL CHROMOSOME, TB40/E/CRE, TAILORED FOR TRANSDUCTION OF EXOGENOUS SEQUENCES

I. Abstract

The study of herpesviruses, including human cytomegalovirus (HCMV), is complicated by viral genome complexity and inefficient methods for genetic manipulation in tissue culture. To facilitate reverse genetics of herpesvirus genomes, isolates have been adapted to grow in *E. coli* as bacterial artificial chromosomes (BACs). Through BAC adaption, viral genomes are easily manipulated using bacterial recombinational systems.

Strict herpesvirus genome packaging requirements require deletion of viral genes for inclusion of the *E. coli* mini-F propagation sequence. Contextual classification of deleted regions as nonessential for growth reduces biological significance due to loss of potentially important uncharacterized functions. To avoid deleting viral genes, several BACs utilize a Cre/LoxP system to self-excise the mini-F sequence upon reconstitution of virus in tissue culture.

Here, we describe the adaptation of Cre/LoxP to modify the mini-F sequence of the HCMV BAC, TB40/E, thus generating a new self-excisable BAC, TB40/E/Cre. By excising the *E. coli* propagation sequence, an approximately 2.7 kbp genome length deficit is created due to a preexisting deletion within the *US2-US6* coding region. We exploit this deficit to incorporate genes of interest fused to an FKBP destabilization domain thereby creating a novel gene transduction system for studying exogenous proteins during HCMV infection. Using TB40/E/Cre, we found genome length-associated differences in growth and demonstrated its utility as a transduction system by significantly regulating the accumulation of an exogenously expressed cellular protein within 2 h.

Because of its flexibility, TB40/E/Cre is a powerful tool that can be adapted to study HCMV replication in a variety of contexts. The work presented in this chapter has been submitted for publication pending review.

II. Introduction

Human cytomegalovirus (HCMV) is a double-stranded DNA virus belonging to the family *Herpesviridae*. HCMV is abundant in the population but only causes minor illness in children and adults with functionally mature immune systems. For those with naïve or compromised immune systems, such as developing fetuses, AIDS patients, or transplant recipients, HCMV infection is associated with several manifestations including hearing loss, gastric ulcers, blindness, liver failure, and encephalitis (9, 218, 219). HCMV is also the leading infectious cause of congenital birth defects and the major non-genetic cause of early-life hearing loss (220, 221). Despite its associated public health impact, HCMV replication is poorly understood when compared to viruses such as HIV and Hepatitis C (222-224). The complexity of herpesvirus genomes greatly contributes to the difficulty of studying their replication. Herpesvirus genomes are 130-240 kbp in size with some containing invertible unique short (US) and unique long (UL) regions (225). HCMV contains the largest known herpesvirus genome at 230-240 kbp which encodes at least 200 protein open reading frames (ORFs) and 14 miRNAs (48, 101, 144, 226, 227). While reverse genetics facilitates the exploration of viral gene function, systems for genetic manipulation of herpes genomes in mammalian cell culture are difficult, time-consuming, and inefficient (228, 229).

Bacterial artificial chromosomes (BACs) allow the high-fidelity propagation of sequences of up to 300 kbp in *Escherichia coli* (*E. coli*) (230, 231). Strains of several

HCMV isolates have been adapted as BACs allowing the use of bacterial systems for mutation of viral sequences before reconstitution and functional analysis of virus in mammalian cells (232-236). New BACs are generated by infecting mammalian cells with viral isolates in the presence of constructs containing a selectable *E. coli* mini-F propagation sequence flanked by viral targeting sequences (234, 237-240). Host-mediated homologous recombination between the HCMV genome and viral targeting sequences leads to the incorporation of the mini-F sequence into the HCMV genome. Following selection (236, 239), recombined genomes are purified and transformed into *E. coli* where they replicate as plasmids and can be further manipulated by recombinational processes (235, 241, 242).

Similar to some classes of tailed bacteriophage, herpesviruses have strict genome length packaging restrictions (225, 243). Because of this, generation of new HCMV BACs has relied on deletion of sufficient viral sequences to accommodate the *E. coli* mini-F sequence (85, 234, 244, 245). In the HCMV BAC strains TR-BAC (TR) and TB40/E BAC clone 4 (TB40/E), the mini-F sequence is substituted into the *US2-US6* locus and is maintained in the viral genome after virus reconstitution in mammalian cells (85, 244). This poses two major problems: i) intentional deletion of *US2-US6* or other viral coding regions assumes the genes are nonessential, a term which is contextually defined by the experiment and ii) the *E. coli* mini-F sequence insertion is generally larger than the region being replaced thereby increasing genome length and potentially interfering with herpesvirus packaging.

Under normal conditions, rolling-circle replication of herpesvirus genomes produces viral genome concatemers (225, 246-248). Viral genomes are inserted into

capsids by the viral terminase complex and an ATP-dependent mechanism until the capsid has reached a structurally defined capacity (249). After passing the capacity threshold, a conformational signal is initiated and terminase subunits cleave the concatemers at designated *pac* sites found within the US and UL inverted terminal repeat regions (225, 249-254). The result is a rigid highly pressurized capsid containing one full complement of the herpesvirus genome (225, 255, 256). If the genome is too short, nascent particles are less infectious possibly due to loss of important genes or a decrease in internal pressure required for injection of the genome into host nuclei upon infection. If the genome is too long, the physiological capacity of the capsid is exceeded and incomplete genomes are packaged or spontaneous deletions are used to compensate. As an example, reconstitution and production of infectious guinea pig cytomegalovirus (GPCMV) virions was reduced when the 233 kbp genome length was decreased by more than 6.5% following deletion of nonessential genes or increased by 3.8% following insertion of an 8.8 kbp *E. coli* mini-F sequence (257). Insertion of the *E. coli* propagation sequence was also correlated with deletion of several-kbp-long regions elsewhere in the genome (257, 258). Likewise, sequence analysis of TR found deletions from *US9-US16* and analysis of TB40/E found spontaneous excision of the remaining portion of *US2* through *US9*, including the *E. coli* mini-F sequence (259). These observations are consistent with genome size being important for production of nascent virus.

Alternatively, other herpesvirus BACs utilize a Cre/Lox system for excision of the *E. coli* propagation sequence following reintroduction to mammalian cells (238, 258, 260, 261). *E. coli* mini-F sequence excision avoids maintenance of length increases in reconstituted virus and mitigates the need for spontaneous mutation as evidenced by the

absence of large-scale deletions in the Cre/Lox-containing Merlin-BAC (Merlin) compared to TR or TB40/E (238, 259). In self-excisable BACs, such as Merlin or the AD169 adapted strain, pAD/Cre, a copy of the Cre recombinase gene containing a synthetic intron (inCre) is inserted adjacent to the *E. coli* mini-F sequence and both are flanked by LoxP sites (239, 262). In bacterial culture, inCre remains inactive but introduction to mammalian cells causes splicing and activation of inCre leading to excision of the *E. coli* propagation sequence (261).

To address the problem of studying genes of interest during infection, we adapted the Cre/Lox system to generate a novel TB40/E-derived self-excisable HCMV BAC, TB40/E/Cre, for the transduction of exogenous sequences. TB40/E was chosen as a template based on preserved endothelial and epithelial cell tropisms compared to other HCMV laboratory strains (85, 244). Relative to a virus with an intact *US2-US6* region, an approximately 2.7 kbp genome length deficit is created following BAC excision. We use the resultant genome length availability to transduce proteins of interest. This new construct: i) alleviates length-associated selective pressures (259), ii) removes the need for deletion of other viral sequences (245, 263), and iii) maintains comparability to previous studies. As a demonstration of its utility, we use TB40/E/Cre to express the cellular trafficking protein Rab3A tagged with the ECFP fluorescent protein and FKBP destabilization domain (264). In this study, we show the power of the TB40/E/Cre transduction system through the controlled accumulation and visualization of Rab3A within the HCMV assembly compartment. In addition to its use as a vector, we used TB40/E/Cre to conduct a preliminary study directly relating HCMV genome size to growth in tissue culture. HCMV strains with genome lengths most similar to wild-type (WT)

isolates had modest growth advantages compared to strains containing extraneous insertions. The ability to adapt TB40/E/Cre for use in various experimental contexts makes it a powerful tool for understanding critical components of HCMV replication and herpesvirus biology as a whole.

III. Materials and Methods

A. Cells and virus.

HCMV strain TB40/E BAC clone 4 was generously provided by Christian Sinzger (University of Tubingen, Germany) and strain pAD/Cre was kindly provided by Dong Yu (Washington University, St. Louis, MO) (239, 244). Viruses were grown in low-passage-number pooled human foreskin fibroblasts (HFFs) in complete Dulbecco's modified Eagle medium (DMEM; Hyclone, Logan, UT; catalog no. SH30243.01) supplemented with 1% nonessential amino acids (Hyclone, Logan, UT; catalog no. SH30238.01), 1% GlutaMax (Gibco, Gaithersburg, MD; catalog no. 35050-061), and 5-10% fetal bovine serum (FBS; Atlanta Biologicals, Atlanta, GA; catalog no. S11150). Virus was titrated by standard plaque assay in HFFs.

BAC recombineering was done in the *Escherichia coli* (*E. coli*) strains SW102 and SW105, provided by Donald L. Court (National Cancer Institute, Bethesda, MD) (235). SW102 contains a heat-inducible lambda phage Red recombinase gene and is unable to utilize galactose due to a *galK* deletion. SW105 also contains temperature-sensitive Red recombinase and *galK* deletion in addition to a gene for arabinose-inducible flippase.

B. Electrocompetency and recombinase induction.

E. coli strain overnights were grown in Luria broth (LB) with appropriate antibiotic selection on a 32°C shaking incubator. The next day, a 1/50 dilution of the culture was

made in antibiotic-LB until an OD_{600} of 0.5-0.7 was reached. Cells were spun down at 4°C at 4,500 x g for 5 min and washed three times with ice cold sterile deionized water (diH_2O) or 10% glycerol in diH_2O before being resuspended in a minimal amount of cold diH_2O or glycerol solution and aliquoted into separate tubes for electroporation or storage at -80°C. To induce recombinase expression, SW102 and SW105 cells were transferred to a shaking 42°C water bath for 15 min after reaching the appropriate OD_{600} and before pelleting in the cooled centrifuge. Following heat shock, the normal protocol was resumed. If frozen, induced cells were used within 48 h. Uninduced cells were used as a control for transformation and recombination efficiency.

C. Construction of recombinant viruses.

Recombineering of HCMV BACs was done as previously described (21, 235). In brief, competent *E. coli* SW102/SW105 cells were electroporated with BAC DNA and selected for by growth on chloramphenicol (Cam)-LB plates. Fragments with a *galK/kan*^{r} selection cassette were PCR amplified from pYD-C630 (provided by Dong Yu) with primers containing 50 bp of overhang homologous for the desired region of insertion into the BAC (Table 2.1, Fig. 2.1 and 2.6). The *galK/kan*^{r} containing amplicons were electroporated into competent and Red recombinase-induced *E. coli* SW102/SW105 cells before plating on kanamycin (Kan)/Cam-GalK indicator plates (MacConkey agar base with 5% D-galactose) for positive selection and screening of colonies. Following incubation at 32°C for two days, colonies were selected based on growth, indicating incorporation of selection cassette into the BAC, and screened based on acid production denoting galactose utilization. Colonies were restreaked onto a second Kan/Cam-GalK indicator plate and grown overnight at 32°C. Following isolation of BAC DNA from

candidate clones, selection cassette insertion was verified by PCR amplification across cloning site junctions and size determination using 0.8% agarose gels in TBE buffer (89 mM Tris [pH7.6], 89 mM boric acid, 2 mM EDTA). Then, fragments containing desired coding sequences were PCR amplified using primers with 50 bp of overhang homologous to those used for insertion of the selection cassette (Table 2.1). These fragments were electroporated into the previously verified *galK/kan*^{r}-containing clones following induction of the Red recombinase and cultures were grown for 4 h on a 32°C shaking incubator prior. Outgrowths were washed 2x with 1x M9 salts, plated on media containing 2-deoxygalactose (2-DOG; Acros Organics, Geel, Belgium; catalog no. 111970050; 1.5 % agar, 1x M63, 0.2 % glycerol, 15 µg/ml Cam, 1 mM $MgSO_4$, 0.2 % 2-DOG, 1 µg/ml biotin, and 45 µg/ml leucine), a bacteriostatic galactose analog, and *galK/kan*^{r}-containing transformants were negatively selected. After growth at 32°C for five days, colonies were streaked for isolation on Cam-GalK plates and grown overnight at 32°C. DNA was isolated from individual colonies, inserts were PCR verified as before, and amplicons were sent in for Sanger sequencing (Genewiz, South Plainfield, NJ). Isolated BAC DNA was also restriction digested and proper band patterns were verified for each clone (see corresponding section below). Following verification, the process was repeated as needed. For the induction of flippase in SW105 cells, 0.1% L-arabinose was added to SW105 cultures in LB and incubated while shaking at 32°C for 1 h. Cells were diluted 1:10 and incubation was resumed for 4-5 h. Cultures were then washed 2x with 1x M9 salts and plated on Cam-GalK indicator plates before incubation overnight at 32°C. Following completion of recombineering, large volume BAC DNA preps were made. For reconstitution of virus, 2 µg of DNA were transfected into 80% confluent HFFs in a T25

(4.4 x 10^4 cells/cm^2) using Lipofectamine 2000 (ThermoFisher, Waltham, MA; catalog no. 11668027) and cells were grown in 10% FBS media until 100% cytopathic effects (CPE) were observed. Infections were harvested and stocks were made for storage at -80°C until use. Construction schematics are shown in Fig. 2.1 and 2.6; the primers are listed in Table 2.1.

D. Restriction endonuclease analysis of BAC and reconstituted virus DNA.

Before transfection BAC DNA samples were purified from SW102 overnights using a Plasmid Midi Kit (Qiagen, Valencia, CA; catalog no. 12143). For reconstituted viruses, T175 flasks of HFFs were transfected with 2 µg of BAC DNA using Lipofectamine 2000 and grown until 100% CPE were evident. Flask contents were scraped, sonicated, and spun at 3,000 x g for 5 min. The supernatant was then layered onto a 20% sorbitol cushion and spun at 100,000 x g for 1 h at 4°C. The virus-containing pellet was resuspended in TNE buffer (10 mM Tris, 1 mM EDTA, 0.1 M NaCl, pH 7.4), treated with DNase I (Promega, Madison, WI; catalog no. M6101), and DNA was isolated using a Blood and Cell Culture DNA Mini Kit (Qiagen, Valencia, CA; catalog no. 13323). Equivalent levels of BAC DNA from before transfection and after transfection were digested using HindIII-HF and EcoRI-HF (New England Biolabs, Ipswich, MA; catalog nos. R3104T and R3101T) for 1 h at 37°C and separated overnight using a large format 0.5% agarose gel in TBE buffer.

E. Virus growth curves.

HFFs were seeded at 1.67 x 10^5 cells per well in 12-well plates with 10% FBS media. The following day, plates were infected at a multiplicity of infection (MOI) of 0.01 or 1.0 in 10% FBS media, incubated for 1-2 h at 37°C, washed with PBS (HyClone, Logan,

UT; catalog no. SH30028.02), and replenished with clean 10% media. Plates were incubated until noted time points at which time they were taken out and processed. For extracellular samples, supernatants were removed and clarified by centrifugation at 1,500 x g and 4°C for 2 min. For intracellular samples, remaining cells were washed once with PBS, fresh 10% FBS media was added, cells were scraped, transferred to a tube, and then sonicated. Following sonication, the samples were spun as before and the pellets were discarded. Virus titers were measured by plaque assay in 24-well plates.

F. Virus genome abundance.

Intracellular and extracellular samples from the viral growth curves were treated with DNase I (Promega, Madison, WI; catalog no. M6101) for 30 min at 37°C prior to DNA isolation using a QIAamp MinElute Virus Spin Kit (Qiagen, Valencia, CA; catalog no. 57704). Samples were assayed by quantitative PCR (qPCR) using iTaq Universal SYBR Green Supermix (Bio-Rad, Hercules, CA; catalog no. 1725121), primers targeting HCMV *UL83*, and 40 cycles on a 7500 Real-Time PCR System (Applied Biosystems, Foster City, CA; catalog no. 4351105). Relative abundance was normalized relative to the TB40/E day 3 sample in each set using the $2^{-\Delta C'T}$ method (3).

G. Immunoblots.

HFFs were grown to confluency and infected with HCMV strains at an MOI of 0.1 or 1.0 in 10% FBS media. Following 1-2 h incubation at 37°C, cells were washed once with PBS, and clean 10% FBS media was added. For Shield-1 experiments, Shield-1 (Cheminpharma, Farmington, CT; catalog no. CIP-AS1) was added to a final concentration of 1 µM at the desired times. At 96 hours post infection (hpi), cells were washed with PBS and lysed using RIPA buffer (0.1 M HEPES [pH 7.4], 0.1% sodium

deoxycholate, 150 mM NaCl, 1% NP-40, 0.1% SDS, and 1x EDTA-free protease inhibitors [Roche, Basel, Switzerland; catalog no. 11836170001]). Lysates were passed through a 27-gauge needle and centrifuged at 14,000 x g and 4°C for 10 min. Protein-containing supernatants were collected for analysis. Protein concentrations were calculated using a bicinchoninic acid (BCA) kit (ThermoFisher, Waltham, MA; catalog no. 23227). Equal amounts of protein were added to 10x sample buffer (65% sucrose, 1% Tris-HCl [pH 7.4], 10 mM EDTA, and 0.3% bromophenol blue) with 5% 2-mercaptoethanol, incubated for 7 min at 100°C, and separated in 12% SDS-polyacrylamide gels before being transferred to nitrocellulose membrane (GE Healthcare, New York, NY; catalog no. 10600007). Membranes were probed with primary antibodies (see Table 2.2) and HRP-conjugated goat anti-mouse/rabbit IgG secondary antibodies (Table 2.2; ThermoFisher, Waltham, MA). Reactive proteins were visualized by reaction with Supersignal West Pico Chemiluminescent substrate (ThermoFisher, Waltham, MA; catalog no. 34080) and exposure to autoradiography film (MIDSCI, St. Louis, MO; catalog no. BX810). Relative protein levels were determined using densitometry and FIJI imaging software (265).

H. Immunofluorescence assays (IFA).

Eight-well chamber slides (LabTek, Nunc, Rochester, NY; catalog no. 177-402) were coated with 0.2% gelatin phosphate buffered saline (PBS) solution for 1 h at 37°C. Following splitting and resuspension in 5% FBS media, HFF were seeded at 2.64 x 10^4 per well and incubated at 37°C. The following day, cells were infected at a multiplicity of infection (MOI) of 0.1 in 5% FBS media and incubated at 37°C for 1-2 h. Cells were washed once with warmed PBS before addition of clean 5% FBS media and continued

incubation for 96 h. For Shield-1 experiments, the compound was added to a final concentration of 1 µM at desired times. At 96 hpi, cells were fixed for 15 min using 4% paraformaldehyde in PBS at pH 7.4 and autofluorescence was quenched by exposing cells to 50 mM ammonium chloride in PBS for 15 min. Cells were then permeabilized for 15-20 min by exposure to 0.2% Triton X-100 in blocking buffer (5% glycine, 10% normal goat serum, and 0.1% sodium azide in PBS) before incubation with blocking buffer for 1 h. Primary antibodies were diluted in blocking buffer before addition to the slide for 1 h at 25°C. Slides were washed three times in PBS prior to incubation with secondary antibodies (Table 2.2) for 1 h at 25°C. Following another series of PBS washes, slides were mounted with Vectashield containing DAPI (4',6-diamidino-2-phenylindole; Vector Laboratories Inc., CA; catalog no. H-1200) and then sealed. Imaging was done using a Nikon Eclipse E800 epi-fluorescence microscope system equipped with a 1.4 MP monochromatic CoolSNAP ES^2 CCD camera (Photometrics, Tucson, AZ) and MetaMorph software (Molecular Devices, LLC., Sunnyvale, CA). False coloring of images was done using FIJI (265).

IV. Results

A. Generation of TB40/E derived strains.

Our primary goal was to develop an HCMV BAC capable of accommodating exogenous sequences to be used to manipulate cellular processes in infected cells. To avoid genome size packaging restrictions without deleting viral sequences, we modified the original TB40/E BAC by making the *E. coli* propagation sequence self-excisable. To accomplish this, we modelled our new BAC, TB40/E/Cre, after the HCMV AD169-derived BAC strain, pAD/Cre (239).

Adaptation of the TB40/E *E. coli* propagation sequence required the incorporation of Cre recombinase, a pair of associated LoxP cleavage sites, and an accessory linker region (LR) (Fig. 2.1). BAC recombineering was used to systematically construct the new BAC through alternating cycles of positive and negative selection using a *galK/kan*^{r} selection cassette and homologous recombination (235). The selection cassette was cloned from the plasmid pYD-C630 and initially targeted to the junction of the truncated *US2* (trUS2) open reading frame (ORF) and adjacent *E. coli* mini-F sequence. Following successful rounds of transformation and recombination in *E. coli* SW102 cells, TB40/E US2 GalK/Kan^r (TB40/E GalK/Kan^r) was generated (BAC 2, Fig. 2.1). An upstream LoxP fragment was then generated using overlapping primer pairs and inserted in place of the selection cassette using a similar method as before (BAC 3, Fig. 2.1). The process was repeated and a fragment containing the LR and CMV major immediate early (MIE) enhancer (MIE$_{Enh}$) was inserted following amplification from the plasmid pECFP-C1 Rab11A (BAC 5, Fig. 2.1). The LR is a 50 bp region of innocuous sequence directly upstream of the MIE$_{Enh}$ without any significant degree of homology to known HCMV sequences. It assists in targeting of amplicons during homologous recombination and mitigates issues related to recombination of the LoxP sites during sequence insertion or deletion. Next, the downstream LoxP site was cloned from pAD/Cre as part of a fragment that included a SV40 promoter (SV40$_P$)-driven *cre* gene. The presence of a synthetic intron interrupting *cre* prevents proper expression of Cre until after transfection into mammalian cells (262). After insertion of another selection cassette, the SV40$_P$/*cre*-LoxP fragment was inserted while oriented downstream of the *E. coli* mini-F sequence so both *cre* and the *E. coli* propagation sequence would be within the bounds of the LoxP

cleavage sites (BAC 7, Fig. 2.1). Finally, the *galK/kan*^{r} selection cassette was inserted to remove the MIE_{Enh} and then subsequently deleted thus generating TB40/E/Cre GalK/Kan^r and TB40/E/Cre, respectively (BAC 8 and 9, Fig. 2.1). Proper insertion of the various fragments was confirmed at each step by PCR amplification and sequencing of junctions, as well as by assessing the overall integrity of the constructs by restriction endonuclease digestion of the whole BAC plasmid (data not shown).

To verify the proper excision of the *E. coli* propagation sequence following recombineering and reconstitution in mammalian cells, restriction mapping of TB40/E/Cre was compared to TB40/E, TB40/E GalK/Kan^r, and TB40/E/Cre GalK/Kan^r both before and after transfection (Fig. 2.2). By monitoring the presence or absence of predicted bands, strain specific differences can be observed including whether the *E. coli* mini-F sequence is maintained. Following HindIII digestion of TB40/E/Cre and TB40/E/Cre GalK/Kan^r, a fragment is present at 6.8 kbp before transfection but is absent after transfection. The missing band corresponds to the altered *E. coli* mini-F sequence and its absence shows the system is functional. Similarly, when digested with EcoRI, a 2.0 kbp band in the TB40/E and TB40/E GalK/Kan^r lanes, regardless of state, indicates the unaltered *E. coli* mini-F sequence whereas a band at 7.1 kbp in the TB40/E/Cre and TB40/E/Cre GalK/Kan^r lanes before transfection indicates the modified *E. coli* mini-F sequence. A 5.9 kbp fragment present in all four BACs is absent in the TB40/E/Cre and TB40/E/Cre GalK/Kan^r reconstituted viruses, demonstrating successful excision of the *E. coli* propagation sequence.

Based on our methods of verification, the newly derived BAC plasmids were able to excise the *E. coli* propagation sequence upon virus reconstitution in mammalian cells.

B. Growth of TB40/E/Cre and the effects of genome length.

To examine the relationship between genome length and virion maturation, we compared growth of TB40/E, TB40/E GalK/Kan^r, TB40/E/Cre, and TB40/E/Cre GalK/Kan^r as a function of genome length. Wildtype isolates of HCMV have genome lengths ranging from ~230-240 kbp. Differences in length can generally be attributed to a mixture of gene duplications and deletions depending on the strain. Even within certain isolates, population heterogeneity can contribute to the observed variation in genome length (244). For TB40/E, the viral encoding region of the genome is approximately 229 kbp in addition to the 7.5 kbp *E. coli* propagation sequence. The 1-10 kbp difference in viral coding capacity of TB40/E relative to directly sequenced isolates is partly due to loss of *IRS1-US1*, part of *US2*, all of *US3-US6*, and other mutations which may have resulted from the initial adaptation of TB40/E as a BAC (244). Because the sequence for the original TB40/E clinical isolate is unavailable, we are unable to determine which mutations were directly caused by BAC generation. Therefore, for the purpose of our study, we compared the lengths of TB40/E and TB40/E/Cre derivatives relative to an approximately 232 kbp long hypothetical pseudo-wildtype TB40/E sequence (pwTB40/E) consisting of the noted 229 kbp TB40/E viral sequence with a reconstituted *US2-US6* region in place of the *E. coli* mini-F sequence (Fig. 2.3). Using pwTB40/E as the benchmark, the 7.6 kbp TB40/E *E. coli* mini-F sequence replaced a 2.7 kbp portion of the *US2-US6* region resulting in a net length increase of 4.9 kbp. Because TB40/E/Cre excises the complete *E. coli* mini-F sequence, the resulting genome length during packaging into the capsid is -2.7 kbp relative to pwTB40/E, or 229 kbp. Insertion of a 2.3 kbp *galK/kan^r* segment, which is under control of a bacterial promoter, was then used as a biologically inert surrogate for

introducing exogenous sequence to the genome of both TB40/E and TB40/E/Cre. After transfection, genome lengths relative to pwTB40/E are as follows: TB40/E/Cre = -2.7 kbp, TB40/E/Cre GalK/Kan^r = -0.4 kbp, TB40/E = +4.9 kbp, and TB40/E GalK/Kan^r = +7.2 kbp (Fig. 2.3).

To characterize virus replication kinetics, we compared the four strains in single-step (MOI = 1.0) and multi-step (MOI = 0.01) growth curves in primary human foreskin fibroblasts (HFFs; Fig. 2.4). No distinct patterns emerged when comparing the intracellular or extracellular growth of the strains following high MOI infection except a slight lag in extracellular TB40/E GalK/Kan^r production. During low MOI infection, intracellular and extracellular titers for TB40/E/Cre and TB40/E/Cre GalK/Kan^r increased at a faster rate than either TB40/E or TB40/E GalK/Kan^r. Unexpectedly, the growth rate of TB40/E GalK/Kan^r appeared to surpass growth of TB40/E by a slight margin despite having the longest overall genome length. Regardless of differences in growth rate, all four viruses reached approximately the same titer at the culmination of the time course. We found a similar pattern when comparing the accumulation of DNase I resistant genomes over the same time course (bottom panels, Fig. 2.4). TB40/E/Cre and TB40/E/Cre GalK/Kan^r, with the smallest genomes, grew faster and almost indistinguishably from each other compared to TB40/E or TB40/E GalK/Kan^r. Likewise, TB40/E GalK/Kan^r genomes accumulated more quickly than TB40/E genomes over the same time course both at the intracellular and extracellular stages. Overall, the growth curves show that TB40/E/Cre and its derivative grow more quickly than strains that maintain the *E. coli* propagation sequence. Additionally, the growth of TB40/E/Cre with

or without insertion of exogenous sequence is identical allowing greater comparability during experiments where expression of foreign sequence is required.

In addition to the growth curves and genome abundance, we assessed expression of the three HCMV kinetic classes of viral proteins (immediate early [IE], early [E], and late [L]); their successive expression is required for production of infectious virions. IE1/2 (IE), pUL44 (E), and pp28 (L) expression levels were evaluated in immunoblots to monitor changes in growth in HFFs (Fig. 2.5A). In comparison to levels of the cellular housekeeping protein, GAPDH, expression of all three classes appeared identical across TB40/E, TB40/E GalK/Kan^r, TB40/E/Cre, and TB40/E/Cre GalK/Kan^r, with the exception of a slight shift in pp28, suggesting growth differences are largely independent of viral protein expression.

Lastly, we compared the characteristic CPE produced by each strain to look for potential issues with spread during infection. HCMV produces a hallmark cytoplasmic virion assembly complex (cVAC) late in infection following viral protein expression and a significant alteration in internal host cell architecture. The cVAC is proposed to facilitate virion maturation and consists of a reniform nucleus with endosomal populations centrally located in a perinuclear, ring-like, Golgi-derived structure. To monitor cVAC formation, we used IFA to image structures present in HFFs (Fig. 2.5B). Infected cells were identified based on the presence of nuclear viral proteins IE1/2 and cellular structures were observed using GM130 to mark the *cis*-Golgi or EEA1 to mark endosome populations. At an early time point (24 hpi; top panels, Fig. 2.5B), a time prior to cVAC formation, there were no differences between TB40/E, TB40/E GalK/Kan^r, TB40/E/Cre,

or TB40/E/Cre GalK/Kan^r. Similarly, at 96 hpi (bottom panels, Fig. 2.5B), when the cVAC should be fully formed, no appreciable differences in cellular morphology were detected.

Our observations suggest that differences in growth rate as a function of genome length are independent of both viral protein expression and cVAC development.

C. Implementation of TB40/E/Cre as a gene transduction vector.

To test the ability of TB40/E/Cre to express a gene of interest, we used the cellular trafficking protein, Rab3A. Rab3A is a GTPase involved in shuttling cargo from Golgi compartments to the plasma membrane and is associated with envelopes of HCMV virions in the cVAC (20, 211, 212).

To express Rab3A from TB40/E/Cre, we first created a TB40/E/Cre derivative that fuses proteins of interest to ECFP and FKBP tags (Fig. 2.6). The fluorescent protein, ECFP, allows protein localization to be monitored. FKBP is a destabilization domain that post-translationally controls protein abundance (264) (Fig. 2.7). In the presence of the soluble stabilizing ligand, Shield-1, the protein is stabilized and accumulates. In the absence of Shield-1, the protein is co-translationally degraded by the proteasome. FKBP allows us to stabilize accumulation of genes of interest on smaller timescales than typically available through other techniques such as plasmid transfection.

Using recombineering as before, BACs were initially modified in *E. coli* SW105 cells (Fig. 2.6). After ECFP-Rab11A was tagged with FKBP using the SW105 arabinose-inducible flippase which excises intervening sequence between FRT cleavage sites, the tagged construct was moved to *E. coli* SW102 cells containing TB40/E/Cre MIE_{Enh} from Fig. 2.1. Incorporation of the fragment reconstituted the MIE enhancer/promoter region ($MIE_{Enh/P}$) and generated TB40/E/Cre FKBP-ECFP-Rab11A (BAC 7, Fig. 2.6). Rab11A

was replaced with *galK/kan*^{r} creating the intermediate TB40/E/Cre FKBP-ECFP-GalK/Kan^r which directly tags genes of interest for transduction (BAC 8, Fig. 2.6). Lastly, the selection cassette was replaced by Rab3A and TB40/E/Cre FKBP-ECFP-Rab3A was completed (BAC 9, Fig. 2.6). As before, each step of the process was verified prior to transfection and reconstitution of infectious virus (data not shown).

To demonstrate the transduction and stability regulation system, stabilization of FKBP-ECFP-Rab3A was determined by immunoblot of infected HFFs (MOI = 0.1) using a time course of Shield-1 additions leading up harvesting of cell lysates at 96 hpi (Fig. 2.8A). Cellular GAPDH and the viral DNA processivity factor, pUL44, was used to monitor the progression of infection. When stained with an anti-Rab3A monoclonal antibody, FKBP-ECFP-Rab3A expression is apparent at the predicted size of 70 kDa even in the absence of Shield-1. The higher molecular weight bands detected by the Rab3A antibody likely represent post-translationally modified forms of FKBP-ECFP-Rab3A which are required for normal Rab3A function. Native Rab3A is a cellular protein of approximately 25 kDa in size. Because Rab3A is expressed at relatively low levels in HFFs (data not shown), it was not detected under the conditions tested due to the significant amount of FKBP-ECFP-Rab3A present. As measured through densitometry, accumulation of the Rab3A construct increases as a function of Shield-1 exposure time with an approximately 4-fold increase in abundance occurring in as little as 2 h (Fig. 2.8B). To demonstrate the reversibility of the system, cells were also exposed to Shield-1 for 12 h, washed, and then incubated in clean media for another 12 h prior to fixation (12 + wash, Fig. 2.8A and B). The withdrawal of Shield-1 was sufficient to stop the continued accumulation of FKBP-tagged Rab3A leading to identical levels as the 12 h time point. Because Rab proteins

associate with membranes after being post-translationally modified, the prolonged persistence of Rab3A following Shield-1 removal may be due to interactions that preclude it from being routed to the proteasome.

To assess intracellular localization of Rab3A as expressed from this construct, internal morphologies of HFFs were compared after infection (MOI = 0.1) with reconstituted TB40/E/Cre or TB40/E/Cre FKBP-ECFP-Rab3A (Fig. 2.8B). Infected cells were identified using an antibody against the nuclear-resident viral protein pUL44. Progression through infection correlates with an increase nuclear pUL44 staining, enabling estimation of the stage of infection in individual cells. GM130 was used to mark the Golgi-ring and the accumulation and localization of FKBP-ECFP-Rab3A was detected using its the ECFP tag. Shield-1 was added according to an identical time course as used for the immunoblots, and cells were fixed for staining at 96 hpi. As in the immunoblots, no FKBP-ECFP-Rab3A was detected during TB40/E/Cre infection alone but a small amount was evident in the absence of Shield-1 during infection with TB40/E/Cre FKBP-ECFP-Rab3A. Likewise, the abundance of the stabilized Rab3A construct increases as a function of time and is markedly different within only 2 h of Shield-1 treatment. Consistent with previous results, when FKBP-ECFP-Rab3A was stabilized, it localized to the cVAC and the plasma membrane. During prolonged exposure to Shield-1, it appears that excessive accumulation of the Rab construct leads to collapse of normally occurring Golgi-ring. This alteration may be caused by secondary or off-target effects of Rab3A expression as Rab3A controlled pathways are required for normal cell homeostasis.

V. Discussion

Several BAC systems have been generated to study HCMV in laboratory settings. The ability to replicate and modify the genome in bacterial culture is a powerful tool for understanding the viral replication cycle but is typically achieved at the cost of viral coding capacity due to genome packaging restrictions. This forces researchers to classify viral sequences as essential versus nonessential despite a lack of functional knowledge and contextual understanding all which contributes to a loss of biological significance. With this in mind, a handful of currently available BACs have been designed using a Cre/LoxP cleavage system to excise the *E. coli* propagation sequence upon transfection into mammalian cells. The Cre/LoxP system decreases the potential for mutations by alleviating genome length restrictions relative to BACs that maintain the *E. coli* mini-F sequence.

Here we describe the adaption of the endothelial-tropic HCMV strain TB40/E to contain a self-excisable *E. coli* mini-F sequence resulting in the novel strain TB40/E/Cre. By adapting a previously characterized strain, we maintain the ability to compare results from TB40/E/Cre infections to earlier observations. In TB40/E, the *E. coli* propagation sequence replaces the *US2-US6* viral gene locus, which contains genes with primarily immunomodulatory roles. In TB40/E/Cre, the *US2-US6* deletion is maintained but the *E. coli* propagation sequence is lost upon introduction to mammalian cells thus creating a small surplus of coding capacity that can be used for transduction of exogenous sequences.

The growth of TB40/E/Cre was compared to the parent strain, TB40/E, and the insertion strains TB40/E GalK/Kan^r and TB40/E/Cre GalK/Kan^r. The inclusion of the

bacterially driven *galK/kan*^{r} selection cassette was used to test the fitness of TB40/E/Cre as a mammalian transduction vector without interference from a biologically active molecule. We show that TB40/E/Cre and its derivative, TB40/E/Cre GalK/Kan^r, grew faster than TB40/E and TB40/E GalK/Kan^r at a low MOI (Fig. 2.4). Additionally, the growth patterns of TB40/E/Cre and TB40/E/Cre GalK/Kan^r were almost completely indistinguishable from each other whereas TB40/E and TB40/E GalK/Kan^r grew at different rates relative to each other. This suggests there may be a confounding variable when expressing exogenous sequence from TB40/E, consequentially reducing its utility as a transduction vector. Unexpectedly, TB40/E GalK/Kan^r, which contains an approximately 8 kbp longer genome compared to WT HCMV isolates and the longest genome of the strains studied here, grew faster than TB40/E alone. There were no significant differences in viral protein expression or generation of the cVAC in infected cells (Fig. 2.5A and B). HCMV strains without a Cre/LoxP system are capable of preferentially and spontaneously losing all or part of the *E. coli* propagation sequence during replication. It may be that TB40/E GalK/Kan^r mutants are closer to the threshold of capsid packaging capabilities so the virus is more predisposed to excising nonessential gene regions following successive rounds of replication. Future studies looking at the genetic content of the various strains over the course of infection may help identify the discrepancies in growth rates.

After demonstrating the ability of TB40/E/Cre to tolerate exogenous sequence, we incorporated a tagged protein transduction system to regulate the abundance of genes of interest over short time intervals (Fig. 2.6-8). Compared to generating stable protein-expressing cell lines or co-transfection/infection experiments, incorporating constructs

into TB40/E/Cre simplifies the process of studying genes of interest during infection. TB40/E/Cre is easily manipulated in bacterial systems and its use as a vector ensures each infected cell carries a copy of the protein of interest. In this instance, we fused the host vesicular trafficking protein Rab3A to ECFP and the destabilization domain, FKBP. By attaching the tags to the N-terminal domain, FKBP is translated first and immediately targets the construct to the proteasome for co-translational degradation unless the soluble ligand, Shield-1 is added to the system and stabilizes FKBP. We use the system to show Rab3A accumulation in infected cells as a function of Shield-1 exposure and demonstrate proper localization of the construct to the cVAC where endogenous Rab3A has been identified as having a role in secondary envelopment and virion egress. The presence of FKBP-ECFP-Rab3A in the absence of Shield-1 may be due to the membrane sequestration of Rab3A following post-translational geranylgeranylation. Despite the incomplete degradation, protein accumulation is able to be modified significantly by addition of Shield-1 with appreciable differences being seen by IFA and Western blot in as few as 2 h post-Shield-1 exposure. This is a marked improvement over other expression systems which typically require 24-48 h before proteins accumulate which is particularly important given the fast nature of many cellular events.

The application of TB40/E/Cre will facilitate the study of viral replication. The combination of the self-excisable BAC and titratable nature of the FKBP/Shield-1 system in TB40/E/Cre gives researchers increasing control of protein accumulation over decreasing time scales. By using TB40/E/Cre to express inhibitors of cellular processes over short periods, it will be easier to avoid off-target effects relative to more traditional techniques such as plasmid transfection. Through proper application, TB40/E/Cre may

be the key to identifying critical control points in viral replication which we can then use for development of novel antivirals.

Table 2.1.

Primers used to generate recombinant viruses

Fragment[a]	Primer sequences	Amplification Target
TB40/E/Cre Generation (Fig. #)		
A	5′ – ACGCAACGCAGCCAGATCACATCCCCTTGCAGTACCAGACGCAGGGCTAGCCTGTTGACAATTAATCATCGGC – 3′	GalK/Kan^r
	5′ – TGTATCTTATCATGTCTGGATCCGATATCGCCGTGGCGGCCGCTCTAGAACTCAGCAAAAGTTCGATTTATTC – 3′	
B	5′ – ACGCAACGCAGCCAGATCACATCCCCTTGCAGTACCAGACGCAGGGCTAGATAACTTCGTATAATGTATGCTA – 3′	LoxP
	5′ – TGTATCTTATCATGTCTGGATCCGATATCGCCGTGGCGGCCGCTCTAGAAATAACTTCGTATAGCATACATTA – 3′	
C	5′ – GCTAGGCGCGCCTGTTTAAACATGGATCCGGCCGCCCTTAATTAACGTGGCCTGTTGACAATTAATCATCGGC – 3′	GalK/Kan^r
	5′ – AAAAGCTGCATGAAAAACACGACGAAAGGCGTTCAGTGTTGGATCAGACTCCTCAGCAAAAGTTCGATTTATTC – 3′	
D	5′ – GCTAGGCGCGCCTGTTTAAACATGGATCCGGCCGCCCTTAATTAACGTGGTATCCCCTGATTCTGTGGA – 3′	LR-MIE$_{Enh}$
	5′ – AAAAGCTGCATGAAAAACACGACGAAAGGCGTTCAGTGTTGGATCAGACTCGTCAATGGGGCGGAGTTGTTACG – 3′	
E	5′ – GCTAGGCGCGCCTGTTTAAACATGGATCCGGCCGCCCTTAATTAACGTGGCCTGTTGACAATTAATCATCGGC – 3′	GalK/Kan^r
	5′ – TAATAACTAATGCATGGCGGTAATACGGTTATCCACAGAATCAGGGGATACTCAGCAAAAGTTCGATTTATTC – 3′	
F	5′ – GCTAGGCGCGCCTGTTTAAACATGGATCCGGCCGCCCTTAATTAACGTGGTGTCAGTTAGGGTGTGGAA – 3′	SV40$_p$-inCre-LoxP
	5′ – TAATAACTAATGCATGGCGGTAATACGGTTATCCACAGAATCAGGGGATAATAACTTCGTATAGCATACATTA – 3′	
G	5′ – TATCCCCTGATTCTGTGGATAACCGTATTACCGCCATGCATTAGTTATTAACCTGTTGACAATTAATCATCGGC – 3′	GalK/Kan^r
	5′ – AAAAGCTGCATGAAAAACACGACGAAAGGCGTTCAGTGTTGGATCAGACTCCTCAGCAAAAGTTCGATTTATTC – 3′	
H	5′ – ATACGAAGTTATTATCCCCTGATTCTGTGGATAACCGTATTACCGCCATGCATTAGTTATTAGAGTCTGATCC – 3′	LR
	5′ – GTCATGGTCTGTAAAAGCTGCATGAAAAACACGACGAAAGCGTTCAGTGTTGGATCAGACTCTAATAACTAAT – 3′	
TB40/E/Cre FKBP-ECFP-Rab3A Generation (Fig. #)		
A	5′ – GCGGGGGACAAAGGACAGTACGACAGATTAGGTGATAGAAACGTTTTTTTCCTGTTGACAATTAATCATCGGC – 3′	GalK/Kan^r
	5′ – CGCTTCGTGTATTTAGACGAATCTCGGCGATAACCGCCGGCGTTGCCGCCCTCAGCAAAAGTTCGATTTATTC – 3′	
B	5′ – GCGGGGGACAAAGGACAGTACGACAGATTAGGTGATAGAAACGTTTTTTTGCAAATGGGCGGTAGGCGTGTA – 3′	MIEP-ECFP-Rab11A-SV40$_{pA}$
	5′ – CGCTTCGTGTATTTAGACGAATCTCGGCGATAACCGCCGGCGTTGCCGCCTAAGATACATTGATGAGTTTGGA – 3′	
C	5′ – GAGGTCTATATAAGCAGAGCTGGTTTAGTGAACCGTCAGATCCGCTAGCGATGGGAGTGCAGGTGGAAACCATC – 3′	FKBP-FRT-GalK/Kan^r-FRT
	5′ – ACCAGGATGGGCACCACCCCGGTGAACAGCTCCTCGCCCTTGCTCACCATGCTGGAGCTCCACCGCGGTGGAAGTTC – 3′	
D	5′ – CAAAATCAACGGGACTTTCCAAAATGTCGTAACAACTCCGCCCCATTGACGCTGTTGACAATTAATCATCGGC – 3′	GalK/Kan^r
	5′ – AAAAGCTGCATGAAAAACACGACGAAAGCGTTCAGTGTTGGATCAGACTCCTCAGCAAAAGTTCGATTTATTC – 3′	
E	5′ – CAAAATCAACGGGACTTTCCAAAATGTCGTAACAACTCCGCCCCATTGACGCAAATGGGCGGTAGGCGTGTA – 3′	MIE$_p$-FKBP-FRT-ECFP-Rab11A-SV40$_{pA}$
	5′ – AAAAGCTGCATGAAAAACACGACGAAAGGCGTTCAGTGTTGGATCAGACTCTAAGATACATTGATGAGTTTGGA – 3′	
F	5′ – ATGGACGAGCTGTACAAGTCCGGCCGGACTCAGATCTCGAGCTCAAGCTTCGAATTCGCACCTGTTGACAATTAATCATCGGC – 3′	GalK/Kan^r
	5′ – ACCTCTACAAATGTGGTATGGCTGATTATGATCAGTTATCTAGATCCGGTGGATCCTGCCCTCAGCAAAAGTTCGATTTATTC – 3′	
G	5′ – TGTACAAGTCCGGCCGGACTCAGATCTCGAGCTCAAGCTTCGAATTCGCAATGGCATCCGCCACAGACTCGC – 3′	Rab3A
	5′ – ATGTGGTATGGCTGATTATGATCAGTTATCTAGATCCGGTGGATCCTGCCTCAGCAGGCGCAGTCCTGGT – 3′	

[a] Fragment designations based on corresponding recombineering schematics

Table 2.2.

Antibodies used for immunoblots and IFA

Antibody target	Type	Source (catalog no.)
Cellular		
GAPDH (36 kDa)	Mouse monoclonal/IgG1, clone GA1R	ThermoScientific (MA5-15738)
GM130 (130 kDa)	Mouse monoclonal/IgG1(κ), clone 35/GM130	BD Biosciences (610822)
EEA1 (180 kDa)	Rabbit polyclonal/IgG	Abcam (ab2900)
Rab3A (25 kDa)	Mouse monoclonal/IgG2b, clone 42.2	Synaptic Systems (107-111)
HCMV		
IE1/2 (72/86 kDa)	Mouse monoclonal/IgG1(κ), clone CH160	Virusys (P1215)
pUL44 (46 kDa)	Mouse monoclonal/IgG1(κ), clone 10D8	Virusys (CA006-100)
pp28 (28 kDa)	Mouse monoclonal/IgG2A (κ), 5C3	Virusys (CA004-100)
Secondary		
Anti-mouse IgG (H+L)	Goat polyclonal, HRP conjugated	Bio-Rad (170-6516)
Anti-rabbit IgG (H+L)	Goat polyclonal, Alexa Fluor 488 conjugated	Invitrogen (A-11034)
Anti-mouse IgG (H+L)	Goat polyclonal, Alexa Fluor 568 conjugated	Invitrogen (A-11031)

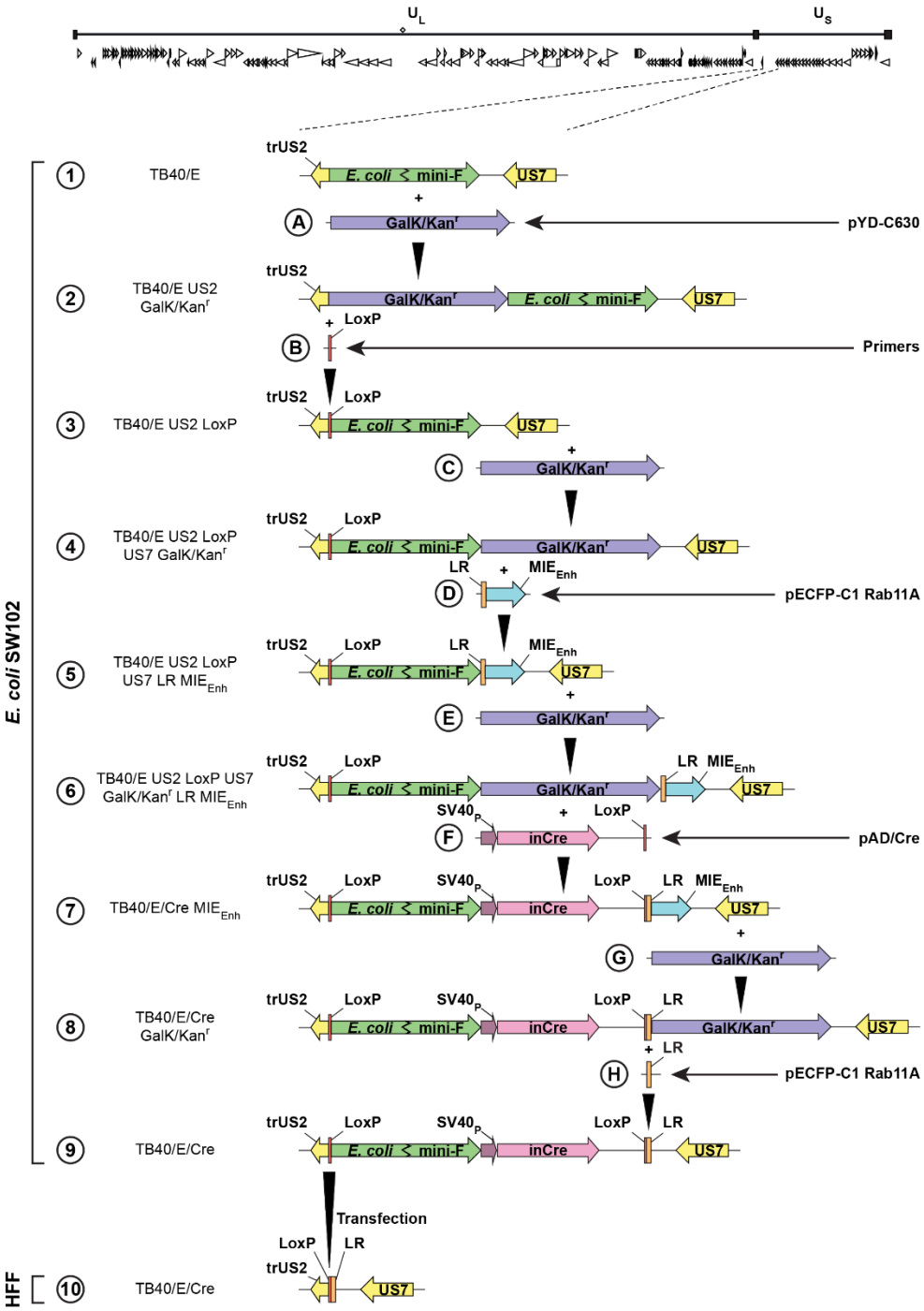

Fig. 2.1. Generation of the self-excisable endotheliotropic HCMV BAC, TB40/E/Cre. Homologous recombination in *E. coli* SW102 cells was used to modify the original TB40/E *E. coli* mini-F propagation sequence which replaces the *US2-US6* region in the HCMV genome. Alternating rounds of positive and negative selection with a *galK/Kanr* cassette were used to insert PCR amplicons containing desired features. Cre recombinase with a synthetic intron (inCre) was inserted adjacent to the *E. coli* propagation sequence and flanked by LoxP cleavage sites. Following transfection, the *cre* intron is removed and the LoxP sites are cleaved resulting in loss of the *E. coli* propagation sequence. Coding sequences are drawn to scale excluding the *E. coli* propagation sequence which is represented as one third the normal length. Letter designations correspond to the primers used in Table 2.1. Abbreviations: unique long region (U_L), unique short region (U_S), truncated *US2* (trUS2), linker region (LR), CMV major IE promoter enhancer region (MIE_{Enh}), SV40 promoter ($SV40_P$).

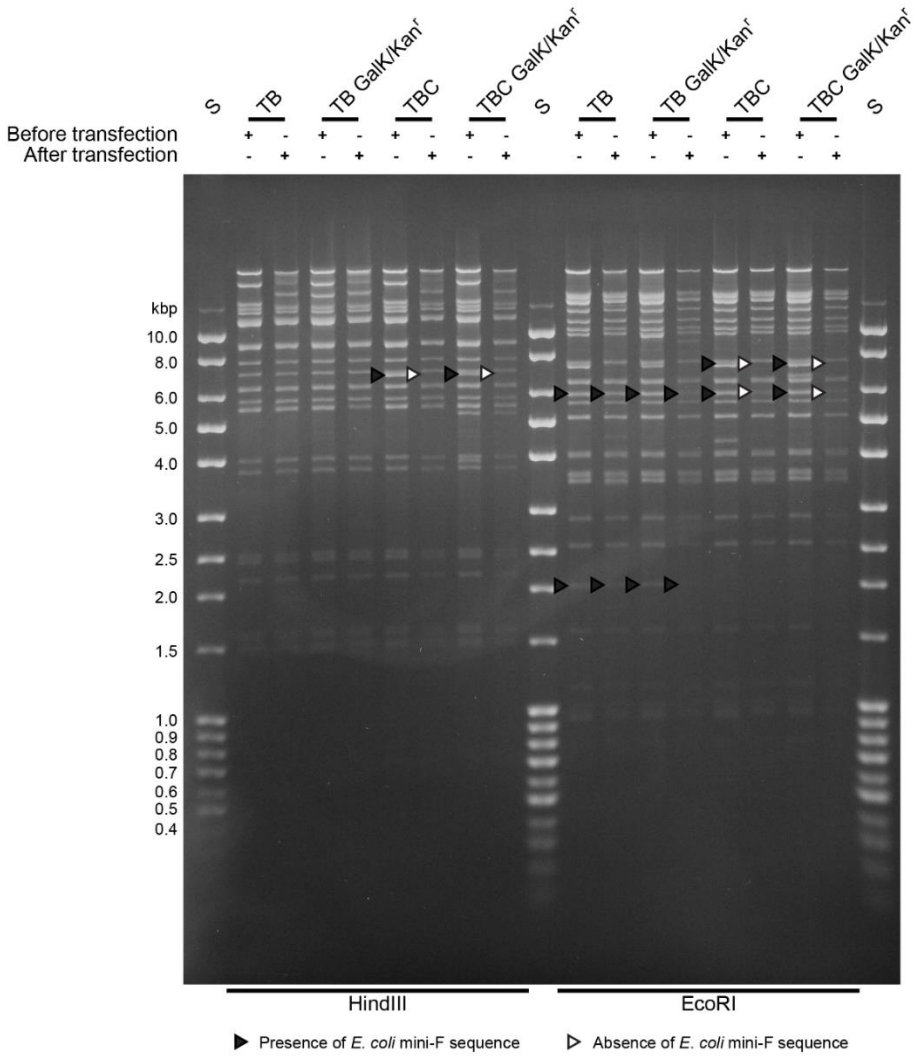

Fig. 2.2. Restriction digestion of HCMV DNA before and after transfection shows successful excision of the E. coli mini-F propagation sequence from TB40/E/Cre derivatives following virus reconstitution. Equal amounts of DNA purified from *E. coli* and DNase I treated virions were digested using HindIII or EcoRI restriction endonucleases. Digests were run overnight on a large format gel and band sizes relative to a standard DNA ladder (S) were visualized with ethidium bromide. Abbreviations: TB40/E (TB), TB40/E/Cre (TBC).

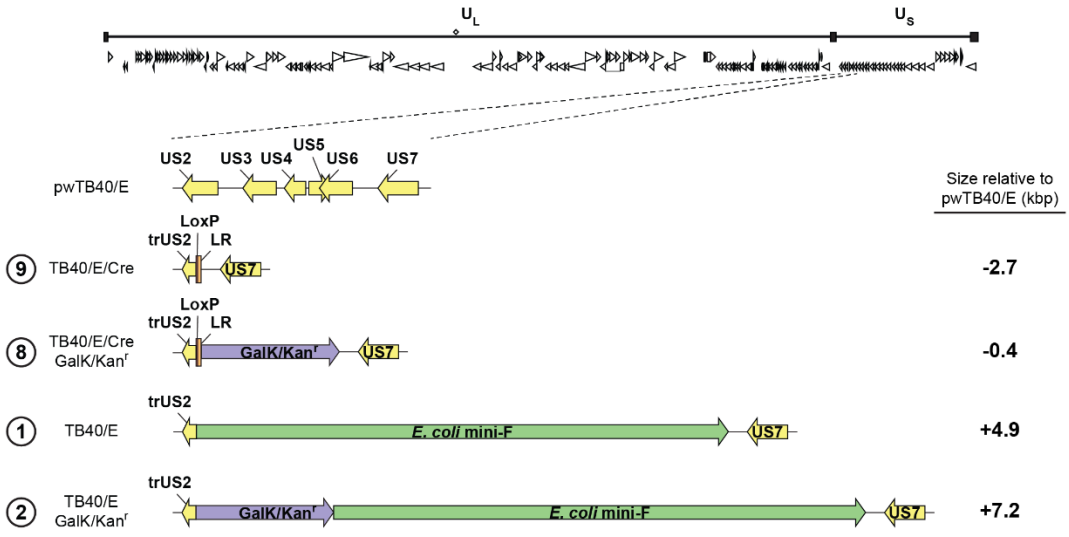

Fig. 2.3. BAC structures and genome lengths following reconstitution relative to a pseudo-wild type TB40/E (pwTB40/E) strain. pwTB40/E is comprised of the TB40/E sequence with an intact *US2-US6* gene region in place of the *E. coli* mini-F propagation sequence. Coding sequences are drawn to scale and number designations correspond to the cloning diagram found in Fig. 1. Abbreviations: truncated *US2* (trUS2), linker region (LR).

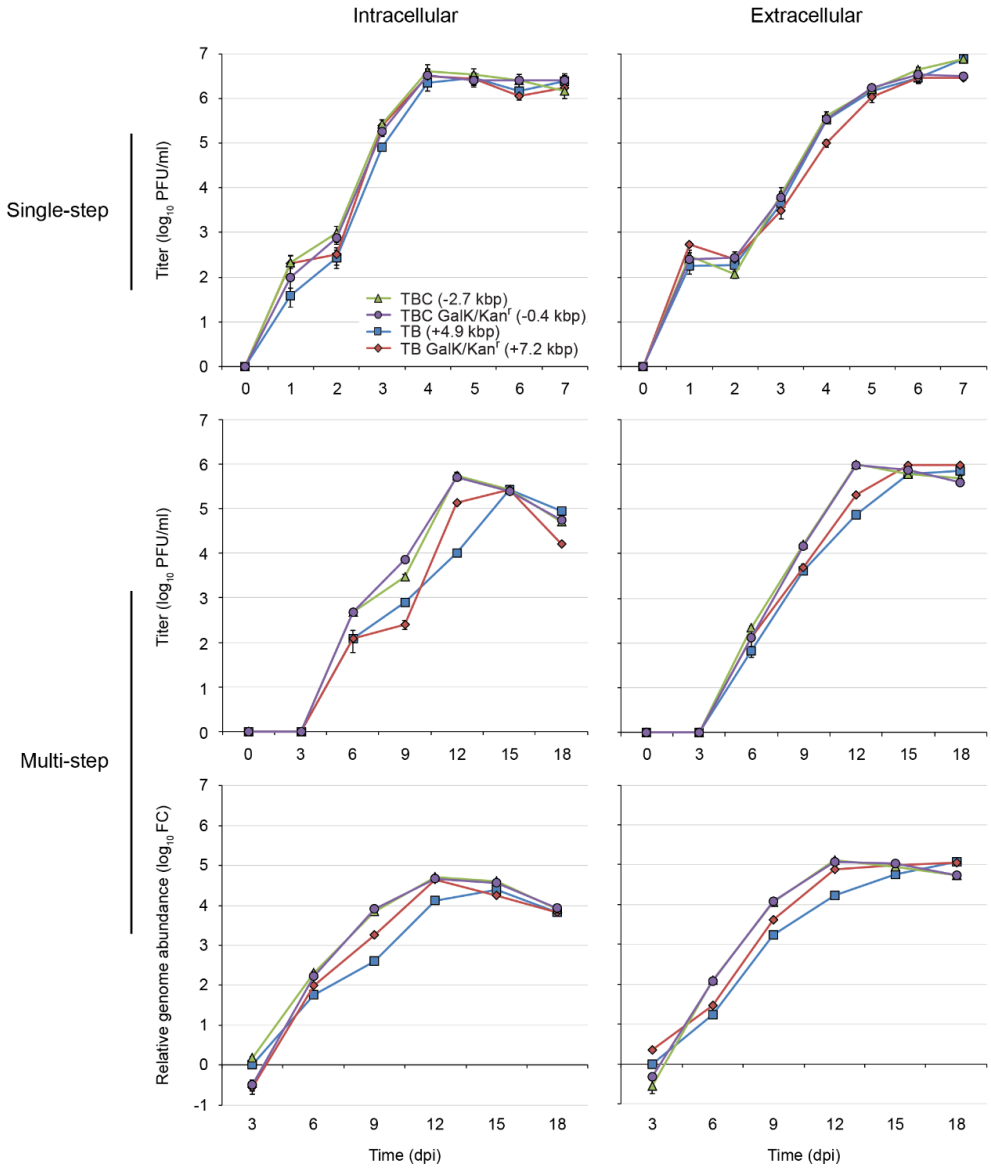

Fig. 2.4. Divergent HCMV genome length-associated growth rates. BAC single-step (MOI 1.0) or multi-step (MOI 0.01) HFF growth rates were determined by plaque assay and genome accumulation. Cellular supernatants were collected for extracellular fractions and remaining cells were washed prior to sonication and harvesting of intracellular fractions. DNase I protected genomes were detected by qPCR and abundances were calculated relative to 3 dpi TB40/E samples using the $2^{-\Delta C'T}$ method (3). Error bars represent standard error of the mean (SEM). Abbreviations: TB40/E (TB), TB40/E/Cre (TBC).

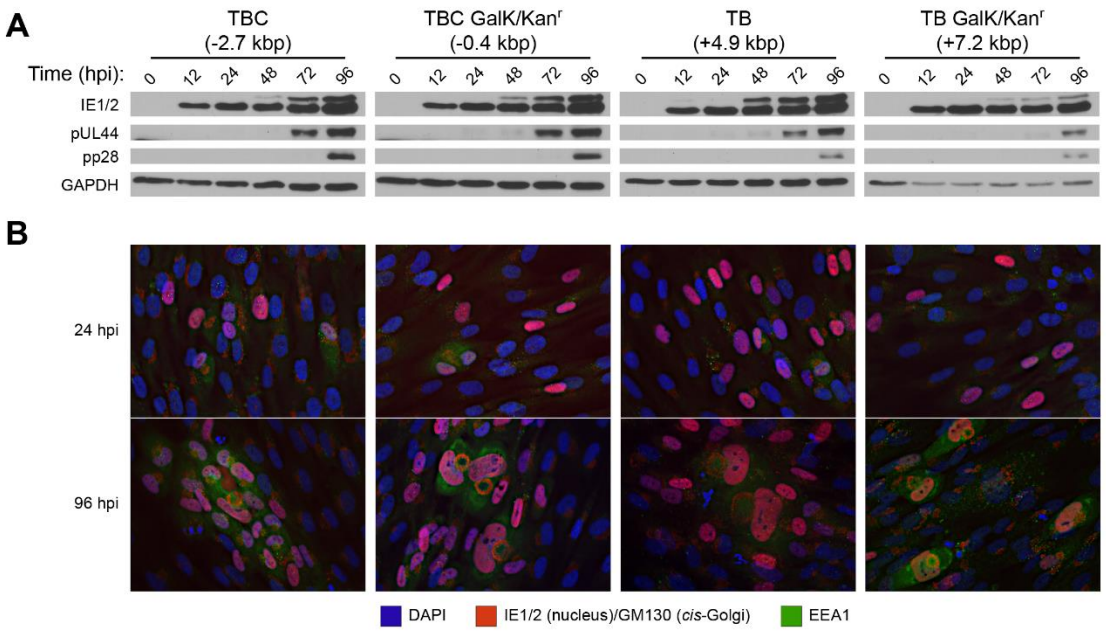

Fig. 2.5. HCMV genome length-associated growth rates are independent of viral protein expression and assembly complex formation. (A) Protein expression of BAC infected HFFs (MOI 1.0) using markers for immediate early (IE1/2), early (pUL44), and late (pp28) viral proteins. (B) Golgi-ring formation and endosome redistribution indicates HCMV assembly complex formation at late time points of infection in HFFs (MOI 0.1). IE1/2 nuclei are positive for infection. Abbreviations: TB40/E (TB), TB40/E/Cre (TBC).

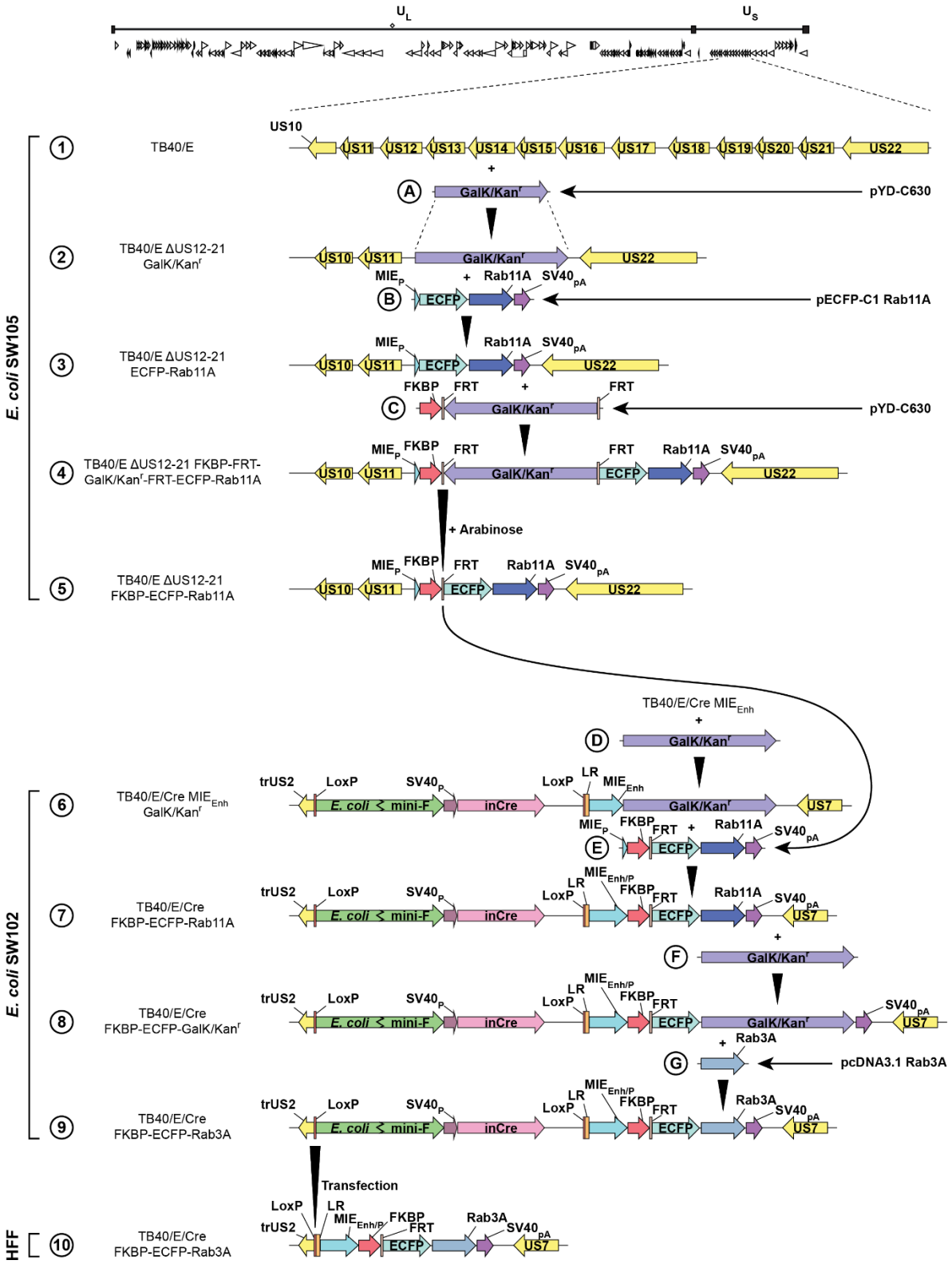

Fig. 2.6. Self-excision of the TB40/E/Cre *E. coli* mini-F propagation sequence creates a genome length reduction that can accommodate exogenous sequence. Homologous recombination of HCMV BACs in *E. coli* strains SW105 and SW102 was used to insert PCR amplicons containing desired sequences through consecutive rounds of positive and negative selection. The Rab11A cellular GTPase protein was tagged with ECFP and the destabilization domain, FKBP, using an arabinose-inducible flippase to cleave FRT sites. FKBP-ECFP-Rab11A was then incorporated into TB40/E/Cre and Rab11A was replaced with the cellular trafficking protein Rab3A. Coding sequences are drawn to scale excluding the *E. coli* propagation sequence which is represented as one third the normal length. Letter designations correspond to the primers used in Table 2.1. Abbreviations: unique long region (U_L), unique short region (U_S), CMV major IE promoter (MIE_P), enhanced cyan fluorescent protein (ECFP), SV40 polyadenylation site ($SV40_{pA}$), FKBP destabilization domain (FKBP), truncated *US2* (trUS2), SV40 promoter ($SV40_P$), Cre recombinase with a synthetic intron (inCre), linker region (LR), CMV major IE promoter enhancer region (MIE_{Enh}), reconstituted CMV major IE enhancer and promoter

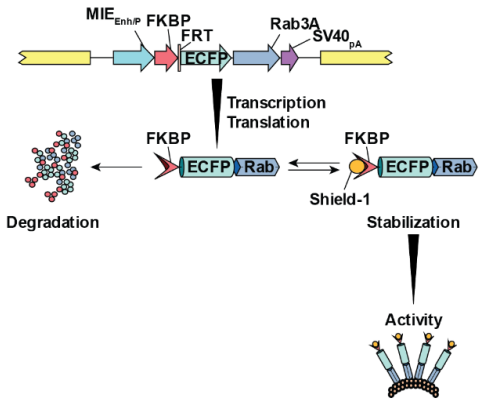

Fig. 2.7. Regulation of function by FKBP/Shield-1 stabilization. FKBP tagged constructs are co-translationally degraded by the proteasome unless reversibly stabilized by the soluble Shield-1 ligand. Abbreviations: CMV major IE enhancer and promoter region ($MIE_{Enh/P}$), SV40 polyadenylation site ($SV40_{pA}$).

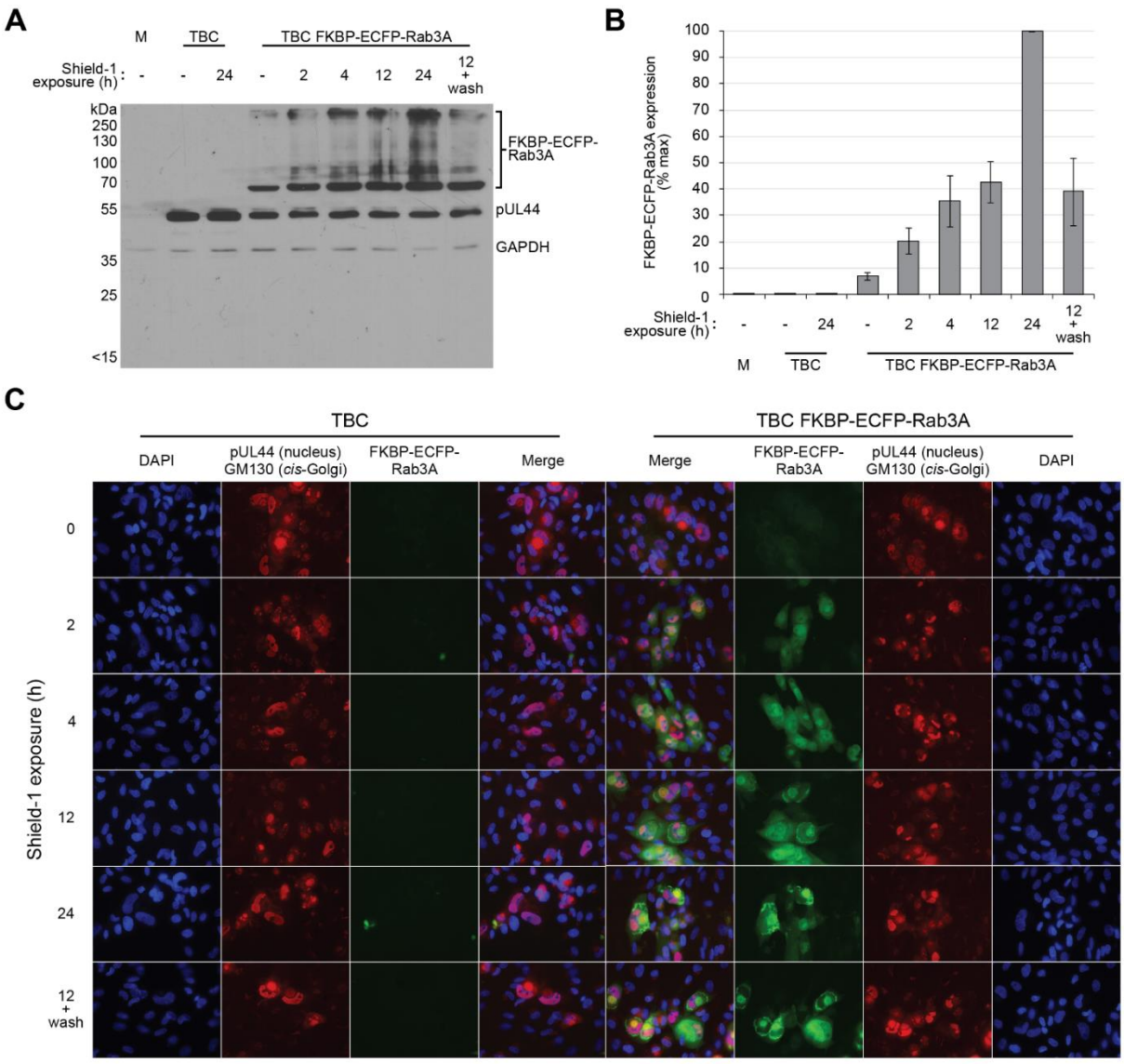

Fig. 2.8. Enhanced accumulation of FKBP tagged Rab3A can be detected within 2 h of exposure to Shield-1. (A) Immunoblot analysis showing accumulation of FKBP-ECFP-Rab3A (70 kDa) in infected HFFs (pUL44; MOI 0.1) following addition of Shield-1. Shield-1 was added at indicated times prior to harvest of cell lysates at 96 hpi. (B) Densitometry analysis of immunoblot in (A). Error bars represent standard error of the mean (SEM). (C) IFA time course of Shield-1 addition showing accumulation and localization of FKBP-ECFP-Rab3A relative to the Golgi-ring (GM130) in infected HFFs (pUL44; MOI 0.1). Shield-1 was added at indicated times prior to fixation and staining at 96 hpi. Abbreviations: TB40/E/Cre (TBC), mock infected control (M).

CHAPTER 3: REGULATION OF THE HOST CYTOPLASMIC COMPARTMENT BY HCMV INFECTION

I. Abstract

Human cytomegalovirus (HCMV) is a persistent pathogen for individuals without functionally competent immune systems. Failure to understand viral assembly has resulted in limited antiviral treatments and the unique biology of HCMV infection has eluded protection by vaccination.

During infection, HCMV causes the dramatic reorganization of host intracellular structures thereby causing formation of the cytoplasmic virion assembly complex (cVAC). The cVAC promotes virion maturation by constituting a viral assembly line.

To understand the role of cellular components during infection, we characterized the role of cellular structures within the endocytic recycling compartment (ERC) as they relate to cVAC formation and virion maturation. We used previously generated transcriptional and proteomic data sets to map regulation of cellular trafficking components throughout the ERC. As a result, we have generated a model for cVAC development and virion maturation which suggests formation of a perinuclear secretory trap utilized for virion assembly and eventual egress using secretory vesicle-like pathways. Using our model, we are able to provide context for previous observations during HCMV replication and provide future opportunities for the development of HCMV specific treatments.

II. Introduction

Human cytomegalovirus (HCMV) is a common viral pathogen capable of causing severe complications in immunologically compromised or naïve individuals. A lack of antiviral target diversity has led to the emergence of antiviral-resistant strains, thereby

removing the last line of defense for patients unable to control the infection. By increasing our understanding of cytoplasmic events during HCMV replication, we can identify and exploit potential targets for the generation of novel therapeutics.

As part of normal HCMV replication, HCMV induces the hallmark reorganization of internal cellular structures at time points late in infection. The restructuring of cellular components leads to the formation of the cytoplasmic virion assembly complex (cVAC) which is proposed to act as a viral assembly line leading to the directed sequential addition of the structural components required to generate nascent virions. The cVAC is a perinuclear structure consisting of a Golgi-derived ring structure with endosome populations at the center. Formation of the cVAC is dependent on cooperation between viral and cellular factors through a process that is not yet understood.

As part of the structural alterations, characteristic membrane populations experience a shift in marker protein identities (19, 23). This shift complicates the classification of host cell-derived membranes used during virion envelopment and egress. Several observations suggest virion envelopes are Golgi-derived and follow a path similar to secretory vesicle (SV) formation and exocytosis (20, 23, 29, 32, 33, 35). Others have looked at the effect of viral regulatory mechanisms on cellular transcripts and protein abundance (2, 23, 266). While individual proteins or processes have been implicated in virion development, an overall map of HCMV-induced trafficking has not yet been presented.

In this study, we utilize previously available data sets to examine the trafficking regulatory processes in the context of HCMV infection. For generation of our model, we map alterations to cellular pathways through the endocytic recycling compartment (ERC)

(Fig. 3.1). The ERC is a functional characterization of normal cellular transport and is required for maintaining homeostasis under normal conditions (reviewed in (267)). Trafficking through the ERC is dependent, in part, on membrane-bound GTPases, including the Rab family of proteins, and various effector molecules attaching to the cytoskeletal network. Importantly, ERC pathways are highly conserved in all cell types.

In this study, we combine the analysis of transcriptional and proteomic data sets to analyze cellular trafficking throughout the ERC as a function of HCMV infection. Through the use of data transformation and a novel metric, we are able to examine global cellular trafficking regulatory patterns induced by viral factors. Our model provides a framework for understanding derivation of host membranes for use in cVAC development and details potential routes of virion egress. In our model, we provide further evidence suggesting HCMV utilizes a SV-dependent pathway for virion envelopment and egress.

Using our model of virion maturation, we provide context for studies examining cytoplasmic events during virion growth. It also provides the opportunity for targeting key regulatory elements which can be exploited for inhibiting HCMV infection in host tissues.

III. Methods

A. Cells and virus.

The viruses used in this study were HCMV Towne, provided by Thomas Shenk (Princeton University, Princeton, NJ), AD169 (ATCC), and AD169-dervied bacterial artificial chromosome (BAC) strain, pAD/Cre, provided by Dong Yu (Washington University, St. Louis, MO). Viruses were grown in low-passage-number pooled human foreskin fibroblasts (HFFs) in complete Dulbecco's modified Eagle medium (DMEM; Hyclone, Logan, UT; catalog no. SH30243.01) supplemented with 1% nonessential amino

acids (Hyclone, Logan, UT; catalog no. SH30238.01), 1% GlutaMax (Gibco, Gaithersburg, MD; catalog no. 35050-061), and 10% fetal bovine serum (FBS; Atlanta Biologicals, Atlanta, GA; catalog no. S11150). Virus was titrated by standard plaque assay in HFFs.

B. Transcriptional and proteomic data sets of HCMV infected cells.

Generation of the transcriptional microarray dataset in our lab has been previously described (1). Briefly, low passage HFFs were mock treated or infected at an MOI of 6.0 using Towne or AD169 and incubated for 12 or 96 h. Upon harvest, RNA was Trizol extracted (Life Technologies, Grand Island, NY; catalog no. 15596-018), and RNA quality was assessed. RNA samples were then loaded onto Illumina HT-12 v4 human bead array chips for detection. Setup of the assay and reading of the chips was done at the Wayne State University Advanced Genomics Technology Center (Wayne State University, Detroit, MI). Results were reported as individual signal intensities.

Generation of the proteomic dataset has also been previously described (2). Briefly, HFFs were infected at an MOI of 10 using the HCMV bacterial artificial chromosome (BAC) strain Merlin. Following appropriate incubation periods, plasma membrane and whole cell lysate samples were isolated, enzymatically digested, and labelled using tandem mass tag (TMT) 8-plex and 10-plex reagents. Labeled samples were then subjected to liquid chromatography and tandem mass spectrometry. For our analysis, available data sets are reported as relative abundances.

C. Bioinformatics analysis.

Initial analysis of microarray data was done using BRB-ArrayTools (v. 4.2.0 beta 2) from Dr. Richard Simon and the BRB-ArrayTools Development Team. Microarray data

for 12 and 96 hours post infection (hpi) samples were compared to mock using the significance analysis of microarray (SAM) function with a false discovery rate of 0.01.

A heatmap of SAM significant genes of interest was generated in R using the limma and gplots packages. Clustering was done using Pearson's correlation coefficient and an average-linker method. Results were normalized on the basis of each individual row and reported as row Z-scores centered around the mean $\log_2$ intensities.

Graphical analysis of dataset relationships was also done using R and r value was calculated using Pearson's correlation coefficient.

D. Transmission electron microscopy.

Infection and imaging of cells infected with the AD169 BAC strain, pAD/Cre, in our lab was previously described (21). In brief, HHFs were infected at an MOI of 0.3 and infections progressed for 120 hpi. Cells were fixed and sent to Dr. Hong Yi at the Robert P. Apkarian Integrated Electron Microscopy Core Facility of Emory University (Atlanta, GA) for staining and imaging.

IV. Results

A. Vesicular transport proteins are differentially regulated over the course of infection

To generate a model of HCMV trafficking within cells, we used a previously generated microarray dataset from our lab to examine transcriptional regulation of vesicle transport during infection with HCMV at early and late time points in viral replication (1). Following infection with HCMV variants Towne and AD169, the cellular transcriptional profile of ~25,000 genes, represented by 47,213 probes, was measured relative to a mock

infected control. By comparing triplicate samples from 12 and 96 hpi, the progression of virally induced transcription regulation was able to be monitored.

Following significance analysis of microarray (SAM) profiling of the transcriptional dataset, probes that passed the filter were examined for roles in cellular vesicle mediated transport. Probes were identified based on known gene ontology classifications and thorough reviews of related literature. In total, 328 probes, representing 328 unique genes, with known functions in vesicular transport were identified.

For a comprehensive overview of regulatory patterns, a heatmap was generated representing the transcriptional profiling of the 328 probes (Fig. 3.2). Construction of the heatmap used Pearson's correlation coefficient to group transcripts based on individually normalized standard deviations around the mean $\log_2$ expression values. Clustering was then performed using an average-linkage method. When examined, the heatmap displays four distinct regulatory patterns including upregulation and downregulation of transcripts at both 12 and 96 hpi. To establish a model of trafficking pathways, the transcriptional data was then compared to measured cellular protein abundances.

B. Transcriptional regulation of HCMV infection correlates with cellular protein abundance

Because transcriptional patterns don't completely correlate with protein translation or protein stability, we compared the whole microarray dataset to a previously characterized proteomic dataset (2). The proteomic data was generated from a series of experiments analyzing whole cell lysate and plasma membrane specific fractions of cellular proteins. Importantly, the proteomic data contained slightly over 8,000 detected proteins so comparison between the two sets were based on only those detected in both

sets. Because the proteomic data was represented as the relative abundance over a series of time points, a summary metric was devised that could be applied to both the transcriptional and proteomic profiles. This was possible because we were interested in the general regulation of pathways over time and not in absolute values.

To transform the data, transcript signal intensities and protein abundance data were independently averaged across all replicates at 12 and 96 hpi. Then, the averages were respectively normalized to control values from mock infected cells resulting in the transcript/protein level fold change (FC) relative to mock. FC values were $\log_2$ transformed and FC_{12hpi} was subtracted from FC_{96hpi} to give the change in $\log_2$ FC ($\Delta\log_2$FC) as seen below.

$$\Delta log_2 FC = log_2\left(\frac{96hpi}{mock}\right) - log_2\left(\frac{12hpi}{mock}\right)$$

By summarizing both data sets using the $\Delta\log_2$FC metric, which is reported in arbitrary units, we focus on the patterns of regulation instead of the absolute values. Next, the $\Delta\log_2$FC values for the Merlin infected proteomic data were graphed against the transcriptional data from AD169 infected cells using a standard coordinate axis (Fig. 3.3).

Comparison of regulatory patterns resulted in a value of r = 0.46 showing the samples are positively correlated but there are still substantial differences.

C. HCMV infected cells favor a secretory vesicle mediated exocytic pathway.

Because the two data sets were overall positively correlated, we proceeded to use the microarray data for establishing a model of HCMV infection because the data were more robust. Using the established roles of the 328 identified probes in regard to positive regulators versus negative regulators of specific pathways, the $\Delta\log_2$FC regulatory patterns were mapped onto pathways throughout the ERC.

The resulting downregulation of all major exocytic pathways and upregulation of all major endocytic pathways with the exception of those required for SV exocytosis suggest a novel pathway for virion egress (Fig. 3.4). By transcriptional analysis, it appears that HCMV drives SV vesicle exocytosis leading to compound exocytic events. Indeed, through imaging by electron microscopy, vesicles containing multiple mature virions and other particles are evident (Fig. 3.5).

V. Discussion

During HCMV infection, virally-induced processes dramatically alter the internal cellular morphology leading to formation of the cVAC (17, 18). As part of the remodeling, several pathways required for normal homeostasis are rerouted or dissociate resulting in an apparent perinuclear secretory trap (19, 42, 44).

By using previously available data, we were able to construct a model of HCMV-induced changes to host secretory systems. While informative, there are a few potential factors that may confound our analysis: i) the viral strains used were different between data sets, ii) the experiments were not setup exactly the same (i.e. MOI of 6.0 versus 10.0), iii) the selection of probes related to transport are subject to individual bias, and iv) mapping of changes to pathway flux is somewhat subjective. While the setup has its flaws, there were still enough correlations to justify use of these data sets for preliminary experiments.

Consistent with previous observations of secretory regulation by HCMV, our modelling predicts a change in the net flux of ERC pathways (19, 20, 42, 44). Under this model, we predict that HCMV promotes the perinuclear accumulation of various components within cells. The concentration of materials in an area coincident with cVAC

development then facilitates cytoplasmic events required for virion maturation (Fig. 3.6). The apparent upregulation of cellular transcripts required for SV vesicle release suggests SV exocytosis may serve as a final pathway for virion egress.

This is supported by previous observations relating virion envelope lipid composition to synaptic vesicles, which follow a similar trajectory, and findings that of SV trafficking proteins associated with HCMV envelopes (20, 29, 32, 33). Additionally, SV exocytosis is mediated through a Ca^{2+} dependent mechanism and during infection with HCMV, Ca^{2+} levels are maintained at substantially elevated levels throughout infection (50). Because SV pathways are highly conserved across diverse cell types, they provide an attractive avenue for HCMV envelopment and egress.

Given the opportunity for further investigation, the various pitfalls could be controlled for and the relationships could be examined in more detail. Using the Δlog_2FC metric under improved conditions may also lead to insight related to regulation of transcriptional activity and protein expression as a result of infection. While approximately half of the investigated transcripts/proteins appeared to follow the same general regulatory pattern, there were some that exhibited increased transcription but decreased protein abundance and vice versa. These techniques can also be applied in the context of infection with other viruses to study viral replication. Understanding the relationship between transcripts and proteins may give context to the effects we see during HCMV infection and cVAC biogenesis.

Through use of our model, we are able to target the various trafficking events that appear to be important for virion maturation. By interfering with key steps, we can identify

critical control points and either validate or improve our current model with the goal of eventually exploiting control points for the development of new therapies.

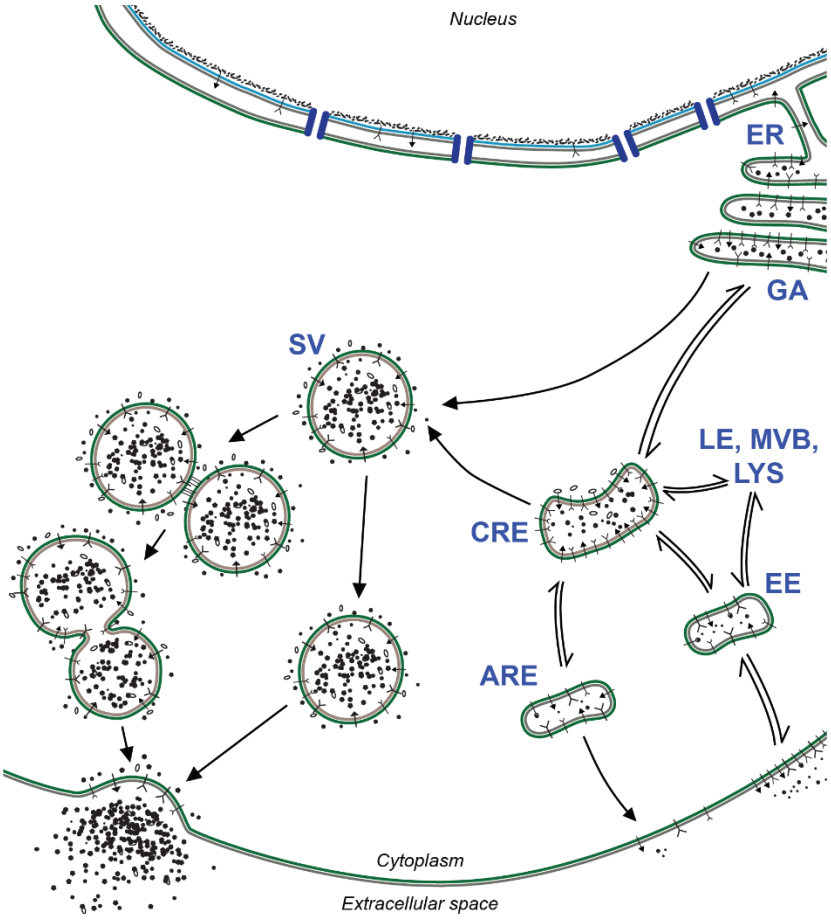

Fig. 3.1. Features of the endocytic recycling compartment (ERC). The endocytic recycling compartment is a functional classification of cellular trafficking events required to maintain homeostasis. Under normal circumstances, inbound materials enter through early endosome (EE) populations before being routed elsewhere such as common recycling endosomes (CRE) or degradative pathways (LE, MVB, LYS). Secretory vesicles (SV) are also generated in this compartment using CRE and Golgi (GA)- derived membranes. During SV exocytosis, vesicles are transported to the plasma membrane and released either independently or through compound exocytosis. Abbreviations: endoplasmic reticulum (ER), Golgi apparatus (GA), common recycling endosomes (CRE), early endosomes (EE), apical recycling endosomes (ARE), late endosomes (LE), multivesicular bodies (MVB), lysosomes (LYS), secretory vesicles (SV).

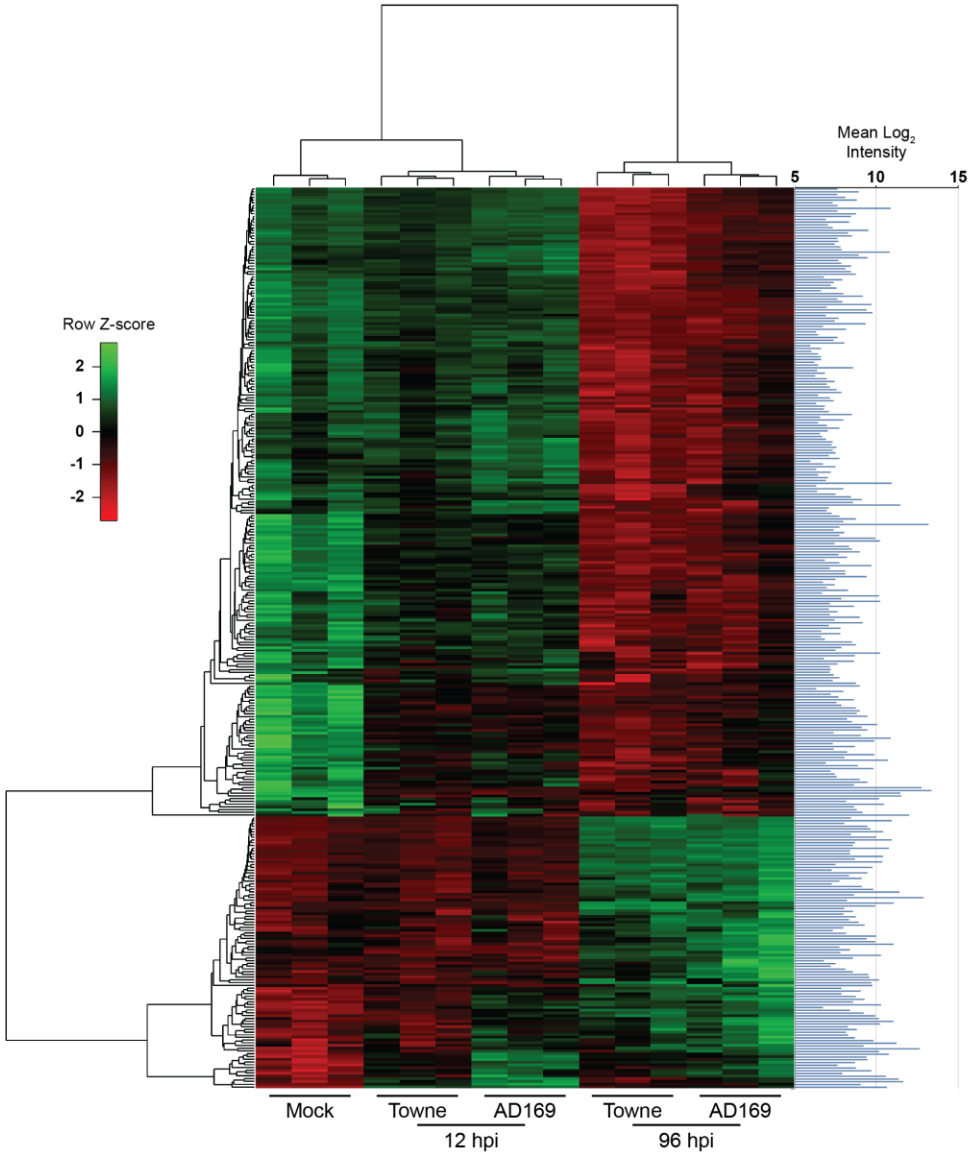

Fig. 3.2. Heatmap demonstrating regulation of cellular trafficking during HCMV infection. HCMV infected HFFs (Towne and AD169; MOI 6.0) were harvested at indicated time points and RNA was extracted for microarray analysis as reported previously (1). Following significance analysis of microarray (SAM) relative to mock cells, 328 significant probes were identified as having roles in vesicle-mediated transport. A heatmap was generated based on standard deviation around the mean log_2 intensity for each individual row. Distance matrices were calculated using Pearson's correlation coefficient and clustering was completed using an average linkage method. Reported Z-scores represent standard deviations from the mean.

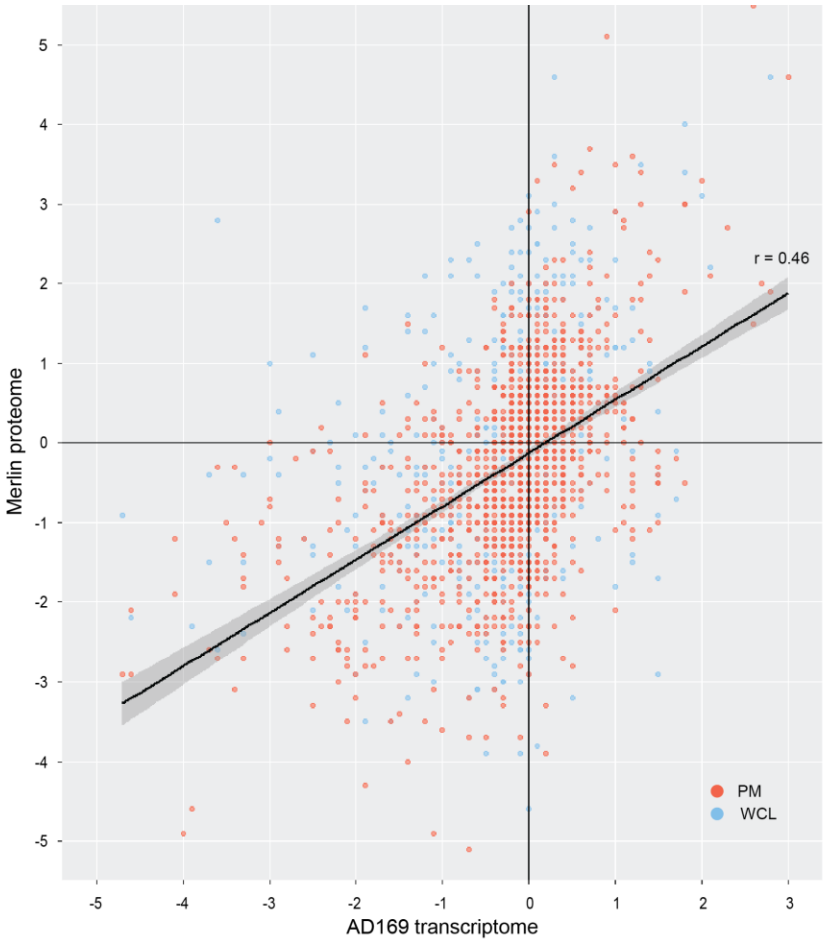

Fig. 3.3. Comparison of proteomic and transcriptional regulation during HCMV infection. Using data sets generated previously (1, 2), proteomic data from HCMV Merlin infected HFFs (MOI 10.0) was compared to transcriptional data for HCMV AD169 infected HFFs (MOI 6.0). By transforming the data using the $\Delta\log_2$FC of protein abundance or transcript intensity relative to mock infected cells, the variation in regulatory patterns of proteins and transcripts during infection was compared. Data represents patterns connecting 12 and 96 hpi relative to mock. Abbreviations: plasma membrane proteome samples (PM), whole cell lysate proteome sample (WCL)

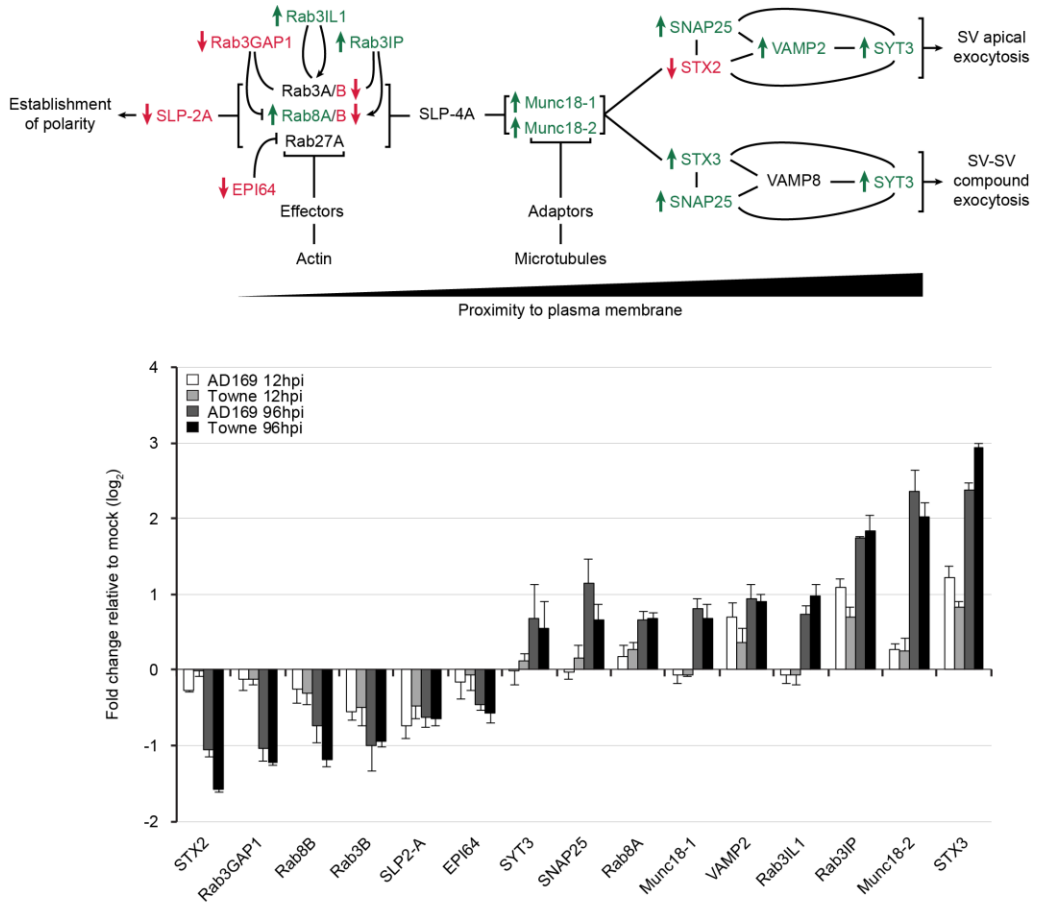

Fig. 3.4. HCMV induced upregulation of secretory vesicle (SV) exocytosis during infection. Following significance analysis of microarray (SAM) filtering, probes were selected for their role in vesicle mediated transportation. As opposed to increased endocytic flux of other pathways in the endocytic recycling compartment, SV vesicle exocytosis-associated transcripts increased. The schematic represents trafficking events required for SV exocytosis with green labeled proteins being upregulated or red labeled proteins being downregulated as a function of HCMV infection. As the figure moves to the right, SVs encounter the plasma membrane and undergo single or compound exocytic events. The graph shows the relative transcript levels of identified proteins over the course of infection with HCMV AD169 or Towne at early (12 hpi) and late (96 hpi) time points.

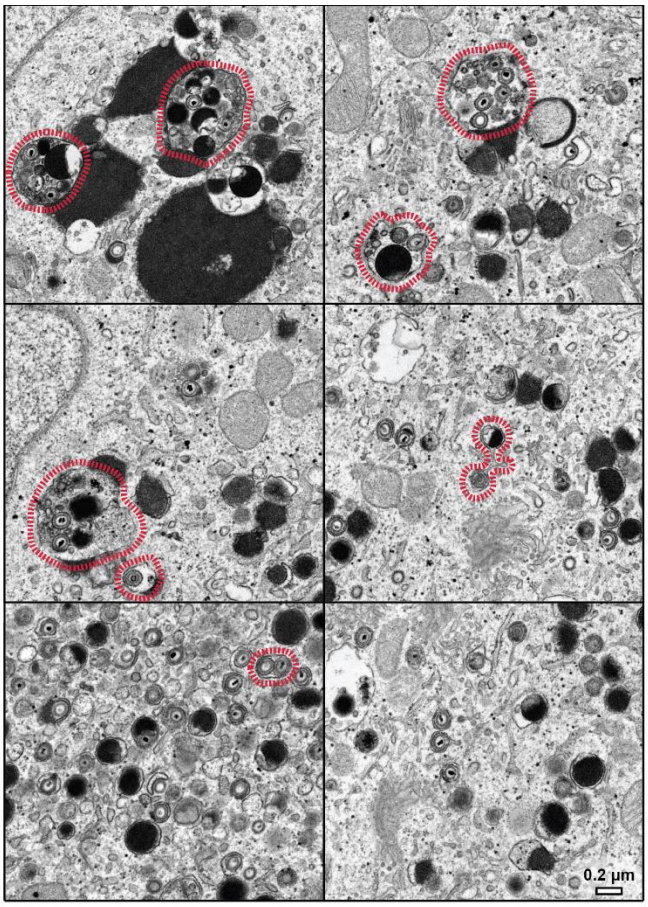

Fig. 3.5. Ultrastructural analysis of HCMV infected cells suggests virion egress by compound exocytosis. Representative images of HFFs infected by the AD169-derived bacterial artificial chromosome (BAC) pAD/Cre (MOI 0.3) show the accumulation of multiple mature viral particles packaged within individual vesicles (red).

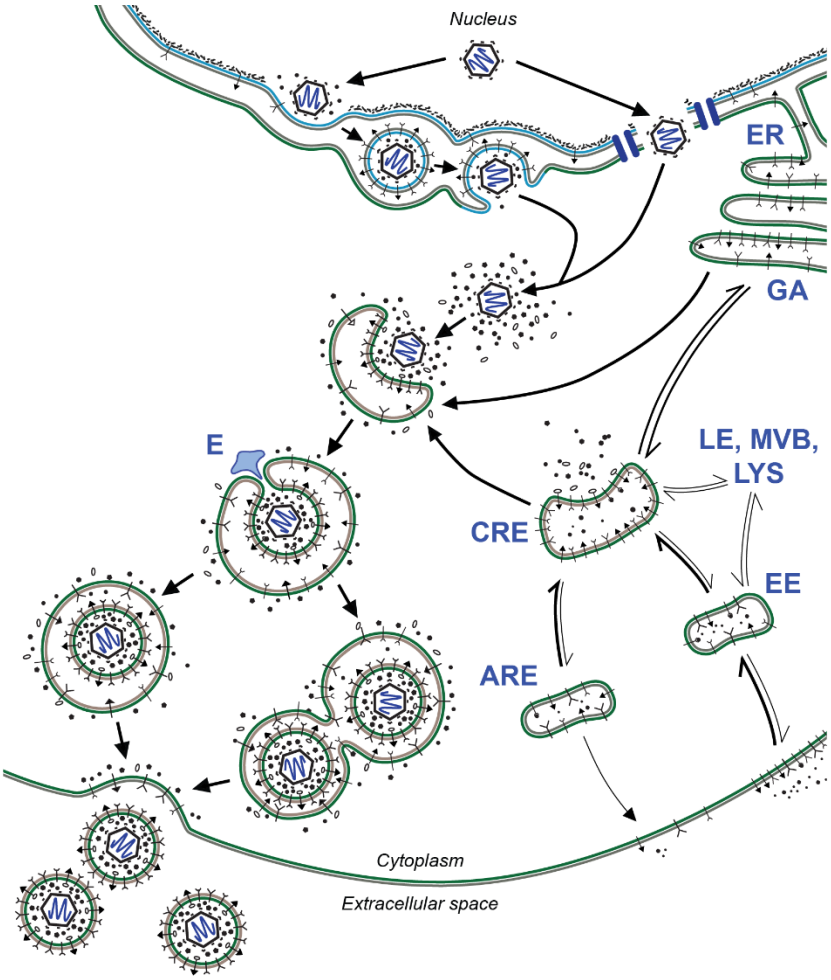

Fig. 3.6. HCMV induced alterations to trafficking within the endocytic recycling compartment (ERC) based on transcriptional data. Following significance analysis of microarray (SAM), 328 significant transcripts were identified as being involved with cellular vesicle-mediated transport. The effects of transcriptional regulation during infection were mapped onto the various pathways within the ERC. The resultant diagram showcases changes in the net flux of various ERC pathways and resultant increase in secretory vesicle exocytosis. Thickness of arrows indicates change in flux relative to uninfected cells with thicker arrows being the favored direction of transport. Abbreviations: endoplasmic reticulum (ER), Golgi apparatus (GA), common recycling endosomes (CRE), early endosomes (EE), apical recycling endosomes (ARE), late endosomes (LE), multivesicular bodies (MVB), lysosomes (LYS), endosomal sorting complex required for transport (ESCRT, E).

CHAPTER 4: GENERAL CONCLUSIONS

Herpesvirus replication cycle relies heavily on remodeling host environments to achieve envelopment and egress of nascent particles. While similar high order requirements exist between the different subfamilies of *Herpesviridae*, details of virion replication differ based on the repertoire of cells infected by each virus. Areas of observed differences include development of an assembly compartment, function of virion structural proteins, composition of virion envelopes, and mechanisms required for membrane scission and virion egress.

In general, herpesviruses hijack host trafficking pathways and direct virion components to a defined assembly region in infected cells, the HCMV cVAC being the most prominent, before exocytosis of fully matured particles. Redirection of trafficking is a result of transcriptional regulation, a complex network of viral protein interactions, and modifications to the metabolic profile of host cells. Key proteins have been identified as having a role in virion maturation but interpretation is difficult due to functional redundancies and downstream cascades of interactions.

As part of this research, we generated a series of novel tools and ideas that will continue to advance the study of HCMV replication. Through the BAC, TB40/E/Cre, genes of interest can be expressed in the context of infection. Through manipulation of cellular and viral processes we will be able to identify pathways integral to HCMV maturation. Through our model of HCMV induced changes to cellular trafficking, we have identified a series of potential targets for further characterization and potential development of novel therapeutics.

By combining all of these advances, functional mutants of cellular trafficking proteins, such as Rab GTPases, can be expressed during infection to inhibit pathways identified as critical control points for virion egress as evidenced by changes in the net output of nascent virions. Likewise, mutated forms of viral proteins purported to be involved in virion maturation and egress could be expressed to look for similar endpoints. Based on prior evidence of cell-specific activities, it will be important to assess trafficking events in all cell types permissive to HCMV infection, particularly epithelial, endothelial, and monocytic lines. Only by using a comprehensive approach will new antiviral targets be identified.

There are still many unanswered questions left but with the advent of new and improved technology, we will be able to probe deeper into depths of virion replication, expanding our knowledge one particle at a time.

REFERENCES

1. **Gurczynski SJ, Das S, Pellett PE.** 2014. Deletion of the human cytomegalovirus US17 gene increases the ratio of genomes per infectious unit and alters regulation of immune and endoplasmic reticulum stress response genes at early and late times after infection. J Virol **88:**2168-2182.
2. **Weekes MP, Tomasec P, Huttlin EL, Fielding CA, Nusinow D, Stanton RJ, Wang EC, Aicheler R, Murrell I, Wilkinson GW, Lehner PJ, Gygi SP.** 2014. Quantitative temporal viromics: an approach to investigate host-pathogen interaction. Cell **157:**1460-1472.
3. **Livak KJ, Schmittgen TD.** 2001. Analysis of relative gene expression data using real-time quantitative PCR and the 2(-Delta Delta C(T)) Method. Methods **25:**402-408.
4. **Beswick TS.** 1962. The origin and the use of the word herpes. Med Hist **6:**214-232.
5. **Davison AJ.** 2010. Herpesvirus systematics. Vet Microbiol **143:**52-69.
6. **McGeoch DJ, Cook S, Dolan A, Jamieson FE, Telford EA.** 1995. Molecular phylogeny and evolutionary timescale for the family of mammalian herpesviruses. J Mol Biol **247:**443-458.
7. **Brown JC, Newcomb WW.** 2011. Herpesvirus capsid assembly: insights from structural analysis. Curr Opin Virol **1:**142-149.
8. **Pellett PE, Roizman B.** 2013. The family Herpesviridae: a brief introduction, p 1802-1822. *In* Knipe DM, Howley PM, Cohen JI, Griffin DE, Lamb RA, Martin MA, Racaniello VR, Roizman B (ed), Fields Virology, 6th ed, vol 2.

9. **Cannon MJ, Schmid DS, Hyde TB.** 2010. Review of cytomegalovirus seroprevalence and demographic characteristics associated with infection. Rev Med Virol **20:**202-213.

10. **Cannon MJ, Davis KF.** 2005. Washing our hands of the congenital cytomegalovirus disease epidemic. BMC Public Health **5:**70.

11. **Adler SP, Nigro G, Pereira L.** 2007. Recent advances in the prevention and treatment of congenital cytomegalovirus infections. Semin Perinatol **31:**10-18.

12. **Cheeran MC, Lokensgard JR, Schleiss MR.** 2009. Neuropathogenesis of congenital cytomegalovirus infection: disease mechanisms and prospects for intervention. Clin Microbiol Rev **22:**99-126, Table of Contents.

13. **Sabin CA, Phillips AN, Lee CA, Janossy G, Emery V, Griffiths PD.** 1995. The effect of CMV infection on progression of human immunodeficiency virus disease is a cohort of haemophilic men followed for up to 13 years from seroconversion. Epidemiol Infect **114:**361-372.

14. **Jabs DA.** 2011. Cytomegalovirus retinitis and the acquired immunodeficiency syndrome--bench to bedside: LXVII Edward Jackson Memorial Lecture. Am J Ophthalmol **151:**198-216 e191.

15. **Nguyen QD, Kempen JH, Bolton SG, Dunn JP, Jabs DA.** 2000. Immune recovery uveitis in patients with AIDS and cytomegalovirus retinitis after highly active antiretroviral therapy. Am J Ophthalmol **129:**634-639.

16. **Lurain NS, Chou S.** 2010. Antiviral drug resistance of human cytomegalovirus. Clin Microbiol Rev **23:**689-712.

17. **Sanchez V, Greis KD, Sztul E, Britt WJ.** 2000. Accumulation of virion tegument and envelope proteins in a stable cytoplasmic compartment during human cytomegalovirus replication: characterization of a potential site of virus assembly. J Virol **74:**975-986.

18. **Das S, Vasanji A, Pellett PE.** 2007. Three-dimensional structure of the human cytomegalovirus cytoplasmic virion assembly complex includes a reoriented secretory apparatus. J Virol **81:**11861-11869.

19. **Das S, Pellett PE.** 2011. Spatial relationships between markers for secretory and endosomal machinery in human cytomegalovirus-infected cells versus those in uninfected cells. J Virol **85:**5864-5879.

20. **Cepeda V, Esteban M, Fraile-Ramos A.** 2010. Human cytomegalovirus final envelopment on membranes containing both trans-Golgi network and endosomal markers. Cell Microbiol **12:**386-404.

21. **Das S, Ortiz DA, Gurczynski SJ, Khan F, Pellett PE.** 2014. Identification of human cytomegalovirus genes important for biogenesis of the cytoplasmic virion assembly complex. J Virol **88:**9086-9099.

22. **Ortiz DA, Glassbrook JE, Pellett PE.** 2016. Protein-Protein Interactions Suggest Novel Activities of Human Cytomegalovirus Tegument Protein pUL103. J Virol **90:**7798-7810.

23. **Jean Beltran PM, Mathias RA, Cristea IM.** 2016. A Portrait of the Human Organelle Proteome In Space and Time during Cytomegalovirus Infection. Cell Syst **3:**361-373 e366.

24. **Ryckman BJ, Jarvis MA, Drummond DD, Nelson JA, Johnson DC.** 2006. Human cytomegalovirus entry into epithelial and endothelial cells depends on genes UL128 to UL150 and occurs by endocytosis and low-pH fusion. J Virol **80:**710-722.

25. **Spear PG, Longnecker R.** 2003. Herpesvirus entry: an update. J Virol **77:**10179-10185.

26. **Seo JY, Britt WJ.** 2007. Cytoplasmic envelopment of human cytomegalovirus requires the postlocalization function of tegument protein pp28 within the assembly compartment. J Virol **81:**6536-6547.

27. **Van Damme E, Van Loock M.** 2014. Functional annotation of human cytomegalovirus gene products: an update. Front Microbiol **5:**218.

28. **Gudleski-O'Regan N, Greco TM, Cristea IM, Shenk T.** 2012. Increased expression of LDL receptor-related protein 1 during human cytomegalovirus infection reduces virion cholesterol and infectivity. Cell Host Microbe **12:**86-96.

29. **Liu ST, Sharon-Friling R, Ivanova P, Milne SB, Myers DS, Rabinowitz JD, Brown HA, Shenk T.** 2011. Synaptic vesicle-like lipidome of human cytomegalovirus virions reveals a role for SNARE machinery in virion egress. Proc Natl Acad Sci U S A **108:**12869-12874.

30. **Koyuncu E, Purdy JG, Rabinowitz JD, Shenk T.** 2013. Saturated very long chain fatty acids are required for the production of infectious human cytomegalovirus progeny. PLoS Pathog **9:**e1003333.

31. **Purdy JG, Shenk T, Rabinowitz JD.** 2015. Fatty acid elongase 7 catalyzes lipidome remodeling essential for human cytomegalovirus replication. Cell Rep **10:**1375-1385.

32. **Cepeda V, Fraile-Ramos A.** 2011. A role for the SNARE protein syntaxin 3 in human cytomegalovirus morphogenesis. Cell Microbiol **13:**846-858.

33. **Fraile-Ramos A, Cepeda V, Elstak E, van der Sluijs P.** 2010. Rab27a is required for human cytomegalovirus assembly. PLoS One **5:**e15318.

34. **Alwine JC.** 2012. The human cytomegalovirus assembly compartment: a masterpiece of viral manipulation of cellular processes that facilitates assembly and egress. PLoS Pathog **8:**e1002878.

35. **Schauflinger M, Villinger C, Mertens T, Walther P, von Einem J.** 2013. Analysis of human cytomegalovirus secondary envelopment by advanced electron microscopy. Cell Microbiol **15:**305-314.

36. **Turcotte S, Letellier J, Lippe R.** 2005. Herpes simplex virus type 1 capsids transit by the trans-Golgi network, where viral glycoproteins accumulate independently of capsid egress. J Virol **79:**8847-8860.

37. **Lee GE, Murray JW, Wolkoff AW, Wilson DW.** 2006. Reconstitution of herpes simplex virus microtubule-dependent trafficking in vitro. J Virol **80:**4264-4275.

38. **Homman-Loudiyi M, Hultenby K, Britt W, Soderberg-Naucler C.** 2003. Envelopment of Human Cytomegalovirus Occurs by Budding into Golgi-Derived Vacuole Compartments Positive for gB, Rab 3, Trans-Golgi Network 46, and Mannosidase II. Journal of Virology **77:**3191-3203.

39. **Sanchez V, Sztul E, Britt WJ.** 2000. Human cytomegalovirus pp28 (UL99) localizes to a cytoplasmic compartment which overlaps the endoplasmic reticulum-golgi-intermediate compartment. J Virol **74:**3842-3851.

40. **Fish KN, Britt W, Nelson JA.** 1996. A novel mechanism for persistence of human cytomegalovirus in macrophages. J Virol **70:**1855-1862.

41. **Cruz L, Streck NT, Ferguson K, Desai T, Desai DH, Amin SG, Buchkovich NJ.** 2017. Potent Inhibition of Human Cytomegalovirus by Modulation of Cellular SNARE Syntaxin 5. J Virol **91**.

42. **Tooze J, Hollinshead M, Reis B, Radsak K, Kern H.** 1993. Progeny vaccinia and human cytomegalovirus particles utilize early endosomal cisternae for their envelopes. Eur J Cell Biol **60:**163-178.

43. **Hollinshead M, Johns HL, Sayers CL, Gonzalez-Lopez C, Smith GL, Elliott G.** 2012. Endocytic tubules regulated by Rab GTPases 5 and 11 are used for envelopment of herpes simplex virus. EMBO J **31:**4204-4220.

44. **Hook LM, Grey F, Grabski R, Tirabassi R, Doyle T, Hancock M, Landais I, Jeng S, McWeeney S, Britt W, Nelson JA.** 2014. Cytomegalovirus miRNAs target secretory pathway genes to facilitate formation of the virion assembly compartment and reduce cytokine secretion. Cell Host Microbe **15:**363-373.

45. **Gottwein E, Corcoran DL, Mukherjee N, Skalsky RL, Hafner M, Nusbaum JD, Shamulailatpam P, Love CL, Dave SS, Tuschl T, Ohler U, Cullen BR.** 2011. Viral microRNA targetome of KSHV-infected primary effusion lymphoma cell lines. Cell Host Microbe **10:**515-526.

46. **Skalsky RL, Corcoran DL, Gottwein E, Frank CL, Kang D, Hafner M, Nusbaum JD, Feederle R, Delecluse HJ, Luftig MA, Tuschl T, Ohler U, Cullen BR.** 2012. The viral and cellular microRNA targetome in lymphoblastoid cell lines. PLoS Pathog **8:**e1002484.

47. **Hertel L, Mocarski ES.** 2004. Global analysis of host cell gene expression late during cytomegalovirus infection reveals extensive dysregulation of cell cycle gene expression and induction of Pseudomitosis independent of US28 function. J Virol **78:**11988-12011.

48. **Grey F, Nelson J.** 2008. Identification and function of human cytomegalovirus microRNAs. J Clin Virol **41:**186-191.

49. **Lucin P, Mahmutefendic H, Blagojevic Zagorac G, Ilic Tomas M.** 2015. Cytomegalovirus immune evasion by perturbation of endosomal trafficking. Cell Mol Immunol **12:**154-169.

50. **Sharon-Friling R, Goodhouse J, Colberg-Poley AM, Shenk T.** 2006. Human cytomegalovirus pUL37x1 induces the release of endoplasmic reticulum calcium stores. Proc Natl Acad Sci U S A **103:**19117-19122.

51. **Sharon-Friling R, Shenk T.** 2014. Human cytomegalovirus pUL37x1-induced calcium flux activates PKCalpha, inducing altered cell shape and accumulation of cytoplasmic vesicles. Proc Natl Acad Sci U S A **111:**E1140-1148.

52. **Williamson CD, Zhang A, Colberg-Poley AM.** 2011. The human cytomegalovirus protein UL37 exon 1 associates with internal lipid rafts. J Virol **85:**2100-2111.

53. **Goulidaki N, Alarifi S, Alkahtani SH, Al-Qahtani A, Spandidos DA, Stournaras C, Sourvinos G.** 2015. RhoB is a component of the human cytomegalovirus

assembly complex and is required for efficient viral production. Cell Cycle **14:**2748-2763.

54. **Poncet D, Pauleau AL, Szabadkai G, Vozza A, Scholz SR, Le Bras M, Briere JJ, Jalil A, Le Moigne R, Brenner C, Hahn G, Wittig I, Schagger H, Lemaire C, Bianchi K, Souquere S, Pierron G, Rustin P, Goldmacher VS, Rizzuto R, Palmieri F, Kroemer G.** 2006. Cytopathic effects of the cytomegalovirus-encoded apoptosis inhibitory protein vMIA. J Cell Biol **174:**985-996.

55. **Schierling K, Buser C, Mertens T, Winkler M.** 2005. Human cytomegalovirus tegument protein ppUL35 is important for viral replication and particle formation. J Virol **79:**3084-3096.

56. **Liu Y, Biegalke BJ.** 2002. The human cytomegalovirus UL35 gene encodes two proteins with different functions. J Virol **76:**2460-2468.

57. **Schierling K, Stamminger T, Mertens T, Winkler M.** 2004. Human cytomegalovirus tegument proteins ppUL82 (pp71) and ppUL35 interact and cooperatively activate the major immediate-early enhancer. J Virol **78:**9512-9523.

58. **Varnum SM, Streblow DN, Monroe ME, Smith P, Auberry KJ, Pasa-Tolic L, Wang D, Camp DG, 2nd, Rodland K, Wiley S, Britt W, Shenk T, Smith RD, Nelson JA.** 2004. Identification of proteins in human cytomegalovirus (HCMV) particles: the HCMV proteome. J Virol **78:**10960-10966.

59. **Womack A, Shenk T.** 2010. Human cytomegalovirus tegument protein pUL71 is required for efficient virion egress. MBio **1**.

60. **Ahlqvist J, Mocarski E.** 2011. Cytomegalovirus UL103 controls virion and dense body egress. J Virol **85:**5125-5135.

61. **Yu D, Silva MC, Shenk T.** 2003. Functional map of human cytomegalovirus AD169 defined by global mutational analysis. Proc Natl Acad Sci U S A **100:**12396-12401.

62. **Bardens A, Doring T, Stieler J, Prange R.** 2011. Alix regulates egress of hepatitis B virus naked capsid particles in an ESCRT-independent manner. Cell Microbiol **13:**602-619.

63. **Zhai Q, Landesman MB, Robinson H, Sundquist WI, Hill CP.** 2011. Identification and structural characterization of the ALIX-binding late domains of simian immunodeficiency virus SIVmac239 and SIVagmTan-1. J Virol **85:**632-637.

64. **Lee CP, Liu PT, Kung HN, Su MT, Chua HH, Chang YH, Chang CW, Tsai CH, Liu FT, Chen MR.** 2012. The ESCRT machinery is recruited by the viral BFRF1 protein to the nucleus-associated membrane for the maturation of Epstein-Barr Virus. PLoS Pathog **8:**e1002904.

65. **Fischer D.** 2012. Dissecting functional motifs of the human cytomegalovirus tegument protein pUL71. Ph.D. thesis. University of Ulm, Ulm, Germany.

66. **Beghetto E, Paolis FD, Spadoni A, Del Porto P, Buffolano W, Gargano N.** 2008. Molecular dissection of the human B cell response against cytomegalovirus infection by lambda display. J Virol Methods **151:**7-14.

67. **Schauflinger M, Fischer D, Schreiber A, Chevillotte M, Walther P, Mertens T, von Einem J.** 2011. The tegument protein UL71 of human cytomegalovirus is involved in late envelopment and affects multivesicular bodies. J Virol **85:**3821-3832.

68. **Meissner CS, Suffner S, Schauflinger M, von Einem J, Bogner E.** 2012. A leucine zipper motif of a tegument protein triggers final envelopment of human cytomegalovirus. J Virol **86:**3370-3382.

69. **To A, Bai Y, Shen A, Gong H, Umamoto S, Lu S, Liu F.** 2011. Yeast two hybrid analyses reveal novel binary interactions between human cytomegalovirus-encoded virion proteins. PLoS One **6:**e17796.

70. **Nozawa N, Kawaguchi Y, Tanaka M, Kato A, Kato A, Kimura H, Nishiyama Y.** 2005. Herpes simplex virus type 1 UL51 protein is involved in maturation and egress of virus particles. J Virol **79:**6947-6956.

71. **Klupp BG, Granzow H, Klopfleisch R, Fuchs W, Kopp M, Lenk M, Mettenleiter TC.** 2005. Functional analysis of the pseudorabies virus UL51 protein. J Virol **79:**3831-3840.

72. **Schleiss MR, McGregor A, Choi KY, Date SV, Cui X, McVoy MA.** 2008. Analysis of the nucleotide sequence of the guinea pig cytomegalovirus (GPCMV) genome. Virol J **5:**139.

73. **Silva MC, Yu QC, Enquist L, Shenk T.** 2003. Human Cytomegalovirus UL99-Encoded pp28 Is Required for the Cytoplasmic Envelopment of Tegument-Associated Capsids. Journal of Virology **77:**10594-10605.

74. **Seo JY, Britt WJ.** 2006. Sequence requirements for localization of human cytomegalovirus tegument protein pp28 to the virus assembly compartment and for assembly of infectious virus. J Virol **80:**5611-5626.

75. **Seo JY, Britt WJ.** 2008. Multimerization of tegument protein pp28 within the assembly compartment is required for cytoplasmic envelopment of human cytomegalovirus. J Virol **82:**6272-6287.

76. **Jones TR, Lee SW.** 2004. An Acidic Cluster of Human Cytomegalovirus UL99 Tegument Protein Is Required for Trafficking and Function. Journal of Virology **78:**1488-1502.

77. **Phillips SL, Cygnar D, Thomas A, Bresnahan WA.** 2012. Interaction between the human cytomegalovirus tegument proteins UL94 and UL99 is essential for virus replication. J Virol **86:**9995-10005.

78. **Phillips SL, Bresnahan WA.** 2011. Identification of binary interactions between human cytomegalovirus virion proteins. J Virol **85:**440-447.

79. **Phillips SL, Bresnahan WA.** 2012. The human cytomegalovirus (HCMV) tegument protein UL94 is essential for secondary envelopment of HCMV virions. J Virol **86:**2523-2532.

80. **Chadha P, Han J, Starkey JL, Wills JW.** 2012. Regulated interaction of tegument proteins UL16 and UL11 from herpes simplex virus. J Virol **86:**11886-11898.

81. **Baines JD, Roizman B.** 1992. The UL11 gene of herpes simplex virus 1 encodes a function that facilitates nucleocapsid envelopment and egress from cells. J Virol **66:**5168-5174.

82. **Maninger S, Bosse JB, Lemnitzer F, Pogoda M, Mohr CA, von Einem J, Walther P, Koszinowski UH, Ruzsics Z.** 2011. M94 is essential for the secondary envelopment of murine cytomegalovirus. J Virol **85:**9254-9267.

83. **Wu JJ, Avey D, Li W, Gillen J, Fu B, Miley W, Whitby D, Zhu F.** 2015. ORF33 and ORF38 of Kaposi's Sarcoma-Associated Herpesvirus Interact and Are Required for Optimal Production of Infectious Progeny Viruses. J Virol **90:**1741-1756.

84. **Guo H, Wang L, Peng L, Zhou ZH, Deng H.** 2009. Open reading frame 33 of a gammaherpesvirus encodes a tegument protein essential for virion morphogenesis and egress. J Virol **83:**10582-10595.

85. **Murphy E, Yu D, Grimwood J, Schmutz J, Dickson M, Jarvis MA, Hahn G, Nelson JA, Myers RM, Shenk TE.** 2003. Coding potential of laboratory and clinical strains of human cytomegalovirus. Proc Natl Acad Sci U S A **100:**14976-14981.

86. **Grainger L, Cicchini L, Rak M, Petrucelli A, Fitzgerald KD, Semler BL, Goodrum F.** 2010. Stress-inducible alternative translation initiation of human cytomegalovirus latency protein pUL138. J Virol **84:**9472-9486.

87. **Liao H, Lee JH, Kondo R, Katata M, Imadome K, Miyado K, Inoue N, Fujiwara S, Nakamura H.** 2014. The highly conserved human cytomegalovirus UL136 ORF generates multiple Golgi-localizing protein isoforms through differential translation initiation. Virus Res **179:**241-246.

88. **Umashankar M, Petrucelli A, Cicchini L, Caposio P, Kreklywich CN, Rak M, Bughio F, Goldman DC, Hamlin KL, Nelson JA, Fleming WH, Streblow DN, Goodrum F.** 2011. A novel human cytomegalovirus locus modulates cell type-specific outcomes of infection. PLoS Pathog **7:**e1002444.

89. **Bughio F, Elliott DA, Goodrum F.** 2013. An endothelial cell-specific requirement for the UL133-UL138 locus of human cytomegalovirus for efficient virus maturation. J Virol **87:**3062-3075.

90. **Bughio F, Umashankar M, Wilson J, Goodrum F.** 2015. Human Cytomegalovirus UL135 and UL136 Genes Are Required for Postentry Tropism in Endothelial Cells. J Virol **89:**6536-6550.

91. **Umashankar M, Rak M, Bughio F, Zagallo P, Caviness K, Goodrum FD.** 2014. Antagonistic determinants controlling replicative and latent states of human cytomegalovirus infection. J Virol **88:**5987-6002.

92. **Caviness K, Cicchini L, Rak M, Umashankar M, Goodrum F.** 2014. Complex expression of the UL136 gene of human cytomegalovirus results in multiple protein isoforms with unique roles in replication. J Virol **88:**14412-14425.

93. **Caviness K, Bughio F, Crawford LB, Streblow DN, Nelson JA, Caposio P, Goodrum F.** 2016. Complex Interplay of the UL136 Isoforms Balances Cytomegalovirus Replication and Latency. MBio **7:**e01986.

94. **Coleman S, Hornig J, Maddux S, Choi KY, McGregor A.** 2015. Viral Glycoprotein Complex Formation, Essential Function and Immunogenicity in the Guinea Pig Model for Cytomegalovirus. PLoS One **10:**e0135567.

95. **Britt WJ, Mach M.** 1996. Human cytomegalovirus glycoproteins. Intervirology **39:**401-412.

96. **Ryckman BJ, Rainish BL, Chase MC, Borton JA, Nelson JA, Jarvis MA, Johnson DC.** 2008. Characterization of the human cytomegalovirus

gH/gL/UL128-131 complex that mediates entry into epithelial and endothelial cells. J Virol **82:**60-70.

97. **Hutt-Fletcher LM.** 2015. EBV glycoproteins: where are we now? Future Virol **10:**1155-1162.

98. **Albecka A, Laine RF, Janssen AF, Kaminski CF, Crump CM.** 2016. HSV-1 Glycoproteins Are Delivered to Virus Assembly Sites Through Dynamin-Dependent Endocytosis. Traffic **17:**21-39.

99. **Maresova L, Pasieka TJ, Homan E, Gerday E, Grose C.** 2005. Incorporation of three endocytosed varicella-zoster virus glycoproteins, gE, gH, and gB, into the virion envelope. J Virol **79:**997-1007.

100. **Bowman JJ, Lacayo JC, Burbelo P, Fischer ER, Cohen JI.** 2011. Rhesus and human cytomegalovirus glycoprotein L are required for infection and cell-to-cell spread of virus but cannot complement each other. J Virol **85:**2089-2099.

101. **Chee MS, Bankier AT, Beck S, Bohni R, Brown CM, Cerny R, Horsnell T, Hutchison CA, 3rd, Kouzarides T, Martignetti JA, et al.** 1990. Analysis of the protein-coding content of the sequence of human cytomegalovirus strain AD169. Curr Top Microbiol Immunol **154:**125-169.

102. **Cha TA, Tom E, Kemble GW, Duke GM, Mocarski ES, Spaete RR.** 1996. Human cytomegalovirus clinical isolates carry at least 19 genes not found in laboratory strains. J Virol **70:**78-83.

103. **Hobom U, Brune W, Messerle M, Hahn G, Koszinowski UH.** 2000. Fast screening procedures for random transposon libraries of cloned herpesvirus

genomes: mutational analysis of human cytomegalovirus envelope glycoprotein genes. J Virol **74:**7720-7729.

104. **Lake CM, Hutt-Fletcher LM.** 2000. Epstein-Barr virus that lacks glycoprotein gN is impaired in assembly and infection. J Virol **74:**11162-11172.

105. **Lake CM, Molesworth SJ, Hutt-Fletcher LM.** 1998. The Epstein-Barr virus (EBV) gN homolog BLRF1 encodes a 15-kilodalton glycoprotein that cannot be authentically processed unless it is coexpressed with the EBV gM homolog BBRF3. J Virol **72:**5559-5564.

106. **Mach M, Kropff B, Dal Monte P, Britt W.** 2000. Complex formation by human cytomegalovirus glycoproteins M (gpUL100) and N (gpUL73). J Virol **74:**11881-11892.

107. **Mach M, Kropff B, Kryzaniak M, Britt W.** 2005. Complex formation by glycoproteins M and N of human cytomegalovirus: structural and functional aspects. J Virol **79:**2160-2170.

108. **Krzyzaniak MA, Mach M, Britt WJ.** 2009. HCMV-encoded glycoprotein M (UL100) interacts with Rab11 effector protein FIP4. Traffic **10:**1439-1457.

109. **Crump CM, Hung CH, Thomas L, Wan L, Thomas G.** 2003. Role of PACS-1 in Trafficking of Human Cytomegalovirus Glycoprotein B and Virus Production. Journal of Virology **77:**11105-11113.

110. **Krzyzaniak M, Mach M, Britt WJ.** 2007. The cytoplasmic tail of glycoprotein M (gpUL100) expresses trafficking signals required for human cytomegalovirus assembly and replication. J Virol **81:**10316-10328.

111. **Mach M, Osinski K, Kropff B, Schloetzer-Schrehardt U, Krzyzaniak M, Britt W.** 2007. The carboxy-terminal domain of glycoprotein N of human cytomegalovirus is required for virion morphogenesis. J Virol **81:**5212-5224.

112. **Chiu YF, Sugden B, Chang PJ, Chen LW, Lin YJ, Lan YC, Lai CH, Liou JY, Liu ST, Hung CH.** 2012. Characterization and intracellular trafficking of Epstein-Barr virus BBLF1, a protein involved in virion maturation. J Virol **86:**9647-9655.

113. **May JS, Smith CM, Gill MB, Stevenson PG.** 2008. An essential role for the proximal but not the distal cytoplasmic tail of glycoprotein M in murid herpesvirus 4 infection. PLoS One **3:**e2131.

114. **Heineman TC, Hall SL.** 2002. Role of the varicella-zoster virus gB cytoplasmic domain in gB transport and viral egress. J Virol **76:**591-599.

115. **Olson JK, Grose C.** 1997. Endocytosis and recycling of varicella-zoster virus Fc receptor glycoprotein gE: internalization mediated by a YXXL motif in the cytoplasmic tail. J Virol **71:**4042-4054.

116. **Alconada A, Bauer U, Hoflack B.** 1996. A tyrosine-based motif and a casein kinase II phosphorylation site regulate the intracellular trafficking of the varicella-zoster virus glycoprotein I, a protein localized in the trans-Golgi network. EMBO J **15:**6096-6110.

117. **Ohno H, Fournier MC, Poy G, Bonifacino JS.** 1996. Structural determinants of interaction of tyrosine-based sorting signals with the adaptor medium chains. J Biol Chem **271:**29009-29015.

118. **Songyang Z, Shoelson SE, Chaudhuri M, Gish G, Pawson T, Haser WG, King F, Roberts T, Ratnofsky S, Lechleider RJ, et al.** 1993. SH2 domains recognize specific phosphopeptide sequences. Cell **72:**767-778.

119. **Radsak K, Eickmann M, Mockenhaupt T, Bogner E, Kern H, Eis-Hubinger A, Reschke M.** 1996. Retrieval of human cytomegalovirus glycoprotein B from the infected cell surface for virus envelopment. Arch Virol **141:**557-572.

120. **Archer MA, Brechtel TM, Davis LE, Parmar RC, Hasan MH, Tandon R.** 2017. Inhibition of endocytic pathways impacts cytomegalovirus maturation. Sci Rep **7:**46069.

121. **Albecka A, Owen DJ, Ivanova L, Brun J, Liman R, Davies L, Ahmed MF, Colaco S, Hollinshead M, Graham SC, Crump CM.** 2017. Dual Function of the pUL7-pUL51 Tegument Protein Complex in Herpes Simplex Virus 1 Infection. J Virol **91**.

122. **Roller RJ, Haugo AC, Yang K, Baines JD.** 2014. The herpes simplex virus 1 UL51 gene product has cell type-specific functions in cell-to-cell spread. J Virol **88:**4058-4068.

123. **Balan P, Davis-Poynter N, Bell S, Atkinson H, Browne H, Minson T.** 1994. An analysis of the in vitro and in vivo phenotypes of mutants of herpes simplex virus type 1 lacking glycoproteins gG, gE, gI or the putative gJ. J Gen Virol **75 (Pt 6):**1245-1258.

124. **Han J, Chadha P, Starkey JL, Wills JW.** 2012. Function of glycoprotein E of herpes simplex virus requires coordinated assembly of three tegument proteins on its cytoplasmic tail. Proc Natl Acad Sci U S A **109:**19798-19803.

125. **Alconada A, Bauer U, Sodeik B, Hoflack B.** 1999. Intracellular traffic of herpes simplex virus glycoprotein gE: characterization of the sorting signals required for its trans-Golgi network localization. J Virol **73:**377-387.

126. **Nozawa N, Daikoku T, Koshizuka T, Yamauchi Y, Yoshikawa T, Nishiyama Y.** 2003. Subcellular localization of herpes simplex virus type 1 UL51 protein and role of palmitoylation in Golgi apparatus targeting. J Virol **77:**3204-3216.

127. **Tirabassi RS, Enquist LW.** 1998. Role of envelope protein gE endocytosis in the pseudorabies virus life cycle. J Virol **72:**4571-4579.

128. **Tirabassi RS, Enquist LW.** 1999. Mutation of the YXXL endocytosis motif in the cytoplasmic tail of pseudorabies virus gE. J Virol **73:**2717-2728.

129. **Kropff B, Koedel Y, Britt W, Mach M.** 2010. Optimal replication of human cytomegalovirus correlates with endocytosis of glycoprotein gpUL132. J Virol **84:**7039-7052.

130. **Spaderna S, Kropff B, Kodel Y, Shen S, Coley S, Lu S, Britt W, Mach M.** 2005. Deletion of gpUL132, a structural component of human cytomegalovirus, results in impaired virus replication in fibroblasts. J Virol **79:**11837-11847.

131. **Jarvis MA, Fish KN, Soderberg-Naucler C, Streblow DN, Meyers HL, Thomas G, Nelson JA.** 2002. Retrieval of Human Cytomegalovirus Glycoprotein B from Cell Surface Is Not Required for Virus Envelopment in Astrocytoma Cells. Journal of Virology **76:**5147-5155.

132. **Jarvis MA, Jones TR, Drummond DD, Smith PP, Britt WJ, Nelson JA, Baldick CJ.** 2003. Phosphorylation of Human Cytomegalovirus Glycoprotein B (gB) at the Acidic Cluster Casein Kinase 2 Site (Ser900) Is Required for Localization of gB to

the trans-Golgi Network and Efficient Virus Replication. Journal of Virology **78:**285-293.

133. **Beitia Ortiz de Zarate I, Cantero-Aguilar L, Longo M, Berlioz-Torrent C, Rozenberg F.** 2007. Contribution of endocytic motifs in the cytoplasmic tail of herpes simplex virus type 1 glycoprotein B to virus replication and cell-cell fusion. J Virol **81:**13889-13903.

134. **Favoreel HW, Van Minnebruggen G, Nauwynck HJ, Enquist LW, Pensaert MB.** 2002. A tyrosine-based motif in the cytoplasmic tail of pseudorabies virus glycoprotein B is important for both antibody-induced internalization of viral glycoproteins and efficient cell-to-cell spread. J Virol **76:**6845-6851.

135. **Foster TP, Melancon JM, Olivier TL, Kousoulas KG.** 2004. Herpes simplex virus type 1 glycoprotein K and the UL20 protein are interdependent for intracellular trafficking and trans-Golgi network localization. J Virol **78:**13262-13277.

136. **Chouljenko DV, Jambunathan N, Chouljenko VN, Naderi M, Brylinski M, Caskey JR, Kousoulas KG.** 2016. Herpes Simplex Virus 1 UL37 Protein Tyrosine Residues Conserved among All Alphaherpesviruses Are Required for Interactions with Glycoprotein K, Cytoplasmic Virion Envelopment, and Infectious Virus Production. J Virol **90:**10351-10361.

137. **Schultz EP, Lanchy JM, Ellerbeck EE, Ryckman BJ.** 2015. Scanning Mutagenesis of Human Cytomegalovirus Glycoprotein gH/gL. J Virol **90:**2294-2305.

138. **Vanarsdall AL, Chase MC, Johnson DC.** 2011. Human cytomegalovirus glycoprotein gO complexes with gH/gL, promoting interference with viral entry into human fibroblasts but not entry into epithelial cells. J Virol **85:**11638-11645.

139. **Wang D, Shenk T.** 2005. Human cytomegalovirus virion protein complex required for epithelial and endothelial cell tropism. Proc Natl Acad Sci U S A **102:**18153-18158.

140. **Kinzler ER, Theiler RN, Compton T.** 2002. Expression and reconstitution of the gH/gL/gO complex of human cytomegalovirus. J Clin Virol **25 Suppl 2:**S87-95.

141. **Coleman S, Choi KY, Root M, McGregor A.** 2016. A Homolog Pentameric Complex Dictates Viral Epithelial Tropism, Pathogenicity and Congenital Infection Rate in Guinea Pig Cytomegalovirus. PLoS Pathog **12:**e1005755.

142. **Dunn W, Chou C, Li H, Hai R, Patterson D, Stolc V, Zhu H, Liu F.** 2003. Functional profiling of a human cytomegalovirus genome. Proc Natl Acad Sci U S A **100:**14223-14228.

143. **Wille PT, Knoche AJ, Nelson JA, Jarvis MA, Johnson DC.** 2010. A human cytomegalovirus gO-null mutant fails to incorporate gH/gL into the virion envelope and is unable to enter fibroblasts and epithelial and endothelial cells. J Virol **84:**2585-2596.

144. **Dolan A, Cunningham C, Hector RD, Hassan-Walker AF, Lee L, Addison C, Dargan DJ, McGeoch DJ, Gatherer D, Emery VC, Griffiths PD, Sinzger C, McSharry BP, Wilkinson GW, Davison AJ.** 2004. Genetic content of wild-type human cytomegalovirus. J Gen Virol **85:**1301-1312.

145. **Theiler RN, Compton T.** 2002. Distinct glycoprotein O complexes arise in a post-Golgi compartment of cytomegalovirus-infected cells. J Virol **76:**2890-2898.

146. **Zhou M, Yu Q, Wechsler A, Ryckman BJ.** 2013. Comparative analysis of gO isoforms reveals that strains of human cytomegalovirus differ in the ratio of gH/gL/gO and gH/gL/UL128-131 in the virion envelope. J Virol **87:**9680-9690.

147. **Molesworth SJ, Lake CM, Borza CM, Turk SM, Hutt-Fletcher LM.** 2000. Epstein-Barr virus gH is essential for penetration of B cells but also plays a role in attachment of virus to epithelial cells. J Virol **74:**6324-6332.

148. **Adler B, Scrivano L, Ruzcics Z, Rupp B, Sinzger C, Koszinowski U.** 2006. Role of human cytomegalovirus UL131A in cell type-specific virus entry and release. J Gen Virol **87:**2451-2460.

149. **Calo S, Cortese M, Ciferri C, Bruno L, Gerrein R, Benucci B, Monda G, Gentile M, Kessler T, Uematsu Y, Maione D, Lilja AE, Carfi A, Merola M.** 2016. The Human Cytomegalovirus UL116 Gene Encodes an Envelope Glycoprotein Forming a Complex with gH Independently from gL. J Virol **90:**4926-4938.

150. **Jean Beltran PM, Cristea IM.** 2014. The life cycle and pathogenesis of human cytomegalovirus infection: lessons from proteomics. Expert Rev Proteomics **11:**697-711.

151. **Li G, Nguyen CC, Ryckman BJ, Britt WJ, Kamil JP.** 2015. A viral regulator of glycoprotein complexes contributes to human cytomegalovirus cell tropism. Proc Natl Acad Sci U S A **112:**4471-4476.

152. **Jiang XJ, Adler B, Sampaio KL, Digel M, Jahn G, Ettischer N, Stierhof YD, Scrivano L, Koszinowski U, Mach M, Sinzger C.** 2008. UL74 of human

cytomegalovirus contributes to virus release by promoting secondary envelopment of virions. J Virol **82:**2802-2812.

153. **Huber MT, Compton T.** 1998. The human cytomegalovirus UL74 gene encodes the third component of the glycoprotein H-glycoprotein L-containing envelope complex. J Virol **72:**8191-8197.

154. **Mori Y, Akkapaiboon P, Yang X, Yamanishi K.** 2003. The human herpesvirus 6 U100 gene product is the third component of the gH-gL glycoprotein complex on the viral envelope. J Virol **77:**2452-2458.

155. **Rasmussen L, Geissler A, Cowan C, Chase A, Winters M.** 2002. The genes encoding the gCIII complex of human cytomegalovirus exist in highly diverse combinations in clinical isolates. J Virol **76:**10841-10848.

156. **Vastag L, Koyuncu E, Grady SL, Shenk TE, Rabinowitz JD.** 2011. Divergent effects of human cytomegalovirus and herpes simplex virus-1 on cellular metabolism. PLoS Pathog **7:**e1002124.

157. **Munger J, Bennett BD, Parikh A, Feng XJ, McArdle J, Rabitz HA, Shenk T, Rabinowitz JD.** 2008. Systems-level metabolic flux profiling identifies fatty acid synthesis as a target for antiviral therapy. Nat Biotechnol **26:**1179-1186.

158. **Spencer CM, Schafer XL, Moorman NJ, Munger J.** 2011. Human cytomegalovirus induces the activity and expression of acetyl-coenzyme A carboxylase, a fatty acid biosynthetic enzyme whose inhibition attenuates viral replication. J Virol **85:**5814-5824.

159. **Chlanda P, Schraidt O, Kummer S, Riches J, Oberwinkler H, Prinz S, Krausslich HG, Briggs JA.** 2015. Structural Analysis of the Roles of Influenza A

Virus Membrane-Associated Proteins in Assembly and Morphology. J Virol **89:**8957-8966.

160. **Roller RJ, Bjerke SL, Haugo AC, Hanson S.** 2010. Analysis of a charge cluster mutation of herpes simplex virus type 1 UL34 and its extragenic suppressor suggests a novel interaction between pUL34 and pUL31 that is necessary for membrane curvature around capsids. J Virol **84:**3921-3934.

161. **Schnee M, Ruzsics Z, Bubeck A, Koszinowski UH.** 2006. Common and specific properties of herpesvirus UL34/UL31 protein family members revealed by protein complementation assay. J Virol **80:**11658-11666.

162. **McMahon HT, Gallop JL.** 2005. Membrane curvature and mechanisms of dynamic cell membrane remodelling. Nature **438:**590-596.

163. **Wakil SJ, Stoops JK, Joshi VC.** 1983. Fatty acid synthesis and its regulation. Annu Rev Biochem **52:**537-579.

164. **Tong L.** 2005. Acetyl-coenzyme A carboxylase: crucial metabolic enzyme and attractive target for drug discovery. Cell Mol Life Sci **62:**1784-1803.

165. **Chin KC, Cresswell P.** 2001. Viperin (cig5), an IFN-inducible antiviral protein directly induced by human cytomegalovirus. Proc Natl Acad Sci U S A **98:**15125-15130.

166. **Seo JY, Cresswell P.** 2013. Viperin regulates cellular lipid metabolism during human cytomegalovirus infection. PLoS Pathog **9:**e1003497.

167. **Landini MP.** 1984. Early enhanced glucose uptake in human cytomegalovirus-infected cells. J Gen Virol **65 (Pt 7):**1229-1232.

168. **Millar AA, Wrischer M, Kunst L.** 1998. Accumulation of very-long-chain fatty acids in membrane glycerolipids is associated with dramatic alterations in plant morphology. Plant Cell **10:**1889-1902.

169. **Markham JE, Molino D, Gissot L, Bellec Y, Hematy K, Marion J, Belcram K, Palauqui JC, Satiat-Jeunemaitre B, Faure JD.** 2011. Sphingolipids containing very-long-chain fatty acids define a secretory pathway for specific polar plasma membrane protein targeting in Arabidopsis. Plant Cell **23:**2362-2378.

170. **Schneiter R, Brugger B, Amann CM, Prestwich GD, Epand RF, Zellnig G, Wieland FT, Epand RM.** 2004. Identification and biophysical characterization of a very-long-chain-fatty-acid-substituted phosphatidylinositol in yeast subcellular membranes. Biochem J **381:**941-949.

171. **Schneiter R, Kohlwein SD.** 1997. Organelle structure, function, and inheritance in yeast: a role for fatty acid synthesis? Cell **88:**431-434.

172. **Yu Y, Maguire TG, Alwine JC.** 2012. Human cytomegalovirus infection induces adipocyte-like lipogenesis through activation of sterol regulatory element binding protein 1. J Virol **86:**2942-2949.

173. **Lewis CA, Griffiths B, Santos CR, Pende M, Schulze A.** 2011. Regulation of the SREBP transcription factors by mTORC1. Biochem Soc Trans **39:**495-499.

174. **Laplante M, Sabatini DM.** 2009. An emerging role of mTOR in lipid biosynthesis. Curr Biol **19:**R1046-1052.

175. **Raiborg C, Stenmark H.** 2009. The ESCRT machinery in endosomal sorting of ubiquitylated membrane proteins. Nature **458:**445-452.

176. **Hurley JH, Hanson PI.** 2010. Membrane budding and scission by the ESCRT machinery: it's all in the neck. Nat Rev Mol Cell Biol **11:**556-566.

177. **Garrus JE, von Schwedler UK, Pornillos OW, Morham SG, Zavitz KH, Wang HE, Wettstein DA, Stray KM, Cote M, Rich RL, Myszka DG, Sundquist WI.** 2001. Tsg101 and the vacuolar protein sorting pathway are essential for HIV-1 budding. Cell **107:**55-65.

178. **Demirov DG, Ono A, Orenstein JM, Freed EO.** 2002. Overexpression of the N-terminal domain of TSG101 inhibits HIV-1 budding by blocking late domain function. Proc Natl Acad Sci U S A **99:**955-960.

179. **Votteler J, Sundquist WI.** 2013. Virus budding and the ESCRT pathway. Cell Host Microbe **14:**232-241.

180. **Shields SB, Oestreich AJ, Winistorfer S, Nguyen D, Payne JA, Katzmann DJ, Piper R.** 2009. ESCRT ubiquitin-binding domains function cooperatively during MVB cargo sorting. J Cell Biol **185:**213-224.

181. **Hurley JH.** 2008. ESCRT complexes and the biogenesis of multivesicular bodies. Curr Opin Cell Biol **20:**4-11.

182. **Hurley JH, Ren X.** 2009. The circuitry of cargo flux in the ESCRT pathway. J Cell Biol **185:**185-187.

183. **Tandon R, AuCoin DP, Mocarski ES.** 2009. Human cytomegalovirus exploits ESCRT machinery in the process of virion maturation. J Virol **83:**10797-10807.

184. **Fraile-Ramos A, Pelchen-Matthews A, Risco C, Rejas MT, Emery VC, Hassan-Walker AF, Esteban M, Marsh M.** 2007. The ESCRT machinery is not required for human cytomegalovirus envelopment. Cell Microbiol **9:**2955-2967.

185. **Kharkwal H, Smith CG, Wilson DW.** 2016. Herpes Simplex Virus Capsid Localization to ESCRT-VPS4 Complexes in the Presence and Absence of the Large Tegument Protein UL36p. J Virol **90:**7257-7267.

186. **Calistri A, Sette P, Salata C, Cancellotti E, Forghieri C, Comin A, Gottlinger H, Campadelli-Fiume G, Palu G, Parolin C.** 2007. Intracellular trafficking and maturation of herpes simplex virus type 1 gB and virus egress require functional biogenesis of multivesicular bodies. J Virol **81:**11468-11478.

187. **Crump CM, Yates C, Minson T.** 2007. Herpes simplex virus type 1 cytoplasmic envelopment requires functional Vps4. J Virol **81:**7380-7387.

188. **Mori Y, Koike M, Moriishi E, Kawabata A, Tang H, Oyaizu H, Uchiyama Y, Yamanishi K.** 2008. Human herpesvirus-6 induces MVB formation, and virus egress occurs by an exosomal release pathway. Traffic **9:**1728-1742.

189. **Pawliczek T, Crump CM.** 2009. Herpes simplex virus type 1 production requires a functional ESCRT-III complex but is independent of TSG101 and ALIX expression. J Virol **83:**11254-11264.

190. **Kumar B, Chandran B.** 2016. KSHV Entry and Trafficking in Target Cells-Hijacking of Cell Signal Pathways, Actin and Membrane Dynamics. Viruses **8**.

191. **Kumar B, Dutta D, Iqbal J, Ansari MA, Roy A, Chikoti L, Pisano G, Veettil MV, Chandran B.** 2016. ESCRT-I Protein Tsg101 Plays a Role in the Post-macropinocytic Trafficking and Infection of Endothelial Cells by Kaposi's Sarcoma-Associated Herpesvirus. PLoS Pathog **12:**e1005960.

192. **Veettil MV, Kumar B, Ansari MA, Dutta D, Iqbal J, Gjyshi O, Bottero V, Chandran B.** 2016. ESCRT-0 Component Hrs Promotes Macropinocytosis of

Kaposi's Sarcoma-Associated Herpesvirus in Human Dermal Microvascular Endothelial Cells. J Virol **90:**3860-3872.

193. **van Spriel AB, van den Bogaart G, Cambi A.** 2015. Editorial: Membrane domains as new drug targets. Front Physiol **6:**172.

194. **Brown D.** 2000. Targeting of membrane transporters in renal epithelia: when cell biology meets physiology. Am J Physiol Renal Physiol **278:**F192-201.

195. **Resh MD.** 2004. A myristoyl switch regulates membrane binding of HIV-1 Gag. Proc Natl Acad Sci U S A **101:**417-418.

196. **Resh MD.** 2004. Membrane targeting of lipid modified signal transduction proteins. Subcell Biochem **37:**217-232.

197. **Mizuno K, Tolmachova T, Ushakov DS, Romao M, Abrink M, Ferenczi MA, Raposo G, Seabra MC.** 2007. Rab27b regulates mast cell granule dynamics and secretion. Traffic **8:**883-892.

198. **Higashio H, Satoh Y, Saino T.** 2016. Mast cell degranulation is negatively regulated by the Munc13-4-binding small-guanosine triphosphatase Rab37. Sci Rep **6:**22539.

199. **Kimura T, Niki I.** 2011. Rab27a in pancreatic beta-cells, a busy protein in membrane trafficking. Prog Biophys Mol Biol **107:**219-223.

200. **Yi Z, Yokota H, Torii S, Aoki T, Hosaka M, Zhao S, Takata K, Takeuchi T, Izumi T.** 2002. The Rab27a/granuphilin complex regulates the exocytosis of insulin-containing dense-core granules. Mol Cell Biol **22:**1858-1867.

201. **Fukuda M.** 2013. Rab27 effectors, pleiotropic regulators in secretory pathways. Traffic **14:**949-963.

202. **Sudhof TC.** 2013. A molecular machine for neurotransmitter release: synaptotagmin and beyond. Nat Med **19:**1227-1231.

203. **Sheng ZH, Rettig J, Cook T, Catterall WA.** 1996. Calcium-dependent interaction of N-type calcium channels with the synaptic core complex. Nature **379:**451-454.

204. **Schiavo G, Stenbeck G, Rothman JE, Sollner TH.** 1997. Binding of the synaptic vesicle v-SNARE, synaptotagmin, to the plasma membrane t-SNARE, SNAP-25, can explain docked vesicles at neurotoxin-treated synapses. Proc Natl Acad Sci U S A **94:**997-1001.

205. **Rizo J, Rosenmund C.** 2008. Synaptic vesicle fusion. Nat Struct Mol Biol **15:**665-674.

206. **Sudhof TC.** 1995. The synaptic vesicle cycle: a cascade of protein-protein interactions. Nature **375:**645-653.

207. **McMahon HT, Sudhof TC.** 1995. Synaptic core complex of synaptobrevin, syntaxin, and SNAP25 forms high affinity alpha-SNAP binding site. J Biol Chem **270:**2213-2217.

208. **Stenmark H.** 2009. Rab GTPases as coordinators of vesicle traffic. Nat Rev Mol Cell Biol **10:**513-525.

209. **Grosshans BL, Ortiz D, Novick P.** 2006. Rabs and their effectors: achieving specificity in membrane traffic. Proc Natl Acad Sci U S A **103:**11821-11827.

210. **Tsuboi T, Fukuda M.** 2006. Rab3A and Rab27A cooperatively regulate the docking step of dense-core vesicle exocytosis in PC12 cells. J Cell Sci **119:**2196-2203.

211. **Handley MT, Haynes LP, Burgoyne RD.** 2007. Differential dynamics of Rab3A and Rab27A on secretory granules. J Cell Sci **120:**973-984.

212. **Miranda-Saksena M, Boadle RA, Aggarwal A, Tijono B, Rixon FJ, Diefenbach RJ, Cunningham AL.** 2009. Herpes simplex virus utilizes the large secretory vesicle pathway for anterograde transport of tegument and envelope proteins and for viral exocytosis from growth cones of human fetal axons. J Virol **83:**3187-3199.

213. **Bello-Morales R, Crespillo AJ, Fraile-Ramos A, Tabares E, Alcina A, Lopez-Guerrero JA.** 2012. Role of the small GTPase Rab27a during herpes simplex virus infection of oligodendrocytic cells. BMC Microbiol **12:**265.

214. **Mazelova J, Ransom N, Astuto-Gribble L, Wilson MC, Deretic D.** 2009. Syntaxin 3 and SNAP-25 pairing, regulated by omega-3 docosahexaenoic acid, controls the delivery of rhodopsin for the biogenesis of cilia-derived sensory organelles, the rod outer segments. J Cell Sci **122:**2003-2013.

215. **Hogue IB, Bosse JB, Hu JR, Thiberge SY, Enquist LW.** 2014. Cellular mechanisms of alpha herpesvirus egress: live cell fluorescence microscopy of pseudorabies virus exocytosis. PLoS Pathog **10:**e1004535.

216. **Hogue IB, Scherer J, Enquist LW.** 2016. Exocytosis of Alphaherpesvirus Virions, Light Particles, and Glycoproteins Uses Constitutive Secretory Mechanisms. MBio **7**.

217. **Johns HL, Gonzalez-Lopez C, Sayers CL, Hollinshead M, Elliott G.** 2014. Rab6 dependent post-Golgi trafficking of HSV1 envelope proteins to sites of virus envelopment. Traffic **15:**157-178.

218. **Fisher RA.** 2009. Cytomegalovirus infection and disease in the new era of immunosuppression following solid organ transplantation. Transpl Infect Dis **11:**195-202.

219. **Nigro G, Adler SP.** 2011. Cytomegalovirus infections during pregnancy. Curr Opin Obstet Gynecol **23:**123-128.

220. **Manicklal S, Emery VC, Lazzarotto T, Boppana SB, Gupta RK.** 2013. The "silent" global burden of congenital cytomegalovirus. Clin Microbiol Rev **26:**86-102.

221. **Smith RJH, Shearer AE, Hildebrand MS, Van Camp G.** 1993. Deafness and Hereditary Hearing Loss Overview. *In* Pagon RA, Adam MP, Ardinger HH, Wallace SE, Amemiya A, Bean LJH, Bird TD, Ledbetter N, Mefford HC, Smith RJH, Stephens K (ed), GeneReviews(R), Seattle (WA).

222. **Freed EO.** 2015. HIV-1 assembly, release and maturation. Nat Rev Microbiol **13:**484-496.

223. **Bartenschlager R, Lohmann V, Penin F.** 2013. The molecular and structural basis of advanced antiviral therapy for hepatitis C virus infection. Nat Rev Microbiol **11:**482-496.

224. **Paul D, Madan V, Bartenschlager R.** 2014. Hepatitis C virus RNA replication and assembly: living on the fat of the land. Cell Host Microbe **16:**569-579.

225. **Davison AJ.** 2007. Comparative analysis of the genomes. *In* Arvin A, Campadelli-Fiume G, Mocarski E, Moore PS, Roizman B, Whitley R, Yamanishi K (ed), Human Herpesviruses: Biology, Therapy, and Immunoprophylaxis, Cambridge.

226. **Stern-Ginossar N, Weisburd B, Michalski A, Le VT, Hein MY, Huang SX, Ma M, Shen B, Qian SB, Hengel H, Mann M, Ingolia NT, Weissman JS.** 2012. Decoding human cytomegalovirus. Science **338:**1088-1093.

227. **Dhuruvasan K, Sivasubramanian G, Pellett PE.** 2011. Roles of host and viral microRNAs in human cytomegalovirus biology. Virus Res **157:**180-192.

228. **Manning WC, Mocarski ES.** 1988. Insertional mutagenesis of the murine cytomegalovirus genome: one prominent alpha gene (ie2) is dispensable for growth. Virology **167:**477-484.

229. **Spaete RR, Mocarski ES.** 1987. Insertion and deletion mutagenesis of the human cytomegalovirus genome. Proc Natl Acad Sci U S A **84:**7213-7217.

230. **Monaco AP, Larin Z.** 1994. YACs, BACs, PACs and MACs: artificial chromosomes as research tools. Trends Biotechnol **12:**280-286.

231. **Shizuya H, Birren B, Kim UJ, Mancino V, Slepak T, Tachiiri Y, Simon M.** 1992. Cloning and stable maintenance of 300-kilobase-pair fragments of human DNA in Escherichia coli using an F-factor-based vector. Proc Natl Acad Sci U S A **89:**8794-8797.

232. **Warden C, Tang Q, Zhu H.** 2011. Herpesvirus BACs: past, present, and future. J Biomed Biotechnol **2011:**124595.

233. **Cui X, Adler SP, Davison AJ, Smith L, Habib el SE, McVoy MA.** 2012. Bacterial artificial chromosome clones of viruses comprising the towne cytomegalovirus vaccine. J Biomed Biotechnol **2012:**428498.

234. **Borst EM, Hahn G, Koszinowski UH, Messerle M.** 1999. Cloning of the human cytomegalovirus (HCMV) genome as an infectious bacterial artificial chromosome

in Escherichia coli: a new approach for construction of HCMV mutants. J Virol **73:**8320-8329.

235. **Warming S, Costantino N, Court DL, Jenkins NA, Copeland NG.** 2005. Simple and highly efficient BAC recombineering using galK selection. Nucleic Acids Res **33:**e36.

236. **Greaves RF, Brown JM, Vieira J, Mocarski ES.** 1995. Selectable insertion and deletion mutagenesis of the human cytomegalovirus genome using the Escherichia coli guanosine phosphoribosyl transferase (gpt) gene. J Gen Virol **76 (Pt 9):**2151-2160.

237. **Paredes AM, Yu D.** 2012. Human cytomegalovirus: bacterial artificial chromosome (BAC) cloning and genetic manipulation. Curr Protoc Microbiol **Chapter 14:**Unit14E 14.

238. **Stanton RJ, Baluchova K, Dargan DJ, Cunningham C, Sheehy O, Seirafian S, McSharry BP, Neale ML, Davies JA, Tomasec P, Davison AJ, Wilkinson GW.** 2010. Reconstruction of the complete human cytomegalovirus genome in a BAC reveals RL13 to be a potent inhibitor of replication. J Clin Invest **120:**3191-3208.

239. **Yu D, Smith GA, Enquist LW, Shenk T.** 2002. Construction of a self-excisable bacterial artificial chromosome containing the human cytomegalovirus genome and mutagenesis of the diploid TRL/IRL13 gene. J Virol **76:**2316-2328.

240. **Messerle M, Crnkovic I, Hammerschmidt W, Ziegler H, Koszinowski UH.** 1997. Cloning and mutagenesis of a herpesvirus genome as an infectious bacterial artificial chromosome. Proc Natl Acad Sci U S A **94:**14759-14763.

241. **Britt WJ, Jarvis M, Seo JY, Drummond D, Nelson J.** 2004. Rapid genetic engineering of human cytomegalovirus by using a lambda phage linear recombination system: demonstration that pp28 (UL99) is essential for production of infectious virus. J Virol **78:**539-543.

242. **Tischer BK, Smith GA, Osterrieder N.** 2010. En passant mutagenesis: a two step markerless red recombination system. Methods Mol Biol **634:**421-430.

243. **Alam TI, Draper B, Kondabagil K, Rentas FJ, Ghosh-Kumar M, Sun S, Rossmann MG, Rao VB.** 2008. The headful packaging nuclease of bacteriophage T4. Mol Microbiol **69:**1180-1190.

244. **Sinzger C, Hahn G, Digel M, Katona R, Sampaio KL, Messerle M, Hengel H, Koszinowski U, Brune W, Adler B.** 2008. Cloning and sequencing of a highly productive, endotheliotropic virus strain derived from human cytomegalovirus TB40/E. J Gen Virol **89:**359-368.

245. **Borst EM, Messerle M.** 2005. Analysis of human cytomegalovirus oriLyt sequence requirements in the context of the viral genome. J Virol **79:**3615-3626.

246. **Boehmer PE, Lehman IR.** 1997. Herpes simplex virus DNA replication. Annu Rev Biochem **66:**347-384.

247. **McVoy MA, Adler SP.** 1994. Human cytomegalovirus DNA replicates after early circularization by concatemer formation, and inversion occurs within the concatemer. J Virol **68:**1040-1051.

248. **Nixon DE, McVoy MA.** 2002. Terminally repeated sequences on a herpesvirus genome are deleted following circularization but are reconstituted by duplication during cleavage and packaging of concatemeric DNA. J Virol **76:**2009-2013.

249. **Borst EM, Kleine-Albers J, Gabaev I, Babic M, Wagner K, Binz A, Degenhardt I, Kalesse M, Jonjic S, Bauerfeind R, Messerle M.** 2013. The human cytomegalovirus UL51 protein is essential for viral genome cleavage-packaging and interacts with the terminase subunits pUL56 and pUL89. J Virol **87:**1720-1732.

250. **Broll H, Finsterbusch T, Buhk HJ, Goltz M.** 1999. Genetic analysis of the bovine herpesvirus type 4 gene locus for the putative terminase. Virus Genes **19:**243-250.

251. **Adelman K, Salmon B, Baines JD.** 2001. Herpes simplex virus DNA packaging sequences adopt novel structures that are specifically recognized by a component of the cleavage and packaging machinery. Proc Natl Acad Sci U S A **98:**3086-3091.

252. **McVoy MA, Nixon DE, Hur JK, Adler SP.** 2000. The ends on herpesvirus DNA replicative concatemers contain pac2 cis cleavage/packaging elements and their formation is controlled by terminal cis sequences. J Virol **74:**1587-1592.

253. **Marks JR, Spector DH.** 1988. Replication of the murine cytomegalovirus genome: structure and role of the termini in the generation and cleavage of concatenates. Virology **162:**98-107.

254. **Deng H, Dewhurst S.** 1998. Functional identification and analysis of cis-acting sequences which mediate genome cleavage and packaging in human herpesvirus 6. J Virol **72:**320-329.

255. **Bauer DW, Huffman JB, Homa FL, Evilevitch A.** 2013. Herpes virus genome, the pressure is on. J Am Chem Soc **135:**11216-11221.

256. **Sae-Ueng U, Li D, Zuo X, Huffman JB, Homa FL, Rau D, Evilevitch A.** 2014. Solid-to-fluid DNA transition inside HSV-1 capsid close to the temperature of infection. Nat Chem Biol **10:**861-867.

257. **Cui X, McGregor A, Schleiss MR, McVoy MA.** 2009. The impact of genome length on replication and genome stability of the herpesvirus guinea pig cytomegalovirus. Virology **386:**132-138.

258. **Cui X, McGregor A, Schleiss MR, McVoy MA.** 2008. Cloning the complete guinea pig cytomegalovirus genome as an infectious bacterial artificial chromosome with excisable origin of replication. J Virol Methods **149:**231-239.

259. **Murrell I, Wilkie GS, Davison AJ, Statkute E, Fielding CA, Tomasec P, Wilkinson GW, Stanton RJ.** 2016. Genetic Stability of Bacterial Artificial Chromosome-Derived Human Cytomegalovirus during Culture In Vitro. J Virol **90:**3929-3943.

260. **Tanaka M, Kagawa H, Yamanashi Y, Sata T, Kawaguchi Y.** 2003. Construction of an excisable bacterial artificial chromosome containing a full-length infectious clone of herpes simplex virus type 1: viruses reconstituted from the clone exhibit wild-type properties in vitro and in vivo. J Virol **77:**1382-1391.

261. **Richards AL, Sollars PJ, Smith GA.** 2016. New tools to convert bacterial artificial chromosomes to a self-excising design and their application to a herpes simplex virus type 1 infectious clone. BMC Biotechnol **16:**64.

262. **Smith GA, Enquist LW.** 2000. A self-recombining bacterial artificial chromosome and its application for analysis of herpesvirus pathogenesis. Proc Natl Acad Sci U S A **97:**4873-4878.

263. **Seo JY, Yaneva R, Hinson ER, Cresswell P.** 2011. Human cytomegalovirus directly induces the antiviral protein viperin to enhance infectivity. Science **332:**1093-1097.

264. **Banaszynski LA, Chen LC, Maynard-Smith LA, Ooi AG, Wandless TJ.** 2006. A rapid, reversible, and tunable method to regulate protein function in living cells using synthetic small molecules. Cell **126:**995-1004.

265. **Schindelin J, Arganda-Carreras I, Frise E, Kaynig V, Longair M, Pietzsch T, Preibisch S, Rueden C, Saalfeld S, Schmid B, Tinevez JY, White DJ, Hartenstein V, Eliceiri K, Tomancak P, Cardona A.** 2012. Fiji: an open-source platform for biological-image analysis. Nat Methods **9:**676-682.

266. **Moorman NJ, Sharon-Friling R, Shenk T, Cristea IM.** 2010. A targeted spatial-temporal proteomics approach implicates multiple cellular trafficking pathways in human cytomegalovirus virion maturation. Mol Cell Proteomics **9:**851-860.

267. **Maxfield FR, McGraw TE.** 2004. Endocytic recycling. Nat Rev Mol Cell Biol **5:**121-132.

ABSTRACT

NAVIGATING HUMAN CYTOMEGALOVIRUS (HCMV) ENVELOPMENT AND EGRESS

by

WILLIAM L. CLOSE

August 2017

Advisor: Dr. Philip E. Pellett

Major: Immunology and Microbiology

Degree: Doctor of Philosophy

Human cytomegalovirus (HCMV) is a ubiquitous viral pathogen. In individuals with fully functioning and mature immune systems, HCMV is associated with mild symptoms prior to establishing latency. In individuals with naïve or compromised immune systems, HCMV is capable of causing severe organ damage. HCMV is the leading infectious cause of congenital birth defects and a major non-genetic cause of hearing loss. Unfortunately, antiviral treatment options lack diversity due to limited knowledge of virion replication. If HCMV replication were better understood, new antiviral treatments could be developed.

In this work, we describe the development and implementation of new tools to study HCMV replication with a focus on envelopment and egress. We generated a novel HCMV bacterial artificial chromosome (BAC) expression system for characterizing the effects of exogenous proteins in the context of HCMV replication. While demonstrating the new BAC, TB40/E/Cre, we are also able to draw conclusions relating HCMV genome size to replication efficiency. In addition, we characterize the transcriptional profile of cellular proteins during HCMV infection. We found that HCMV causes significant alteration in host mRNA expression and targets a number of transcripts related to vesicle-

mediated trafficking. By tracing the effects of HCMV on cellular trafficking, we propose a model of virion envelopment and egress.

Through this work, we now have the capability to test our predictions and determine the route of viral maturation and exocytosis in host cells. By constructing a map of HCMV replication, we provide critical control points for use in developing novel antiviral therapies.

AUTOBIOGRAPHICAL STATEMENT

William L. Close

EDUCATION:

Ph.D., Immunology and Microbiology
Wayne State University School of Medicine, Detroit, MI, August 2017

Bachelor of Science in Microbiology with Business Concentration
University of Wisconsin – La Crosse, La Crosse, WI, May 2012

WORK EXPERIENCE:

2010 – 2012 Microbiology Quality Assurance Intern
City Brewing Company, La Crosse, WI

AWARDS:

2017 American Society for Virology 36th Annual Meeting Travel Grant
American Society for Virology

2016 Second Place, Poster Presentation, Graduate and Postdoctoral Research Symposium
Wayne State University

2016 Honorable Mention, Poster Presentation, 20th Annual Graduate Student Research Day
Wayne State University

2015-2017 Thomas C. Rumble Fellow
Wayne State University

PUBLICATIONS:

2017 Close WL, Bhandari A, Hojeij M, Pellett PE. Generation of a novel human cytomegalovirus bacterial artificial chromosome tailored for transduction of exogenous sequences. *Virus Research*. *Under revision.*

2013 Tiruveedhula VV, Witzigmann CM, Verma R, Kabir MS, Rott M, Schwan WR, Medina-Bielski S, Lane M, **Close W**, Polanowski RL, Sherman D, Monte A, Deschamps JR, Cook JM. Design and synthesis of novel antimicrobials with activity against Gram-positive bacteria and mycobacterial species, including M. tuberculosis. *Bioorganic & Medicinal Chemistry.* 21(24):7830-7840.